SECULAR VARIATION OF COSMOGENIC NUCLIDE PRODUCTION FROM CHLORINE-36 IN FOSSIL PACK RAT MIDDENS:

Implications for Cosmogenic Nuclide Dating and Potential Application as a Groundwater Tracer

by

Mitchell Aaron Plummer

A thesis submitted in partial fulfillment of the

requirements for the degree of

Master of Hydrology

New Mexico Institute of Mining and Technology

Abstract

Since the advent of ^{14}C dating in the early 50's, there has been a continuing effort to assess the effect of secular variation of production of ^{14}C on ^{14}C activity. It is now widely accepted that long-term variations in ^{14}C activity are caused by fluctuations in the strength of the earth's magnetic field. This study attempts to shed light on the nature and source of ^{14}C activity variations through a proxy record of its production, namely the production record of another cosmogenic radionuclide, ^{36}Cl. Chlorine-36/chlorine ratios representative of the meteoric water taken up plants should be well represented in the crystalline urine contained in fossil packrat middens; packrats derive their water solely from plants and deposit a substantial amount of concentrated urine in their middens. We have measured $^{36}Cl/Cl$ ratios in 33 ancient packrat middens in an effort to reconstruct the production history of cosmogenic isotopes. Results suggest that the $^{36}Cl/Cl$ ratio of infiltration declined by ~50% to 100% at the close of the Pleistocene. While this is not inconsistent with the general trend in the predicted production record, the magnitude of the change at that period in time is greater than that suggested by available paleomagnetic records and by other records of the secular variation of cosmogenic nuclide production. It is possible that this large change was caused by local variations in the flux of stable chloride in the area that may have occurred as a result of the climate change.

As with other cosmogenic nuclides production such as ^{14}C and ^{10}Be, reconstruction of the cosmogenic nuclide production record from ^{36}Cl ratios in packrat middens is not without complications. Perhaps the most difficult of these factors is that we cannot determine fluxes of solute fallout from the middens, only relative concentrations. Because concentrations of ^{36}Cl in the middens are necessarily measured relative to stable chlorine, variations in $^{36}Cl/Cl$ ratios may be due to a variable ^{36}Cl flux or a variable stable chloride flux or a combination thereof. The two effects are not easily separable as an independent record of stable chloride flux is not available. While this limits our ability to determine the actual production record of ^{36}Cl, the record of $^{36}Cl/Cl$ ratio variation is ultimately most useful for

another purpose - that of an environmental tracer. Because chloride is conservative in the subsurface, the secular variation of $^{36}Cl/Cl$ ratio could provide an excellent tool for soil moisture and groundwater tracing. If the recharge system is advection-dominated and flow is essentially via piston displacement, a ^{36}Cl profile along a flow path should also preserve a record of production of the isotope. In such a system, solute deposition rates may be inferred based on chloride concentrations and groundwater fluxes estimated from groundwater dating or flow modeling. An estimate of the flux of ^{36}Cl is then independent of stable chloride flux variations. We have measured $^{36}Cl/Cl$ ratios in a vertical vadose zone profile in the desert near Socorro, New Mexico and from groundwater samples of the San Juan aquifer in northern New Mexico. These records of $^{36}Cl/Cl$ ratio variation and those developed by other investigators are discussed in regard to potential application of the ^{36}Cl production record as a groundwater tracer. The most significant pattern observed in the midden, soil moisture, and groundwater archives is that each displays a large decrease (50% - 100%) in $^{36}Cl/Cl$ ratios during the last 20 kyr, though the abruptness and magnitude of this change varies considerably between the different archives. The timing and direction of that shift are consistent with ^{14}C studies, which indicate that the atmospheric ^{14}C activity was at least 20% higher prior to about 12 ka. This, and the fact that archives from remote locations display this decrease, suggests that the change is not due simply to local changes in stable chloride flux. The observed variations may well be attributable to cosmogenic nuclide production rate variations, in which case either the available global paleointensity data are inaccurate or we need an improved model of the production and distribution of cosmogenic nuclides or the response of production to modulating effects such as variations in the intensity of the earth's magnetic field.

Acknowledgments

I am extremely thankful for the assistance and long-standing patience of my adviser, Dr. Fred Phillips. Many thanks also to the members of my committee who provided valuable criticism during my defense and in their review of this thesis. June Fabryka-Martin applied a particularly attentive eye to the manuscript and that effort is gratefully acknowledged. Thanks to my fellow students who have also enjoyed the struggle of learning, for many conversations about ^{36}Cl, atmospheric physics, hydrology and other fascinating scientific tomfoolery. I would not now be as painfully aware of the many flaws in this document without the continual growth that comes from such interaction.

For her many wily ways and means of distracting me from completing anything less significant than her entertainment and education, I thank my beautiful daughter, Sara. She did much to increase the time necessary to complete this work and has been a joy throughout. My parents also deserve more than a little thanks; without their having encouraged curiosity and resourcefulness at an early age, I might never have been able to find reward in focusing on such an arcane subject for such a long period of time. Finally, I could not have accomplished anything here without the unending support of my beloved wife, Catherine.

Table of Contents

List of Tables

List of Figures

Section One

Secular Variation of Cosmogenic Isotope Production

> *An investigation of this subject leads one into many fields of study, including geology and anthropology, astronomy, solar physics, nuclear and cosmic-ray physics, meteorology, climatology, oceanography, biology, chemistry, pedology, and history [Damon, Lerman, and Long 1978].*

Cosmogenic Nuclides and their Uses

The use of cosmogenically produced nuclides as dating tools in the earth sciences began about 1950, when Willard F. Libby and co-workers published the first results of radiocarbon measurements. Since then, cosmogenic nuclides have been applied to an increasing number of problems in the geosciences, particularly since the advent of accelerator mass spectrometry (AMS) in the early 1970's, which allows measurement of the rare isotopes in ratios commonly below background levels.

Cosmogenic radionuclides commonly used in the geosciences today include ^{14}C, ^{10}Be, ^{26}Al, ^{36}Cl, ^{3}He, and ^{21}Ne. Several of these isotopes are produced in the earth's stratosphere by interaction of atmospheric gases with galactic corpuscular radiation known as "cosmic rays." Production of many of these nuclides also occurs at the earth's surface by nuclear interactions between rock minerals and cosmic-rays. Many of the cosmogenic nuclides, as well as other radionuclides used in the geosciences such as tritium, have also been produced in abundance by anthropogenic activity and this has provided yet another tool for environmental researchers.

As with ^{14}C, radionuclides such as ^{36}Cl may be used for dating based on their decay rates and some assumed initial specific activity for the material being dated. The application of cosmogenic nuclides has been extended to dating of geomorphic surfaces based on the rate of buildup of in-situ produced cosmogenic isotopes such as ^{26}Al, ^{10}Be, and ^{36}Cl [Phillips, 1986; Lal, 1991; Nishizumi, 1986]. Concentrations of cosmogenic isotopes have been used to further our understanding of the nature of climate variations by providing a means of

deciphering the precipitation variations recorded in glacial ice [Raisbeck, 1990; Beer, 1994; Lal, 1987].

Secular Variation of Production - Previous Work

Variations in Atmospheric ^{14}C Content

Most students are introduced to the method of radiocarbon dating with the assumption that the initial activity of ^{14}C in organic carbon over time is essentially constant. The possibility that the production rate of ^{14}C has varied in time, however, was recognized by Libby and his co-workers at the time of publication of their first results. At that time Libby assumed that the exchange of carbon dioxide in the atmosphere with the bicarbonate of the oceans occurred quickly compared to other changes in the ocean-atmosphere system. He thus presumed that this very large combined carbon reservoir would respond to changes in the ^{14}C production rate "only extremely sluggishly" [Suess, 1986].

Production of ^{14}C in the upper atmosphere occurs when neutrons produced by cosmic rays interact with nitrogen. Although energetic solar flare particles produce ^{14}C and other cosmogenic nuclides, the long-term contribution due to this effect is estimated to be quite small compared with the galactic cosmic ray production [Raisbeck *et al.*, 1990]. Changes in the production rate of ^{14}C, as well as other cosmogenic nuclides such as ^{10}Be and ^{36}Cl, may thus result from changes in the flux of cosmic rays penetrating the earth's atmosphere. Such variations in the penetrating flux may arise due to variations in the flux of galactic cosmic radiation and/or solar radiation impinging on the earth's magnetosphere, to changes in the degree of shielding provided by the earth's magnetosphere, or to modulation by magnetic disturbances in the heliosphere associated with solar flares [Sternberg, 1992]. Variations in atmospheric ^{14}C activity may also be attributed to other factors. Several researchers have suggested that because the ocean contains over 40 times as much radioactive ^{14}C than is present in the atmosphere, substantial changes in atmospheric ^{14}C could arise from relatively small changes in oceanic ventilation associated with climatic changes [Bard *et al.*, 1990]. Stuiver *et al.*, [1991] describe the phenomenon as follows.

The atmosphere, biosphere, mixed layer ocean, and deep ocean all play a role in ^{14}C storage and exchange. The ^{14}C concentrations in these reservoirs is ultimately set by the ^{14}C production rate in the atmosphere and by the exchange rate between, and size of, the various reservoirs. For example, the waters in the most isolated part of the world oceans (water below 1500-m depth in the NW Pacific Ocean) have $^{14}C/^{12}C$ isotope ratios three-fourths that of the atmosphere (Stuiver et al., 1983). A change in upwelling rate of these ^{14}C deficient waters influences atmospheric ^{14}C content.

Cosmic and solar radiation consists primarily of highly energetic charged atomic particles. A significant fraction of these particles are deflected by the earth's magnetic field so that the flux of cosmic and solar rays is inversely proportional to the intensity of the earth's dipole field. The possibility of such a geomagnetic control on the production rate of ^{14}C was recognized as early as 1956, when Elsasser *et al.* [1956] commented on the implications of results of measurements of remanent magnetism of ancient bricks fired in France. These measurements indicated that the earth's magnetic field intensity had decreased by ~65% during the previous 2,000 years. Elsasser pointed out that if that intensity variation was global, then the "incident flux of cosmic rays and the rate of production of radio carbon must have increased during this period."

Dendrochronology provides a means of calibrating the ^{14}C dating technique by comparing ^{14}C ages for cellulose samples to actual ages based on ring counting and tree-ring correlation. This provides a very accurate means of evaluating changes in ^{14}C activity over time but is, of course, only applicable over that period of time for which dendrochronological records exist. As such records were extended, it became evident that there were significant discrepancies between those ages given by radiocarbon measurements and dendrochronology. By 1958, H. de Vries, had described variations in the back-calculated initial ^{14}C activities of wood from the 15th and 17th centuries [Suess, 1986]. Libby considered these minor variations to be within the experimental error of the measurements and suggested that errors may have been made in the dendrochronological dating used by DeVries. However, Suess had already shown that the exchange rate of carbon dioxide between atmosphere and ocean was not sufficiently fast to exclude the possibility of variations of a few percent, consistent with the results of DeVries [Suess, 1986].

Development of the dendrochronological calibration has continued and at present these records are well-constrained back approximately 9,700 years [Stuiver and Braziunas, 1991]. The overall pattern of this record shows a variation of ^{14}C activity of about 120%, with a dominant long-term periodicity of 10,000 - 12,000 years and shorter-term periods of about 2000 and 200 years [Sternberg, 1992]. The difference between the accepted modern ^{14}C activity and the measured paleo-activity is termed the atmospheric $\Delta^{14}C$, expressed as a per mille difference. It is widely accepted that the long-term variation observed in the $\Delta^{14}C$ record is due to modulation by the earth's varying geomagnetic field. Shorter term variations are generally believed to be related to solar cycles of magnetic flux. The latter control on cosmogenic production is not well understood but "appears to arise mainly because the interplanetary magnetic fields embedded in the outflowing solar wind are disturbed by shock waves associated with energetic solar flare events" [Raisbeck *et al.*, 1990].

Due, in part, to this interest in understanding the source of variations in ^{14}C, there has been a considerable effort to develop an accurate reconstruction of the secular variation of the earth's dipole moment. McElhinny and Senanayake [1982] produced one of the more commonly used reconstructions of paleointensity variations during the past ~10,000 years. A hypothetical cosmogenic production history can be calculated from that record using the production model given by Elsasser [1956]. Stuiver [1991] demonstrated that the fit between this calculated production history and the pattern of variation of atmospheric ^{14}C preserved in ~10,000 years of tree rings is quite good (Figure 1-1). While there are discrepancies between the calculated production curve and the data, the fit generally suggests a strong correlation between geomagnetic field strength and ^{14}C activity. It should be noted that this comparison assumes variations in ^{14}C activity are due only to changes in the production rate and also neglects the damping effects imposed on the ^{14}C response due to atmosphere-ocean exchange.

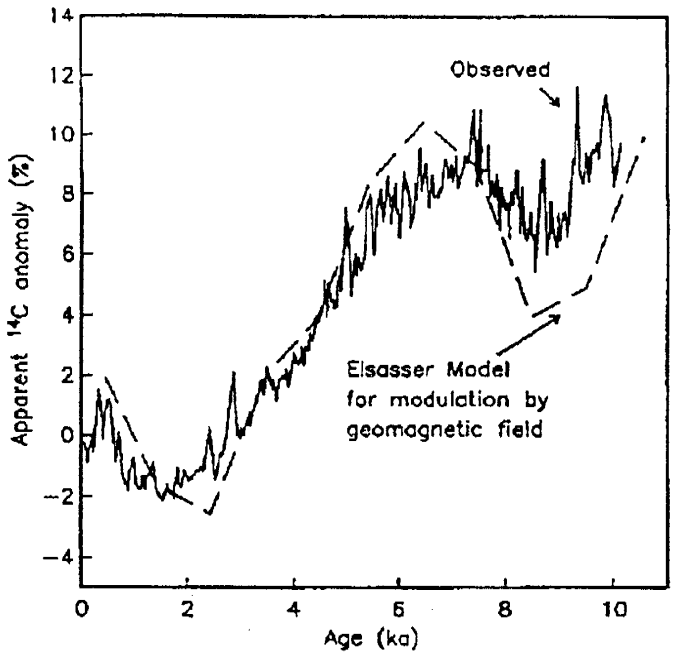

Figure 1-1. Comparison of observed variations in ^{14}C production by Stuiver et al. [1986] and those predicted by the dipole moment data compiled by McElhinny and Senanayake [1982] using the production model described by Elsasser [1956]. From Tauxe, 1993.

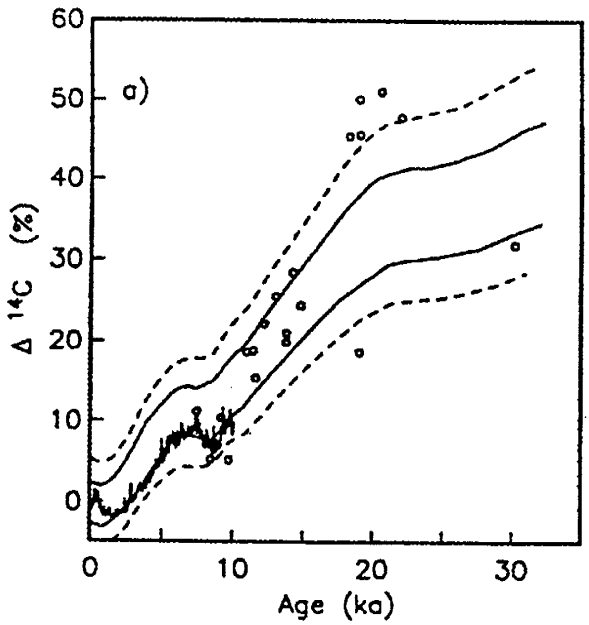

Figure 1-2. $\Delta^{14}C$ data plotted versus age. Solid and dashed lines assume uncertainties of 5% and 10%, respectively, on the dipole moment data of McElhinny and Senanayake [1982]. Circles are based on comparing U-Th ages with radiocarbon ages. Uncertainties have been left off for clarity. Redrawn by Tauxe [1993] from Bard et al. [1990].

The superiority of dendrochronology as a means of determining past ^{14}C activities stems from the fact that it essentially provides a "true" age for each sample. Similarly, if a set of carbon-containing samples can be dated with a more accurate chronometer that is independent of cosmic ray flux, then those samples can also be used to determine the secular variation history of ^{14}C activity. Bard *et al.* [1990] demonstrated that uranium-thorium dating can provide a more accurate chronometer than ^{14}C for at least the past ~30,000 years. Bard *et al.* obtained

^{14}C and U-Th ages for a set of corals raised off the island of Barbados and compared the ^{14}C activity calibration obtained from this method to that obtained by dendrochronology (Figure 1-2a). Sample ages ranged between approximately 6,000 and 28,000 years. Their calibration showed excellent agreement with the dendrochronological calibration and indicated that before 9,000 years BP the ^{14}C ages are systematically younger than the U-Th ages, with a maximum difference of ~3,500 years at ~20,000 years BP. To simulate the ^{14}C activity variation that would have resulted from variations in the earth's dipole field strength, Bard *et al.* used the paleo-dipole moment reconstruction of McElhinny and Senanayake [1982], ^{14}C production calculations of Lal [1988], and a simple box model of the ocean-atmosphere exchange process. They found "clear agreement" between the calculated signal and their U-Th/^{14}C comparison.

More recently, a nearly continuous high-resolution record of global paleointensity variations for the past 80 ka has been developed by Tric *et al.* [1992] (Figure 1-3). This dipole moment history is based on measurements of remanent magnetism in cored sediments from the Tyrhennian and Mediterranean seas. In 1991, Mazaud *et al.* examined the relationship between geomagnetic field strength and ^{14}C activity by comparing the results of dendrochronologically calibrated ^{14}C variations and measurements of corals by Bard *et al.* [1990] to a ^{14}C activity signal based on the Tric *et al.* [1992] record. Mazaud *et al.* also used Lal's [1988] production calculations and the two-box model of ocean-atmosphere exchange demonstrated by Houterman *et al.* (1973) to convert instantaneous production rates calculated from field intensity changes to ^{14}C activity (Figure 1-4). They noted a "remarkable agreement" between the $\Delta^{14}C$ signal and the calibrated ^{14}C ages of corals by U-Th dating, especially in the interval 7-15 ka. Data at and before 20 ka, however, are considerably more scattered and less well correlated to the predicted activity record. Tauxe *et al.* [1993] indicate that some of the discrepancies between the geomagnetic-based signal and the atmospheric ^{14}C record may be due to Mazaud *et al.*'s choice of virtual dipole moment (VDM) reconstruction, which emphasizes a trough in the Mediterranean record of paleointensity at approximately 30 ka. Tauxe *et al.* suggest that combining data from all the

sources of global paleointensity data "would yield results in much better agreement with the observed age anomalies."

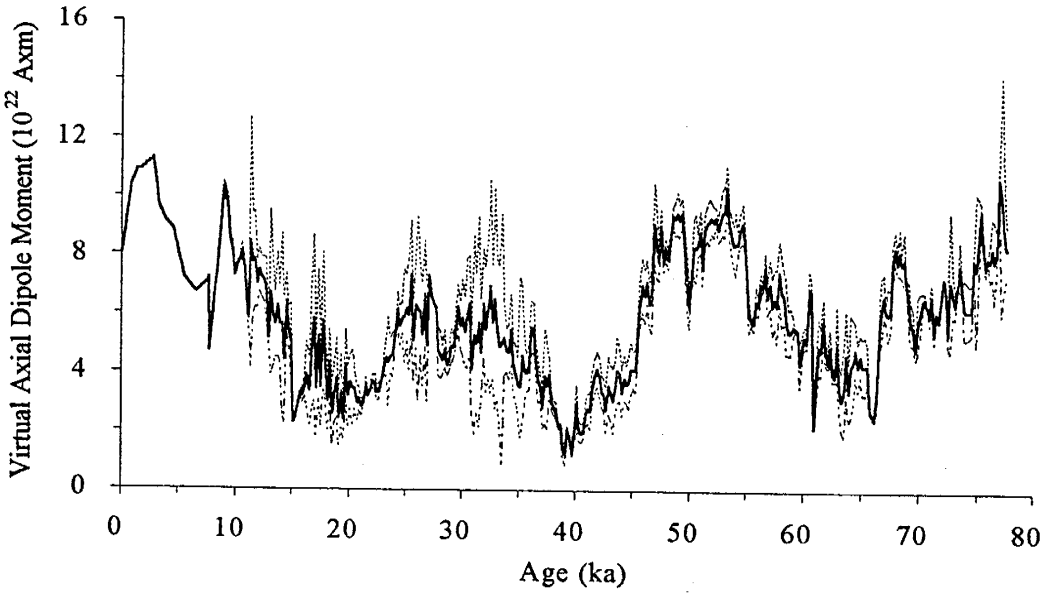

Figure 1-3. The field intensity record obtained by Tric et al.[1992]. Dotted lines correspond to uncertainties (+/- one standard deviation) in Virtual Axial Dipole Moment determinations. Solid line between 0 and 10 ka represents data of McElhinny and Senanayake [1982]. Present day value is approximately 8 x 10^{22} Axm.

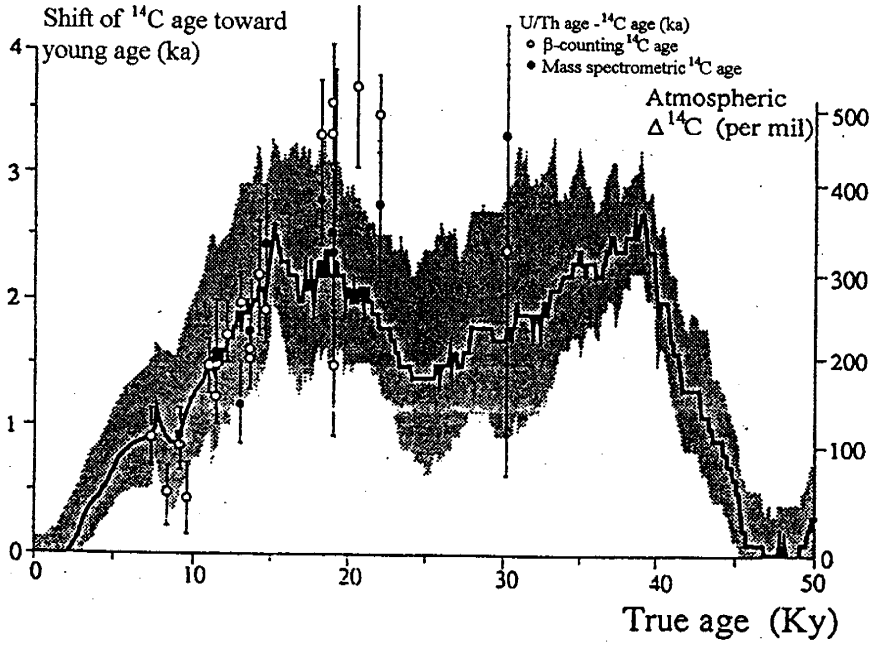

Figure 1-4. Calibration of the radiocarbon time scale, together with spot calibrations of ^{14}C ages obtained from U-Th ages determinations. Open symbols show ^{14}C ages determined by β-counting ^{14}C disintegrations. Closed symbols show ^{14}C ages determined by accelerator mass spectrometry. Shaded area corresponds to uncertainties of the magnetic intensities given by Tric et al.[1992]. From Mazaud et al., 1991.

The time-scale for the paleomagnetic record of Tric *et al.* is based primarily on correlation of oxygen isotope measurements of some of the cores with oxygen isotope records [Tric *et al.*, 1992]. Chronology of the marine isotope record is, in turn, based on the Paterne *et al.* [1988] tephrochronology for the past 60,000 years. This chronology was developed by correlation of marine ash-layers with terrestrial volcanic deposits dated by ^{14}C and/or K-Ar methods [Paterne *et al.*, 1988]. The most recent ash layers used in the tephrochronology (C-2 and C-4 in the notation of the authors) were radiocarbon dated at approximately 12.3 and 19.6 ka. Older ash layers, the youngest of which is dated at 33.5 ka, were dated using the K-Ar method which would not be affected by variations in the cosmic ray flux. The resultant time-scale is thus a hybrid of ^{14}C and "true" ages, which introduces some error in when comparing production histories based on this paleomagnetic record with archives of cosmogenic nuclide production.

While the Bard *et al.* [1990] data seem to provide a reliable record of the secular variation of atmospheric ^{14}C activity prior to about 9 ka, Stuiver and others have questioned its validity because the record disagrees with $^{14}C/^{12}C$ records from some varved lake sediments [Edwards *et al.*, 1993]. Recently, Edwards *et al.*, [1993] measured ^{14}C and ^{230}Th ages of fossil corals from the Huon Peninsula, Papua New Guinea. Radiocarbon ages of these samples ranged from 7 to 11 ka. Atmospheric $\Delta^{14}C$ for that period, based on the difference in ages produced by the two methods, are generally consistent with dendrochronological calibration data, the floating varve chronology of Becker and Trimborn [1991], and with the Barbados coral data for the period between 13 and 11 ka. The Huon Peninsula data (Figure 1-5) are of higher temporal resolution however, due to greater sample density and smaller analytical errors, and this record suggests that there was a large $\Delta^{14}C$ decrease within a short time interval (~1300 years) between about 13 and 10 ka. Edwards *et al.* note that this is the "most prominent feature in the record of atmospheric $^{14}C/^{12}C$ variations over the last 20,000 years and represents almost two-thirds of the total lowering of atmospheric $\Delta^{14}C$ between 19 and 11 ka." Because this prominent decrease in atmospheric $\Delta^{14}C$ activity does not correspond to a similarly dramatic increase in the magnetic record, Edwards *et al.* suggest that the changes in the earth's dipole moment may not have caused most of the

decrease in ^{14}C seen between 19 and 11 ka. They further note that the average rate of atmospheric $\Delta^{14}C$ decrease is similar to that which would occur due to decay if the ^{14}C production stopped completely. This also suggests that production variations due to geomagnetic changes are not the only, nor perhaps even the primary, control on atmospheric ^{14}C activity for that period.

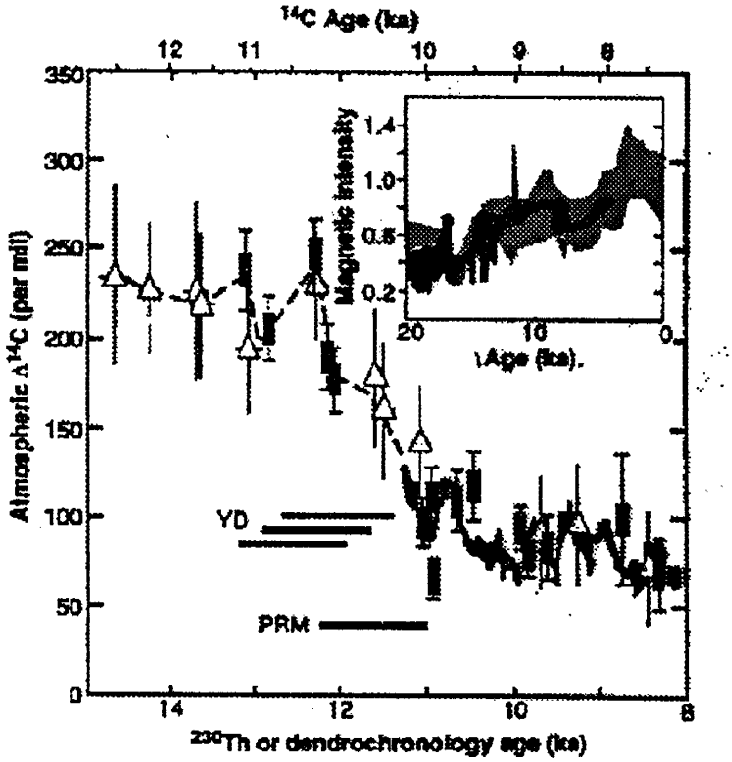

Figure 1-5. Atmospheric $\Delta^{14}C$ between 15 and 8 ka. Inset shows a portion of the Tric et al. [1992] paleointensity record of the geomagnetic dipole. Time is in ^{230}Th years on the lower x axis and in conventional ^{14}C years on the upper x axis. Solid boxes are Papua New Guinea data; triangles are Barbados data. The stippled curve is based on dendrochronology. The dashed curve is a spline drawn through the coral data, which are consistent with each other and generally consistent with the dendrochronology. The bars labeled YD represent the timing of the Younger Dryas on the basis of ice-core data: upper bar, latest possible timing; middle bar, best estimate; and lower bar, earliest possible timing. The other bar represents the timing of the period of reduced melting (PRM) from the Huon Peninsula core. The Papua New Guinea data show a rapid decrease in $\Delta^{14}C$ between 12.3 and 11.0 ka, which is the most prominent feature yet identified in records of atmospheric $\Delta^{14}C$ and is synchronous with the PRM. This decrease represents almost two-thirds of the total decrease in $\Delta^{14}C$ between 19 and 11 ka. From Edwards et al., 1993.

The Huon Peninsula coral data also provide information concerning sea level changes. That record apparently indicates that the large decrease in ^{14}C seen between 13 and 10 ka was synchronous with a period of reduced melting, suggesting that the decrease was related to global melt rates. Because of this correlation, Edwards *et al.* hypothesize that the reduced

melting rate during that period is associated with an increase in oceanic ventilation and thus a decrease in atmospheric ^{14}C activity. The authors thus suggest that the observed pattern of $\Delta^{14}C$ variation between 13 and 10 ka is due to a change in the partitioning of ^{14}C between the atmosphere and the ocean that was superimposed on the gradual lowering of average $\Delta^{14}C$ caused by the increasing intensity of the Earth's magnetic dipole field strength between 20 and 10 ka.

Other Archives of Cosmogenic Nuclide Variation

While dendrochronology provides the most accurate means of determining actual ^{14}C activity over time, that record does not reflect the actual instantaneous production of the isotope. This is because ocean-atmosphere carbon exchange and rapid terrestrial uptake and release of atmospheric carbon filter the production signal, damping high-frequency oscillations in the production signal and preserving to some extent earlier production variations [Mazaud, 1991]. It is therefore useful to determine the paleo-production record using a cosmogenic isotope that better reflects the instantaneous production record. ^{10}Be and ^{36}Cl are suitable radionuclides because they are both rapidly removed from the atmosphere in solid rather than gaseous form and are not involved in complicating exchange processes as is ^{14}C. In considering what variations in terrestrial archives of either of these nuclides implies for the radiocarbon time-scale, we must consider the relative sensitivity of each to the relevant modulating mechanisms. Blinov [1988] calculated the global production rates of each of these nuclides using a hadronic cascade model to produce the following plots of predicted relative production variations due to solar and geomagnetic modulation (Figure 1-6 and Figure 1-7).

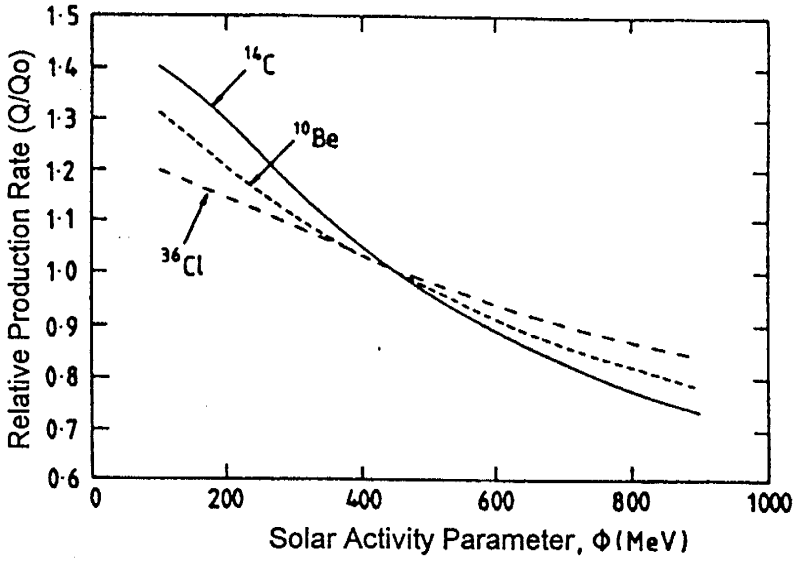

Figure 1-6. The dependence of the relative cosmogenic isotope (for ^{14}C, ^{10}Be, and ^{36}Cl) production rate (Q/Qo) on the level of solar activity. Q(ϕ=450 MeV) = Qo. From Blinov, 1988.

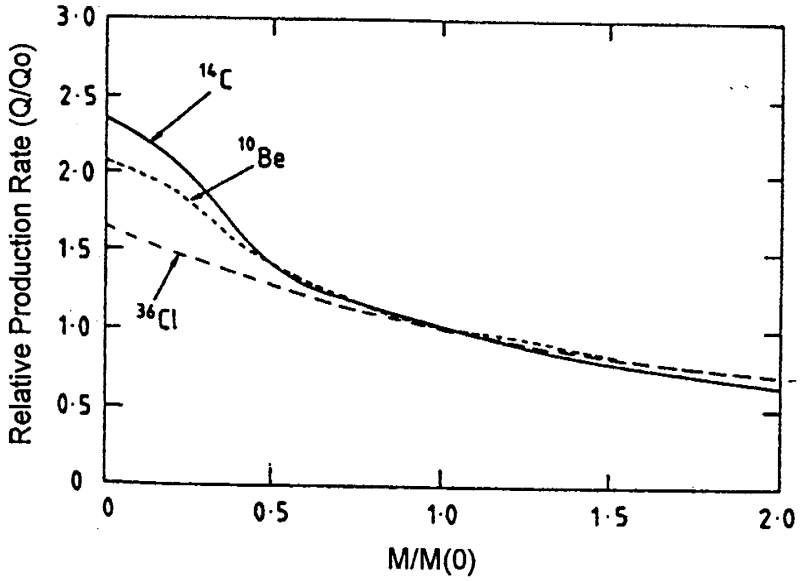

Figure 1-7. The dependence of the relative cosmogenic isotope (for ^{14}C, ^{10}Be, and ^{36}Cl) production rate (Q/Qo) on the geomagnetic moment variations. Q(M/Mo=1) = Qo. From Blinov, 1988.

Due to the orientation of magnetic field lines, cosmogenic production is highly latitude dependent. About two-thirds of the latitude-dependent production of ^{10}Be and ^{36}Cl occurs in the stratosphere, where the residence of aerosols is sufficient to ensure complete mixing throughout that layer [Beer et al., 1987]. Annual mixing of the stratosphere and troposphere occurs at the mid-latitudes, so that the amount of stratosphere-derived fallout

decreases with distance from those latitudes. About one-third of the production of ^{10}Be and ^{36}Cl occurs in the troposphere where it is rapidly removed by precipitation and/or dry fallout. The flux of troposphere-derived ^{10}Be and ^{36}Cl is thus more strongly a function of the latitude-dependent local production rate, increasing with distance from the equator. The location of a terrestrial archive, sampling resolution and other factors thus have a profound effect on the sensitivity of the record to the various modulating mechanisms. These and other conditions, which may introduce variations not directly related to production rate variations, are equally important in the interpretation of the concentration variations seen in terrestrial archives of the various cosmogenic nuclides.

^{10}Be Records

^{10}Be is produced by cosmic ray interaction with oxygen and nitrogen and has a residence time in the upper atmosphere of 1.5 years or less [Beer, 1990]. Excellent temporal records of ^{10}Be concentrations, of varying length and resolution, have been obtained from glacial ice cores in Greenland and Antarctica. A 906-meter core at Dome C, Antarctica, provides a record of ^{10}Be concentration extending back approximately 30 ka [Raisbeck *et al.*, 1981] and highly detailed ^{10}Be records from Byrd station, Antarctica, and Camp Century, Greenland, extend back approximately 10 ka (Figure 1-8) [Beer *et al.*, 1987]. Raisbeck *et al.* [1987] later reported ^{10}Be concentrations in 92 samples from an approximately 2,000-meter ice core from Vostok, Antarctica. Adopting the time-scale of Lorius *et al.* [1985], these data provide an approximately 150-ka record of ^{10}Be concentration variations (Figure 1-9).

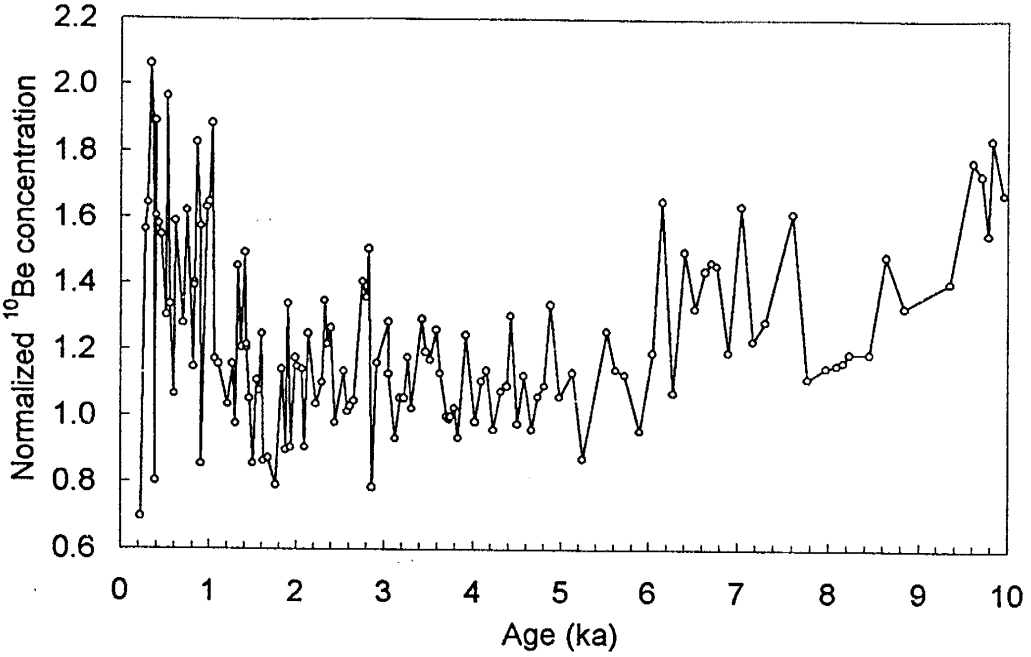

Figure 1-8. ^{10}Be data from Camp Century ice core from Beer et al.,1988. Sample ^{10}Be concentration (normalized to estimated present concentration) vs. sample age. Note that sample thicknesses are constant while dating resolution decreases with age. Redrawn from Beer et al., 1988.

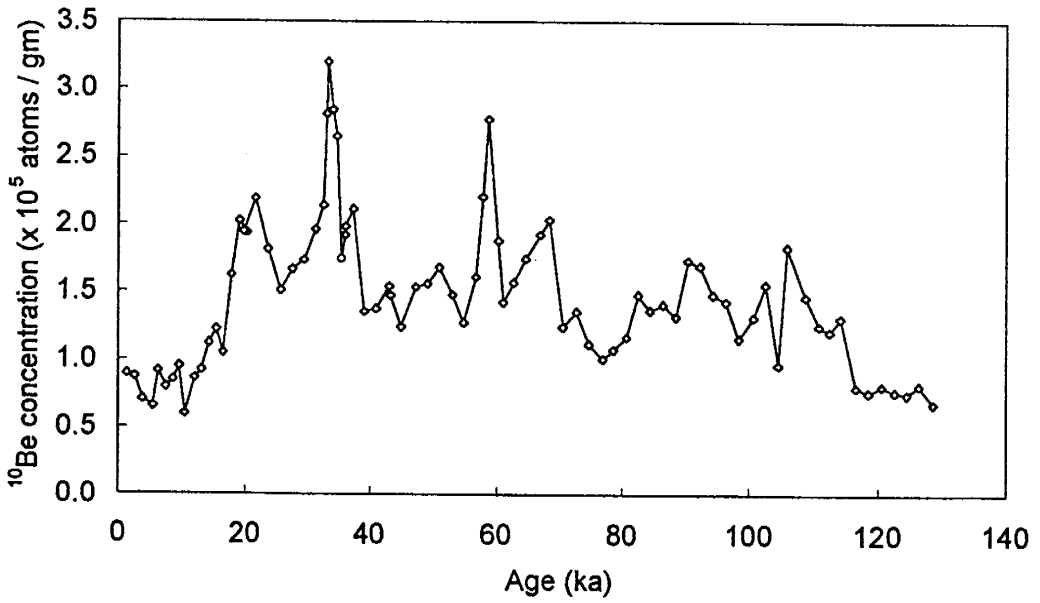

Figure 1-9. ^{10}Be concentration as a function of sample age in the Vostok ice core. Small corrections (<7%) have been made using the time-scale adopted by Lorius et al. Redrawn from Raisbeck et al., 1987.

Concentration variations observed in these records have been attributed to several mechanisms which can alter the concentration of ^{10}Be in polar ice. These include variations in the amount of precipitation with which the Be is deposited, variations in the atmospheric distribution of ^{10}Be, production rate variations due to changes in solar and/or cosmic ray flux incident to the earth's magnetosphere, and variations in the modulation of the incident solar and cosmic rays by the solar wind and by the earth's magnetic field. As seen in Figure 1-6 and Figure 1-7, the sensitivity of the ^{10}Be production rate to changes in solar activity and geomagnetic field strength is quite similar to that of ^{14}C.

A prominent feature of the longest record of ^{10}Be concentration (Vostok, Figure 1-9) is a dramatic decrease in ^{10}Be concentration between approximately 20 ka and 10 ka This and the most of the other main features of that profile are well-correlated with the oxygen isotope record of temperature from the same core, indicating that those large-scale ^{10}Be concentration variations are primarily due to variable precipitation rather than to variable cosmogenic production. It is generally held that precipitation rates at the Antarctic sites are controlled primarily by the water vapor pressure, and thus temperature, above the tropospheric inversion layer [Raisbeck *et al.*, 1987]. Assuming a fixed relationship between δD and accumulation rate, Raisbeck *et al.* [1992] calculated a history of ^{10}Be deposition rates from ^{10}Be concentration data in the Vostok core (Figure 1-10).

Large concentration decreases near the end of the last glacial maximum are also evident in ice cores from Dome C, Antarctica [Raisbeck *et al.*, 1987] and Camp Century, Greenland [Beer *et al.*, 1988]. These changes, again, are generally attributed to a significant increase in precipitation that presumably occurred with the onset of warmer climatic conditions. The increase in temperature that would have caused such an increase in precipitation is plainly seen in the $\delta^{18}O$ records of both the Greenland and Antarctic sites [Raisbeck *et al.*, 1987; Beer *et al.*, 1988].

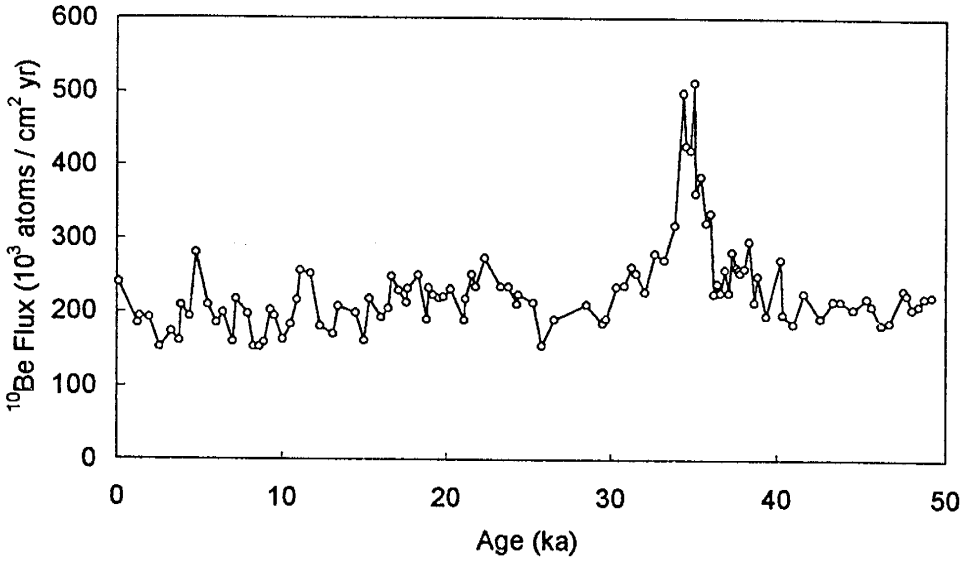

Figure 1-10. ^{10}Be flux at Vostok, Antarctica as a function of time based on the timescale of Jouzel et al. [1989]. Redrawn from Raisbeck et al., 1992.

The Vostok record of ^{10}Be concentration includes two prominent peaks, at approximately 35 ka and 60 ka before present, which appear to reflect actual variations in the flux of ^{10}Be rather than precipitation rate variations (Figure 1-9). These peaks, each representing a period of approximately 1,000 years, are not well correlated with the $\delta^{18}O$ record and the depths containing the peaks do not show evidence, such as an increases in concentrations of other aerosol components, of a significant decrease in precipitation rate. Raisbeck *et al.* [1985] have identified the 35 ka peak in the Dome C record and Beer [1992] indicates that the same peak is clearly present in the Byrd station record and appears to be present in the Camp Century record as well. Reeh *et al.* [1991] applied a different time-scale to the Camp Century core and also concluded that the 60 ka peak is evident in that core.

Several hypotheses have been advanced as the cause for these anomalous high periods of ^{10}Be concentration. Although the peaks in deposition rate could have been caused by changes in atmospheric circulation patterns, Raisbeck *et al.* [1985] contend that the increases were most likely due to increased production of ^{10}Be in the atmosphere. Sonett *et al.* [1987] suggested that the concentration peaks may be associated with ancient supernovae, which would have increased the atmospheric cosmic ray flux by cosmic ray acceleration in propagating interstellar shock waves enveloping the heliosphere. More recently Beer *et al.*

[1992] compared the Antarctic and Greenland records and examined correlations between ^{10}Be, $\delta^{18}O$, and SO_4 concentrations in the Camp Century core. Beer *et al.* [1992] also concluded that the most likely cause for the ^{10}Be peak at ~35 ka is an increase in production rate. As Beer *et al.* point out, if this is the case, the effect is apparently global and should also be reflected in the secular variation of other cosmogenic nuclides such as ^{14}C and ^{36}Cl.

High frequency variations in the ^{10}Be concentration record are well-preserved in the polar ice records. Highly detailed records of ^{10}Be concentration variations in the Milcent ice core from Greenland, Raisbeck *et al.*, 1990; Beer *et al.*, 1990; Oeschger and Beer, 1990] appear to record the 11-yr. Schwabe cycle as well as ~200-year and longer periodicities. Based on calculations of the magnitude of production variations expected to result from solar and geomagnetic modulation, Lal [1987] argued that short-term variations in the Greenland and Antarctic records are likely due to a combination of changes in precipitation rates and stratosphere-troposphere exchange and mixing. Lal stresses that while the observed patterns exhibit good inverse correlation with certain solar patterns, the correlation is due to the climatic effects of a varying solar activity rather than solar modulation of cosmogenic production. Beer *et al.* [1988, 1994a, 1994b] however argue that the good correlation of short-term ^{10}Be variations with short-term variations in atmospheric ^{14}C activity is convincing evidence that the ^{10}Be variations do reflect solar modulation of production. Raisbeck *et al.* [1990] also conclude that the "remarkable correlation with ^{14}C ... as well as a recent comparison of ^{10}Be from Arctic and Antarctic ice cores argue strongly in favor of a production rate origin for the main 100-200-year structure in the ^{10}Be record". Moreover, Beer [personal communication, March 31, 1995] indicates that recent calculations by Reedy suggest that the observed production rate variations are indeed within expected limits based on revised calculations of production modulation by the solar wind.

Beer *et al.* [1988], Oeschger and Beer [1990] and Raisbeck *et al.* [1992] have also compared the long-term variations in the polar ^{10}Be records in order to determine whether these records showed evidence of geomagnetic control. They generally concluded that while the ^{10}Be record does not show evidence of a geomagnetic field control on production, this is likely due to the high-latitude location of the polar records. At high latitudes, fallout from

locally produced cosmogenic production is a much larger fraction of the total deposition than at low latitudes [Lal, 1987]. At the poles there is very little modulation of the cosmic ray flux by the geomagnetic field so that field strength variations have a negligible effect on the local production rate of cosmogenic nuclides.

Several investigators have attempted to model atmospheric $\Delta^{14}C$ variations based on those ^{10}Be records, such as the Camp Century data of Beer et al., that are believed to reflect actual production rate variations. These attempts have met with varying success. In general, the ^{10}Be record does not appear to explain the large $\Delta^{14}C$ decrease seen in the Barbados and Huon Peninsula coral records, even if the peak in ^{10}Be concentration seen at 35 ka lasts for several thousand years. Raisbeck *et al.* [1992] conclude that the ^{14}C discrepancy cannot be related to the ^{10}Be peak observed in Antarctic ice ~35 ka B.P. unless the ^{10}Be peak is due to some mechanism having a much larger $^{14}C/^{10}Be$ production ratio than that of present galactic cosmic ray particles.

There have been several attempts to examine archives of ^{10}Be which may better reflect production rate modulation by geomagnetic variations. Lao *et al.* [1992] examined ^{10}Be accumulation rates in Pacific sediments believed to reflect average global production rates of that nuclide. A comparison of deposition rates between the Holocene and the last glacial period indicated that the production rate of ^{10}Be must have been at least 25% higher during the glacial maximum period.

^{36}Cl Records

Several researchers have examined temporal records of ^{36}Cl as a means of determining the production variation of cosmogenic nuclides. Priller *et al.* [1990] measured the $^{36}Cl/Cl$ ratio in a series of old wines from Germany and compared the results with records of sunspot activity. They concluded that "a correlation between the sun spot number and the $^{36}Cl/Cl$ ratios in the samples could not be confirmed."

Both ^{36}Cl and ^{10}Be concentration variations in the Dye 3 core from Camp Century have been reported for a period including the Maunder minimum of solar activity (~1645 to

1700) [Elmore et al., 1987; Suter et al., 1987]. Concentrations of both ^{36}Cl and ^{10}Be are significantly higher during that period, consistent with the higher $\Delta^{14}C$ measured via dendrochronology [Elmore et al., 1987]. This suggests that the polar record preserves production rate variations of both nuclides caused by a varying solar wind. In both studies, however, the $^{10}Be/^{36}Cl$ ratios of the samples fluctuated by a factor of up to 5, considerably greater than the variation observed for either nuclide. Production calculations indicate that the ratio should be relatively constant for the two nuclides (<10%) [Suter et al., 1987]. Elmore *et al.* hypothesized that the unexpected variation may be due to climatic effects such as "changes in air circulation between the stratosphere and the troposphere in the polar region in combination with chemical processes that affect aerosol chlorine differently from aerosol beryllium." Suter *et al.* [1987] concluded that the unexpected variations in the $^{10}Be/^{36}Cl$ ratio were likely due to differences in atmospheric transport effects, in which case the $^{10}Be/^{36}Cl$ ratio may turn out to be "a useful tool for studying past atmospheric transport and mixing processes."

Suter et al. [1987] also report concentrations of both ^{36}Cl and ^{10}Be across the transition from the Wisconsin to the Holocene (Figure 1-11). Concentrations of both nuclides decrease by a factor of about two during that period. As discussed previously, the decrease in ^{10}Be concentration across that transition is generally attributed to a change in precipitation rate.

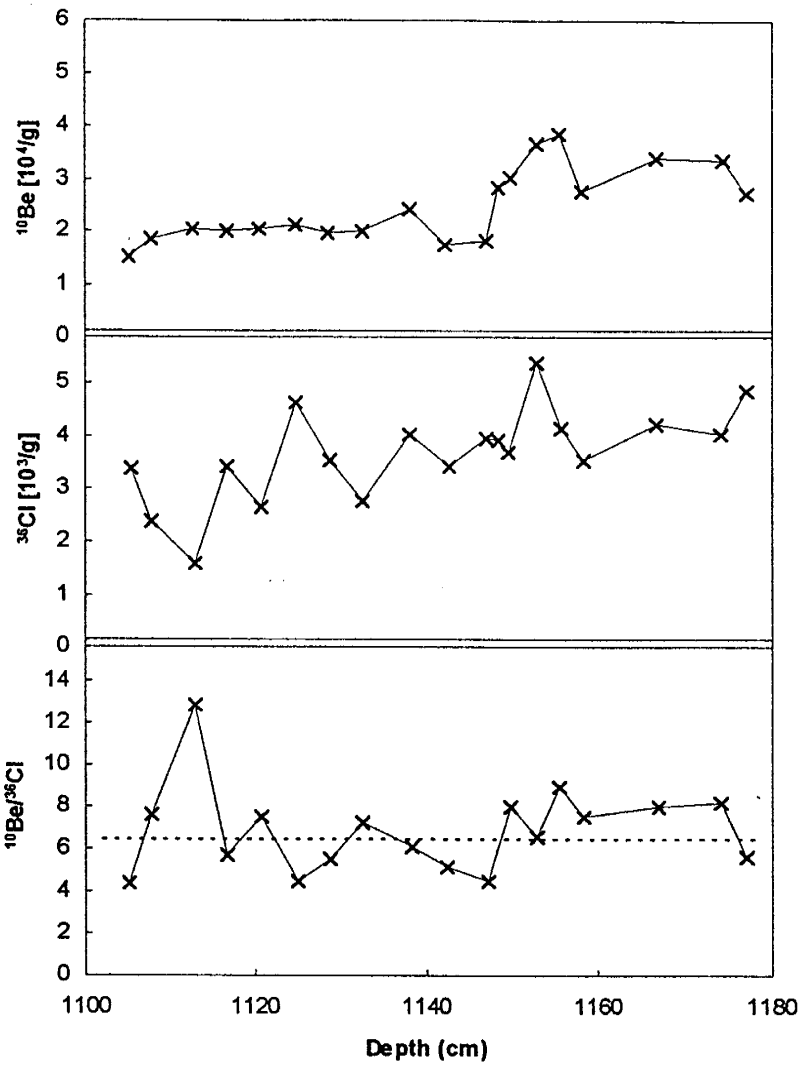

Figure 1-11. Profiles of ^{10}Be, ^{36}Cl and ^{10}Be/^{36}Cl from Camp Century from the depth interval of 1100 - 1180 m. This interval corresponds to the end of the transition between glacial and post glacial times. The mean value of the ^{10}Be/^{36}Cl ratio is about 6.5 (dashed line). Redrawn from Suter et al., 1987.

Focus of Present Study

In this study, I report the results of an examination of the ^{36}Cl production record as recorded in chloride contained in ancient packrat middens. I further discuss the potential use of the production signal as a groundwater and soil-moisture tracer and examine temporal records of ^{36}Cl preserved in (1) a vertical vadose zone profile from desert near Socorro, New Mexico and (2) radiocarbon-dated groundwater samples from the San Juan aquifer in northern New Mexico. Other temporal records of ^{36}Cl in soil moisture and groundwater samples, provided by other investigators, are also examined in this light.

While reconstruction of the record of secular variation of cosmogenic isotope production clearly has benefits in refining the ^{14}C dating method, the secular variation record in itself may also prove a useful environmental tracer. Environmental tracers are substances that have been introduced into the environment by anthropogenic or natural means and whose movement through the medium of interest is readily detectable. Both tritium and ^{36}Cl were produced and globally distributed as a result of nuclear weapons testing between ~1950 and 1964. These radio-isotopes were gradually removed from the atmosphere by precipitation and dry fallout and injected into the subsurface environment by natural recharge processes. The fallout pattern and time of injection of these isotopes at a given location can be determined by studies of atmospheric transport processes and records of fallout at other sites. The bomb "pulse" of these isotopes into the environment thus serves as a tracer that, when identified in the subsurface, can be used to estimate transport rates within the subsurface. Similar use can be made of the secular production record of cosmogenic isotopes if the variation is significantly stronger than the background noise due to other sources of variation. In the case of ^{36}Cl, this would also provide a very long-term tracer if the signal can be directly related to a driving force for which an independent record of variation is available. As a basis for each of the following three discussions, I therefore review here ^{36}Cl production mechanisms, mixing of ^{36}Cl with stable chloride in the atmosphere, and removal of ^{36}Cl and Cl from the atmosphere.

Production of ^{36}Cl, Mechanisms and Distribution

Cosmic Ray Interaction with the Atmosphere

Both solar and cosmic radiation contribute to the atmospheric production of cosmogenic isotopes. The primary component of this radiation is highly charged protons. The flux of cosmic rays has been estimated as ~1 particle cm^{-2} s^{-1} and approximately 90% of that flux consists of protons [Pal, 1967]. Cosmic ray energies are typically 10 - 100 GeV. Solar radiation also consists predominantly of protons, but with lower energies, typically about 100 MeV. While the actual flux of solar radiation is much greater (typically ~10^3 particles cm^{-2} s^{-1}), averaged over time, most of the particles responsible for nuclear reactions in the atmosphere come from outside of the solar system [Lal & Peters, 1967]. Protons which

penetrate the earth's magnetosphere are scattered, both elastically and inelastically, upon impact with the earth's atmosphere. In inelastic scattering, nuclear reactions transfer some of the energy of the incident proton to one or more neutrons. These neutrons are ejected from the affected nucleus with sufficient energy to cause several other atomic transmutations which also release neutrons. The overall result is such that a "cascade" of neutrons is produced by the impact of each proton with the atmosphere.

^{36}Cl Production, Mechanisms and Modulating Effects

Chlorine-36 is produced in the earth's atmosphere principally by spallation of argon-40 through interaction with cosmic ray primary particles (protons) or secondary particles (neutrons). While other atmospheric nuclear reactions also produce ^{36}Cl, those production rates are negligible by comparison. Such reactions include neutron activation of ^{36}Ar and neutron capture by ^{35}Cl. Neutron activation of ^{36}Ar is minor because of the much greater abundance and capture cross-section of ^{14}N [R.Reedy, pers. comm., 1/26/96] while neutron capture of ^{35}Cl is probably negligible because of the short residence time of Cl in the atmosphere.

Cosmogenic nuclide production occurs throughout the atmosphere, with approximately 60% of the total occurring in the stratosphere and 40% in the troposphere [Bentley *et al.*, 1986]. The mean global production rate of ^{36}Cl has been calculated by several investigators. Most recently Blinov [1989] corroborated earlier calculations of Oeschger *et al.* (1969) estimating the mean production rate due to spallation of ^{40}Ar as ~20 atoms m^{-2} sec^{-1} [Dowgiallo *et al.*, 1990]. Production rates are, however, modulated by solar and geomagnetic effects so that the rate is not constant over time.

Modulation of Production by the Earth's Magnetic Field

Because of their charge, a significant fraction of the incident cosmic and solar protons is deflected by the earth's magnetic field. Deflection occurs at the edges of the magnetosphere, several earth radii away from the Earth's surface. Therefore only changes of the earth's virtual dipole moment (VDM), not local field intensity variations, will effectively modulate the production rate of cosmogenic isotopes [Bard et al., 1990].

Variations in the production rate of ^{36}Cl and the other cosmogenic isotopes may therefore result from variations of the cosmic ray flux reaching the earth's magnetosphere or by variations in the degree of shielding provided by the earth's magnetosphere. While this shielding is primarily a function of the intensity of the earth's dipole moment, the solar wind also attenuates the cosmic radiation flux. Figure 1-12 illustrates the effect of variations in the intensity of the earth's dipole field on the penetration of the earth's atmosphere by solar and cosmic rays.

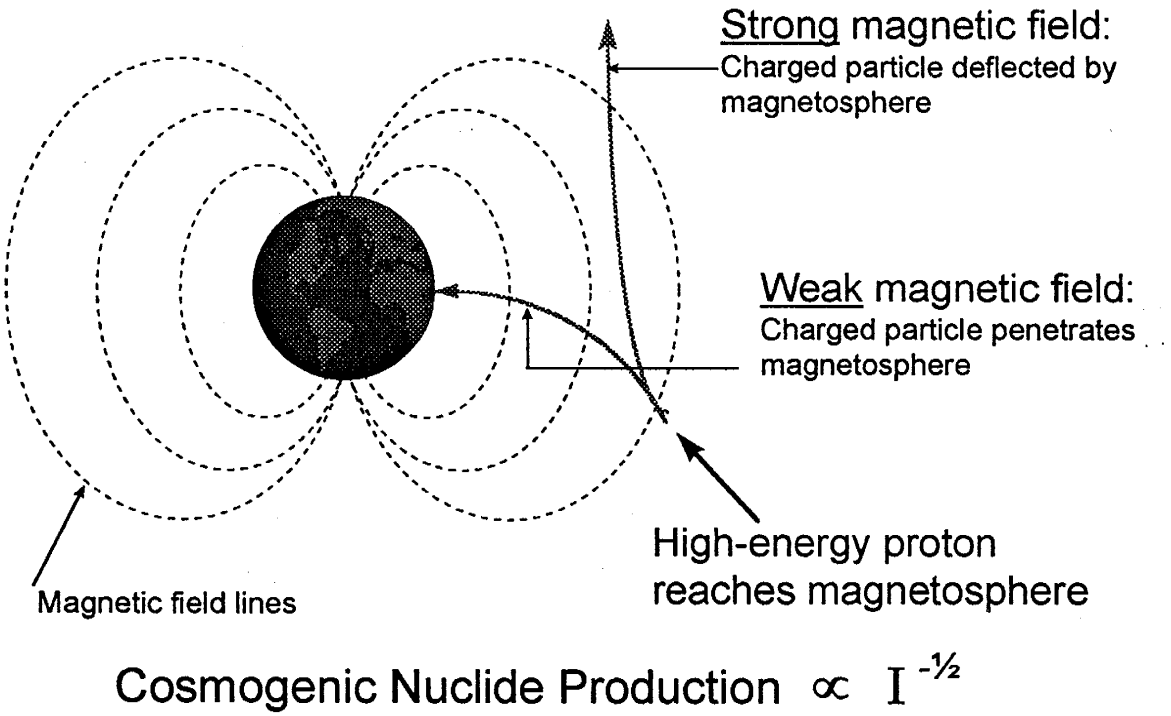

Figure 1-12. Effect of variations of dipole moment (I) on penetration of solar and cosmic radiation.

The integrated global atmospheric production rates of several cosmogenic isotopes, as a function of magnetic field intensity, have been calculated by Blinov *et al.* [1989]. Figure 1-7 shows the expected production rate of ^{36}Cl, as well as ^{10}Be and ^{14}C, as a function of relative magnetic field strength. Blinov *et al.* indicate that in the range of p = 0.5 to 1.5, the production function for ^{36}Cl is approximately

$$Rate = p^{0.36}$$

where p is the ratio of the magnetic field intensity at some time t to the current field strength {i.e. p = m/m(0)}.

Modulation of Production by the Solar Wind

As with ^{10}Be, ^{36}Cl production in the atmosphere should be modulated by the solar wind. Solar modulation is strongly cyclical with periods of ~2000, 200 and 11 years. If both the period averaged by a given archive of ^{36}Cl and the frequency of sampling is sufficiently small, any or all of these periodicities may be recorded. The magnitude of solar modulation effects for ^{36}Cl production may be estimated from variations observed in ^{10}Be archives because the sensitivity of each of these nuclides to cosmic ray intensity variations is similar (see Figure 1-6). Beer *et al.* [1988] report that ^{10}Be fluctuations with a periodicity of ~200 years have a peak to peak amplitude of about 40% in the Camp Century record. Oeschger and Beer [1990] indicate that ^{10}Be production variations associated with the 11-year sunspot cycle are on the order of 20 - 30%.

Removal of ^{36}Cl from the Atmosphere

Trace constituents remain in the stratosphere only a few years before entering the troposphere via vertical mixing [Newell, 1971]. Chlorine-36 produced in the stratosphere is then mixed with troposphere-derived ^{36}Cl and stable Cl in the troposphere and rapidly removed by precipitation or as dry fallout. The mean residence time of small particles in the troposphere is about 30 days or less [Newell, 1971, Turekian, 1977]. The ratio of ^{36}Cl to stable chlorine (i.e. the $^{36}Cl/Cl$ ratio) in precipitation thus depends on the production rate of the radionuclide in the atmosphere, the degree and pattern of mixing between the stratosphere and troposphere, and the amount of stable chloride present in the troposphere.

$^{36}Cl/Cl$ Variations due to Changes in Flux of Stable Chloride

Examination of ^{36}Cl concentrations in any geologic archive generally rely on measurement of the $^{36}Cl/Cl$ ratio. If the ^{36}Cl deposition rate can be determined independent of the chloride deposition rate, then ^{36}Cl flux variations can be examined directly. In a discussion of the ^{36}Cl variations in packrat middens, we are constrained to consider $^{36}Cl/Cl$ ratios; the

rate of meteoric deposition of chloride or ^{36}Cl cannot be determined from the midden deposits. In Section Three, I discuss $^{36}Cl/Cl$ variations measured in a soil profile. There again, we are constrained to examination of isotopic ratios because the ages of the soil samples are estimated from the amount of chloride present in the soil. In Section Four, I discuss $^{36}Cl/Cl$ ratios in groundwater. There, the flux of ^{36}Cl and Cl can be examined independently to some extent because the groundwater ages are determined from ^{14}C measurements.

Because we are so often constrained to examination of $^{36}Cl/Cl$ variations, we must consider factors other than cosmogenic production rate variations which can alter the $^{36}Cl/Cl$ ratio of precipitation and recharge. Principal among these factors is potential variation in the flux of stable chloride. The following discussion thus concerns the sources of stable chloride in the atmosphere and the distribution of that chloride in fallout.

Stable Chloride Flux

Atmospheric chlorine is present adsorbed to particulate matter, in solution as chloride and in gaseous form as HCl or Cl_2. These forms are removed from the atmosphere by precipitation and dry. A considerable amount of data is available regarding concentrations of Cl in precipitation and this is generally regarded as the dominant form of deposition. In contrast, few data have been collected regarding rates of dry deposition and conclusions based on existing information are often contradictory. Feth [1981] provides the following summary.

> *The literature is somewhat contradictory with reference to the influence of dry fallout on the Cl concentrations in continental water, partly, at least, because of varying methods of defining and sampling "precipitation." Speaking of the inland, arid parts of Israel, Yaalon (1961, p. 13) said "the ... precipitated salt will be mainly by deposition of dry salts." Junge and Gustafson (1957, p. 164) reported tests at Boston, Mass., where "two collectors were exposed side by side; one open to precipitation only, and the other open continuously. On the average, the open gauge collected twenty-five percent more Cl as a result of the dry fallout." Koyama and others (1965, p. 3) calculated that the increment from dry fallout was 2.3 times the increment from precipitation excluding dry fallout for the islands of Japan, but Tsunogai (1975) estimated that only 20 percent of Cl brought landward from the sea was deposited as dry fallout.*

Similar uncertainty is associated with the importance of gaseous contributions to the Cl in precipitation and the source of the gaseous forms is likewise imperfectly understood.

> *Its origin has variously been ascribed to reaction of ozone with sea-salt particles in the atmosphere and to reaction of NaCl and H_2SO_4. Valach (1967) took issue with those hypotheses on the basis of calculations that led him to conclude that such reactions would yield only 5-50 percent of the gaseous chlorine observed. He suggested that volcanic emissions probably supply the rest. Limited studies suggest that the quantities of gaseous chlorine and of Cl in the atmosphere are comparable in magnitude. Undoubtedly some of the Cl in precipitation is from the gaseous source, whatever its origin. [Feth, 1981]*

Some of the difficulty involved in understanding the nature of the chloride cycle is suggested by available studies of the chloride balance in drainage basins. It is generally assumed that virtually all of the chloride that is returned to the sea by rivers comes from rainfall or other forms of precipitation, i.e. that it is recycled chloride from the ocean. This assumption is not entirely supported by the available data however. Hem [1985] notes that relatively few investigations "have included enough actual measurements of quantities of chloride brought into a drainage basin in rainfall as well as quantities carried out in streamflow to ascertain how closely this assumption can be verified. In all studies to date in the United States, where enough data have been obtained to permit reliable computations to be made, the amount of chloride brought in by rainfall seems inadequate to explain the amounts appearing in runoff." In one such study, Van Denburgh and Feth considered the Cl balance in 11 river basins of the Western United States:

> *The study indicated that tonnages of Cl brought by rain and snow into the 11 river basins made up from about 2 to nearly 20 percent of the Cl tonnages removed from those basins in an average year. The Pecos River, with its abundant near-surface deposits of halite but low precipitation and runoff, yielded an estimate of 1.6 percent: the Willamette and Rogue River basins, underlain by much less soluble and less chlorine-rich rocks but near the ocean, yielded estimates of 16 percent and 17 percent respectively. The average for the 11 river basins was 8.5 percent. [Feth, 1981]*

Hem [1985] references several other such studies and concludes that "the widely published assumption that chloride loads of rivers represent recycled oceanic chloride is not entirely vitiated by individual examples such as those mentioned, but these examples certainly imply that not all oceanic chloride reaches streams by way of rainfall." In his review of chloride in

natural continental water, Feth [1981] likewise concludes that "whatever the worldwide average percentage of airborne (cyclic) Cl in streamflow ultimately turns out to be, present data strongly indicate that there are wide variations in that percentage from region to region, depending on variables such as climate, urban development, nearness to the sea, and geology of the river basin." While leaching of sediments probably accounts for most of the chloride not brought in by precipitation and dry fallout, these studies attest to the difficulty of estimating the relative importance of the various contributions of chloride in natural systems.

Sources of Chloride

Chloride may be introduced to the atmosphere from several sources in addition to salt particles and brine droplets airborne from the sea. Feth [1981] notes that these include "beds of halite, saline crusts of desert basins -- both those at present land surface and older deposits buried in the valley fill -- magmatic gases, brines, and human and animal wastes" and again indicates that these sources do not seem to explain Cl concentrations found in water in many areas.

OCEANIC SOURCES

Most of the chloride flux to the continental interior is probably derived from salt particles borne aloft from the ocean surface. Chloride and other ionic solutes are injected into the atmosphere over the oceans primarily by the bursting of bubbles at the ocean surface (in contrast, water droplets blown from waves on the surface are generally too large to remain in suspended in the atmosphere). Most of the aerosols produced over the mid-oceans are rapidly removed by precipitation. Nearer the coasts, these aerosol particles are transported inland by dominant air circulation patterns. The concentration of chloride in precipitation decreases approximately exponentially with distance from the coast. While some of this decrease is due to cumulative removal by precipitation, Junge and Werby [1958] indicate that "the rapid drop reflects primarily the dilution of sea spray particles in the lowest 2 to 3 km of the troposphere, where most rain is formed. This dilution occurs when maritime air masses, with the highest concentration of sea-spray particles in the ground layers, move inland as vertical mixing tends to produce a uniform vertical distribution." A study of

airborne chloride conducted by Woodcock [1959] also suggested that a large part of the decrease in chlorinity of rains with distance inland is due to "differences in the amounts of salt in the sub-cloud layer over the sea, and the mixing of this layer as it flows inland."

Continental Sources

The contribution of chloride from sources other than the oceans is poorly known and undoubtedly highly variable spatially. Evidence from studies of ion concentrations and ratios of modern precipitation [Junge and Werby, 1958] indicates that even in humid climates, marine-derived aerosols are mixed with a significant amount of terrestrial dust, generally of lower Cl concentration and higher Ca, K, and Na concentration. Junge and Werby [1958] examined the ratio of sodium to chloride in precipitation throughout the United States (Figure 1-13). The average Cl-/Na+ ratio, by weight, in sea water is 1.800 [(Sverdrup *et al*, 1946) in Junge and Werby, 1958]. Junge and Werby argue that the lower Cl-/Na+ ratio in precipitation that occurs even near the coast is due to addition of Na+ from continental sources. Junge [1963] suggested (p. 322) that in arid regions salts deposited at land surface by evaporation of precipitation or evaporation of rising ground water may be a source of Cl aerosols. As an example, Junge and Werby [1958] note that the salt flats in the area of Brownsville and Laredo, Texas, "are known to produce fairly high concentrations of salt in the air." Eriksson [1960] suggests that the excess Na+ in coastal regions is due to gaseous removal of Cl- that does not affect Na+.

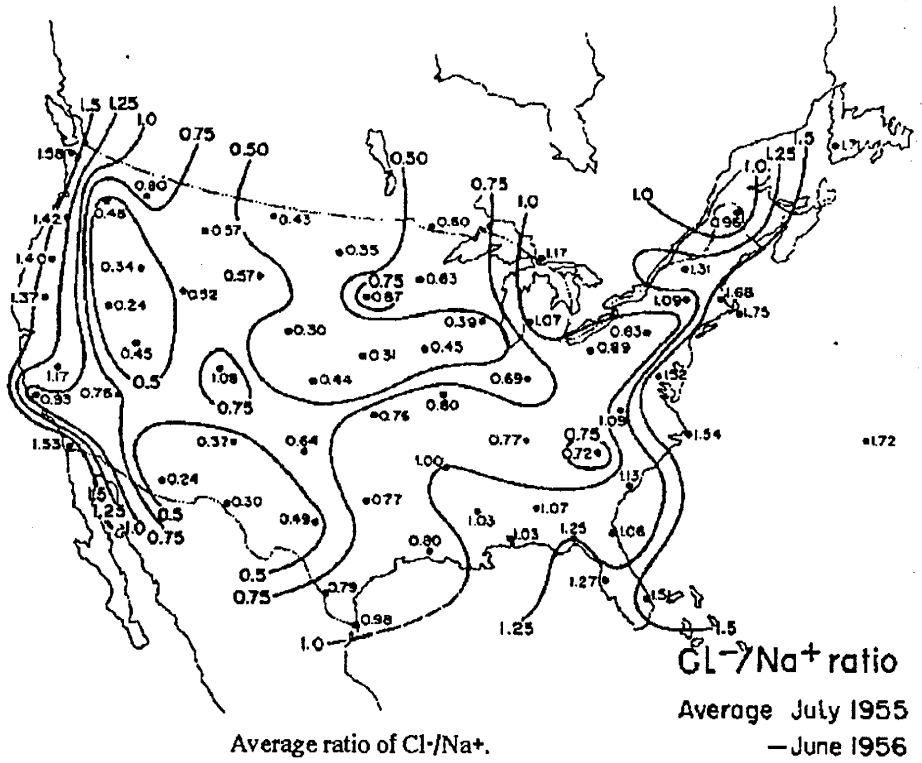

Figure 1-13. Average Cl-/Na+ ratios across the United States. From Junge and Werby, 1958.

Gambel (1961) used the ratio Ca/Cl to infer that, except in immediate coastal areas, continental aerosols provide the larger part of soluble material brought down in precipitation. He concluded that Cl derived by deflation of arid-land basins exerts only small influence on the Cl content of rainfall. Gambel's data were, however, drawn from Junge and Werby [1958] and hence are governed by the distribution of Junge and Werby's sampling points, by the fact that their samples did not include dry fallout, and that sampling stations in the more arid parts of the Southwest were few [Feth, 1981]. More recently, however, Sequeira [1993] concluded that the deflation of soil and loess in arid and semiarid areas is responsible for the large-scale average distribution pattern and extreme concentrations of excess calcium in background precipitation in the northern hemisphere. Bird *et al.* [1991] indicate that similar factors likely affect the $^{36}Cl/Cl$ ratios of precipitation in Australia: "large-scale dust storms redistribute chloride from surface layers, including salt lakes and make it impossible to distinguish dry precipitation of cosmogenic ^{36}Cl from recycled chloride; most chloride travels relatively short distances but occasional events move massive quantities of solids over large distances."

Feth [1981] summarizes results of several other researchers as follows.

> *Eardley (1969, p. 21) estimated, on the basis of 1-year samples from five collecting stations supplemented by snowpack profile analyses, that about 14,000 t of Cl are brought to the Great Salt Lake watershed each year from the Pacific Ocean, and some 28,000 t found in precipitation are of local derivation, thus recycled within the basin. Wedman (1964, p. 66-67) calculated that on the average 30,000 t of salt are removed by deflation yearly from the Sebkra Sedjoumi, a saline playa southwest of Tunis, Tunesia, and that a layer less than 1 mm thick over the surface of the 28 km² area of the salt flat would supply that quantity. He remarked that dust storms occur commonly and the dust has a salty taste. Data from Wedman's table 4 suggest that nearly one-third of the total load might be Cl.*
>
> *In summary, aerosols contribute measurable quantities of Cl to precipitation almost everywhere; many such aerosols originate from the ocean, and their effect is most evident in coastal areas. We know less about the continental sources, but areas within range of the influence of aerosols derived by deflation of continental salt deposits might be strongly influenced by such airborne salts.*

It is clear then that the chloride concentration and overall ionic composition of recharge depends heavily on the relative contributions of from marine, continental, and other sources such as volcanic emissions. This must be also be considered in any estimation of the potential variability of the ionic composition of recharge. Terrestrial sources of chloride which may be temporally variable are often site-specific. Such sources are discussed in context in following sections.

Temporal Variations in Stable Chloride Flux

Long-term variations of atmospheric aerosol concentrations are neither well known nor well studied. "Since the development of the Aitken counter in the 1800s, instruments for counting particle concentration have been available but no long-term series of measurements was inaugurated and continued at clean remote sites bridging the time span from then to the present (or even a reasonable portion of that span)" Twomey [1977]. In 1950, W.D. Crozier investigated variations of dry fallout of Cl particles in Socorro, New Mexico, in an attempt to obtain information that would be useful in air trajectory studies. Crozier hoped that the chloride peaks in New Mexico could be correlated with marine storms, as had been done in two previous studies that had tracked chloride intrusions as far east as Illinois. Systematic spot collections of dry chloride fallout were made at ground level over the period from September 1949 to December 1951. Although Crozier concluded

from the data that the "correlation between precipitation and chloride abundance is not very impressive," he also listed among the conclusions of his study that (1) "it is sometimes possible to trace chloride-bearing air back to regions of marine disturbance, and it seems reasonable to believe that high chloride-particle concentrations usually originate in such regions" and (2) "there is a tendency for high chloride-particle concentrations to be associated with passage of cold fronts." Variations in the daily particle counts in that study were as large as three orders of magnitude. Unfortunately, the study did not measure the distribution of particle sizes and Crozier notes that "particle sizes were small at the times when the abundance was high." While Crozier's study measured only dry deposition of chloride, it seems likely that this would be a relative indicator of the amount of chloride present in the atmosphere, and therefore a reasonable indicator of the amount available for removal by precipitation.

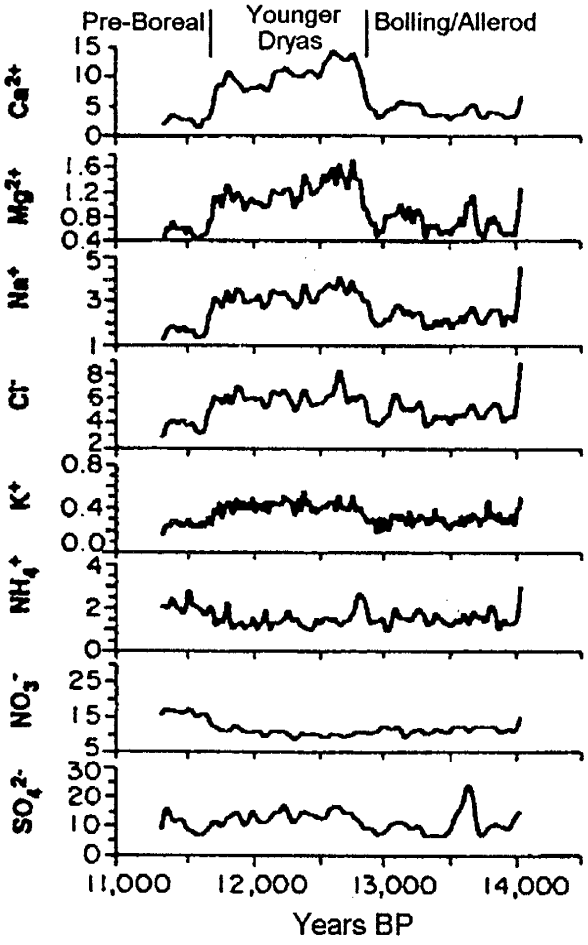

Figure 1-14. Robust spline smooth of various ionic constituents of precipitation (in flux in kilograms per kilometer squared per year) covering the time period approximately 11,322 to 14,035 years ago as measured in the GISP2 ice core from central Greenland [Mayewski et al., 1993].

RECORDS OF CL DEPOSITION IN ICE-CORES

The long-term record of atmospheric chemistry preserved in ice-cores from the poles provides some information about the temporal variation of chloride flux. Mayewski *et al.* [1993] present detailed records of the flux of chloride and other ions during the Younger Dryas (~12,900 BP to 11,600 BP) developed from the U.S.-Greenland Ice Sheet Project (GISP2). This record (Figure 1-14) indicates a substantial decrease in both chloride flux and flux variability at the termination of the Younger-Dryas. Chloride flux appears to decrease from about 6 kg/(km^2*yr) to 4 kg/(km^2*yr) over an approximately 100-year period beginning at about 11,700 BP. Legrand *et al.* [1988] present data from the Vostok ice core which records atmospheric chemistry changes over the last ~160,000 years. This record also indicates a substantial reduction in chloride flux at the termination of the Younger-Dryas (Figure 1-15).

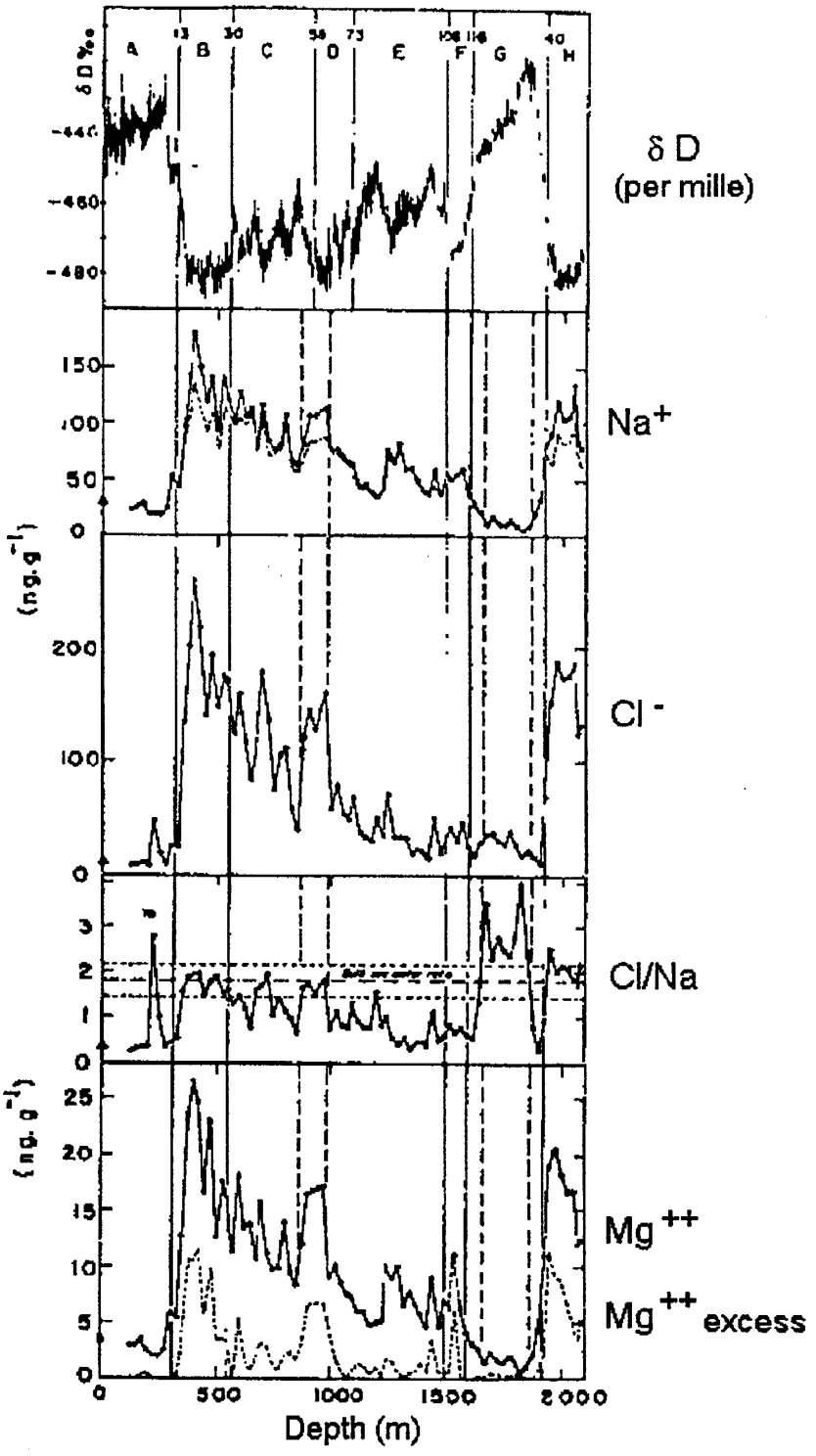

Figure 1-15. Vostok ice core: isotope and marine trace element profiles. (a) Deuterium isotope profile from Jouzel et al. (1988); solid vertical lines refer to the successive climatic stages (A-H) defined by Lorius et al. (1985). Vertical dashed lines are used when the chemical profiles divisions are slightly different from those defining climatic stages (see text). (b) Total Na, dashed line corresponds to the marine Na. (c) Chloride. (d) Cl/Na weight ratio. (e) Magnesium, dashed line refers to the excess-magnesium. From Legrand et al., 1988.

Mixing of ^{36}Cl with Stable Chloride and Resultant Spatial Distribution of ^{36}Cl

Because production of ^{36}Cl occurs in greater proportion in the stratosphere, its fallout pattern is strongly influenced by the mechanism through which mixing with the troposphere occurs. Most of the transfer of air from the stratosphere to the troposphere is thought to occur close to the tropopause level near the median latitude jet stream (Figure 1-16) [Newell, 1971].

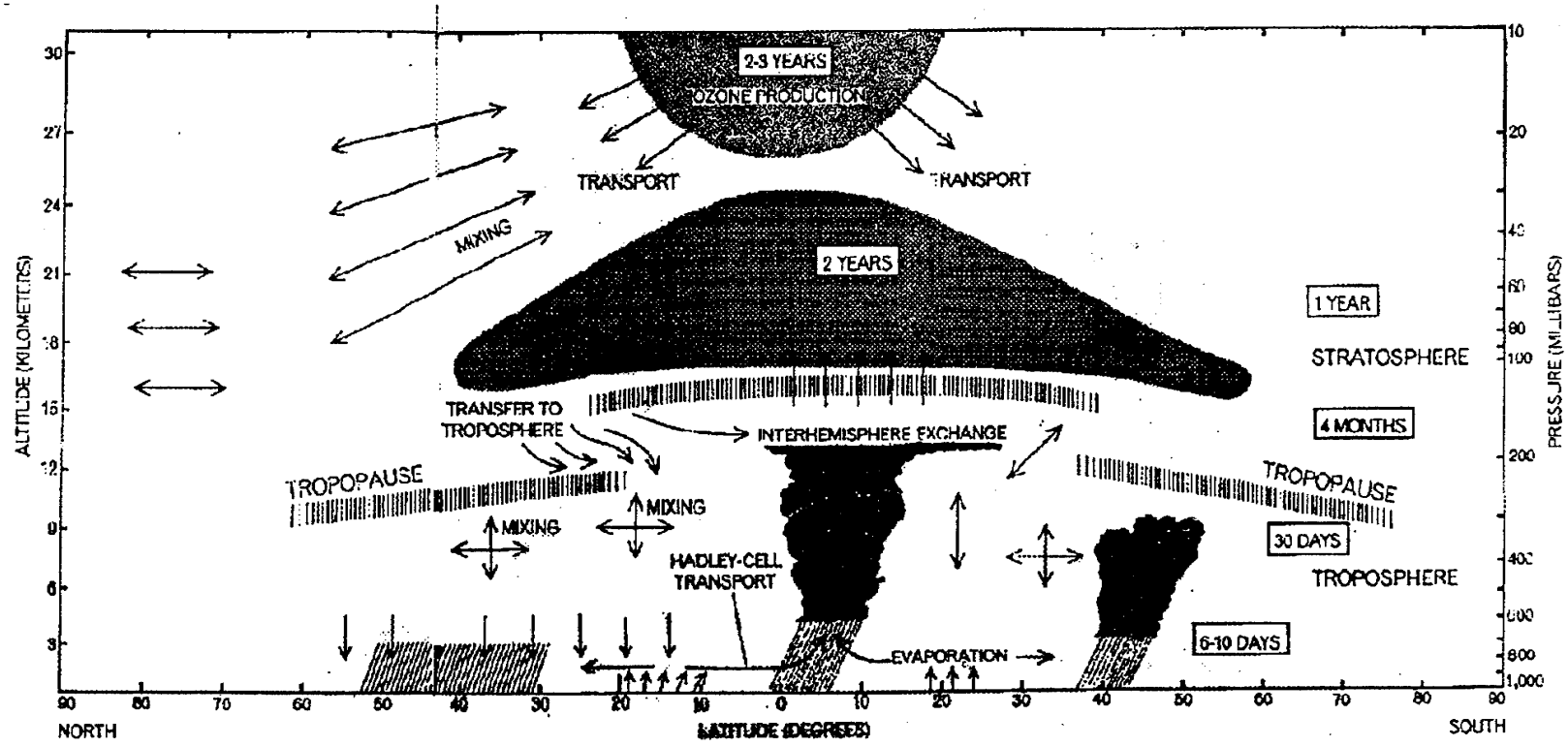

Figure 1-16. Schematic diagram of the earth's atmosphere and transport mechanisms within it. Distribution and movements of ozone, water, and aerosols, or small solid and liquid particles, are indicated in the schematic diagram drawn along a line of longitude. Boxed figures are residence times for aerosols. The tropopause is the boundary between the troposphere and the stratosphere; its altitude varies with latitude as indicated. From Newell, 1971.

Fallout is thus greatest at the mid-latitudes with a latitudinal dependence as shown in Figure 1-17. This dependence is based on data from the fallout of long-lived radioisotopes produced during nuclear weapons testing [Lal and Peters, 1967].

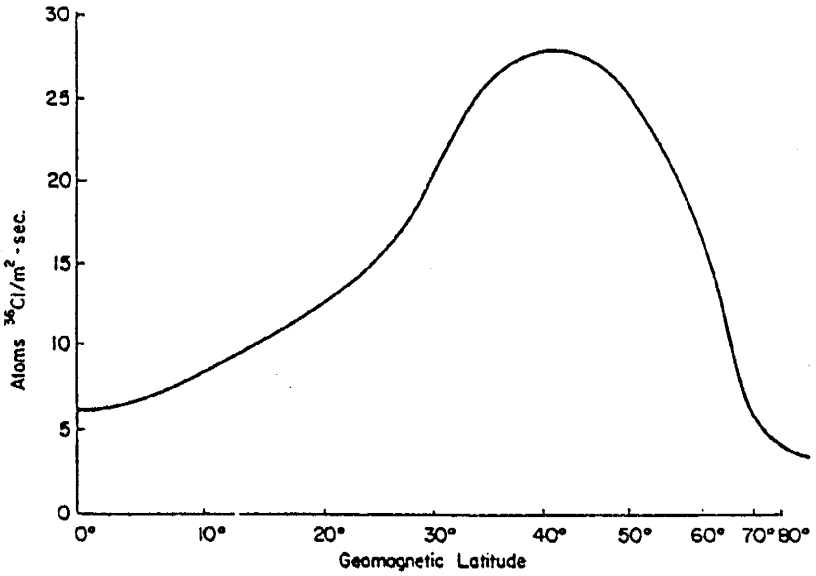

Figure 1-17. Latitudinal dependence of ^{36}Cl fallout. From Bentley et al., 1986.

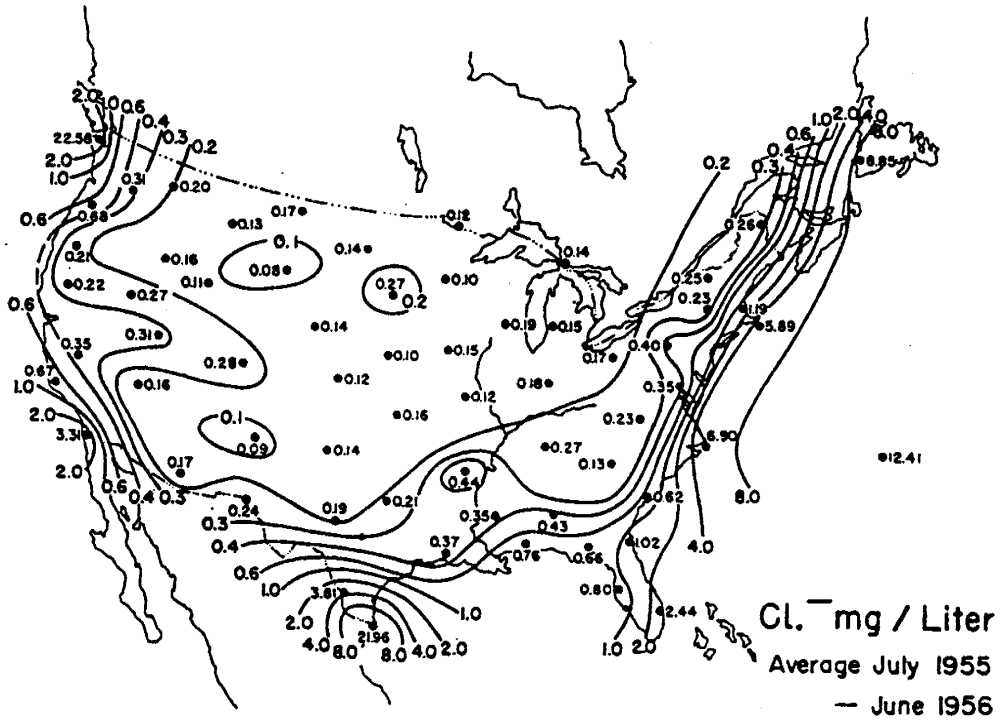

Figure 1-18. Average Cl- concentration in precipitation. From Werby et al., 1958.

This ^{36}Cl fallout distribution is superimposed on the atmospheric concentration distribution of stable chloride. If it is assumed that the fallout of chloride (dry and wet) is directly proportional to its concentration in the troposphere, the results of Junge and Werby [1958] (Figure 1-18) may be used as a measure of the amount of stable chloride with which the ^{36}Cl fallout will be diluted. Accordingly, Bentley *et al.* [1986] superimposed the latitude-dependent ^{36}Cl fallout calculated by Lal and Peters [1967] on a slightly modified form of the chloride concentration distribution described by Junge and Werby [1958] to predict the spatial variation of the $^{36}Cl/Cl$ ratio within the United States (Figure 1-19).

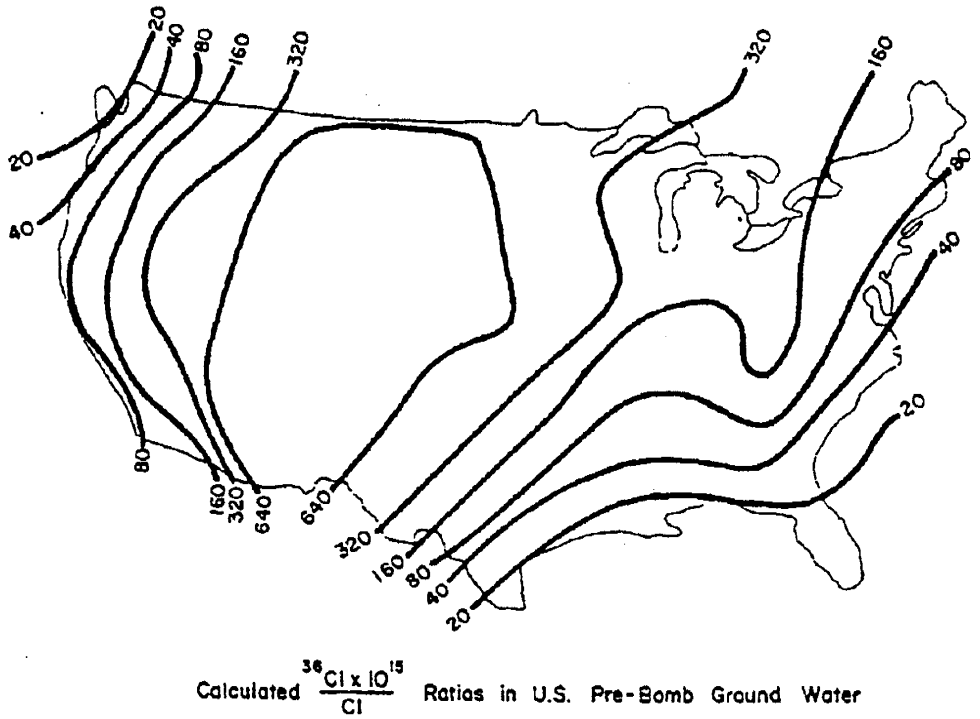

Figure 1-19. Calculated ^{36}Cl ratios in precipitation and dry fallout over the United States. From Bentley et al., 1986.

The pattern predicted by Bentley *et al.* is based on the assumption that the atmospheric chloride available for mixing with the injected ^{36}Cl is directly reflected by the concentrations of Cl in precipitation, as would be the case if the pattern of decreasing Cl concentration with distance inland is due primarily to cumulative washout by precipitation. As discussed previously, the decrease in Cl concentrations due to cumulative removal is likely a minor effect compared to vertical mixing of aerosols in the atmosphere as air masses move inland. It seems likely that the annual turnover of the tropopause would allow thorough mixing of

the injected ^{36}Cl atoms with the entire column of stable chloride in the troposphere, not just that in the lower troposphere where precipitation originates. Accordingly, estimates of the spatial distribution of $^{36}Cl/Cl$ ratios in precipitation should probably be based on superposition of the latitudinal fallout dependence of Lal and Peters [1967] with atmospheric chloride concentration distribution data rather than precipitation chemistry data as has been previously assumed. Since some studies [Fabryka-Martin *et al.*, 1987] indicate fairly good agreement of $^{36}Cl/Cl$ measurements of modern pre-bomb recharge with the Bentley *et al.* [1986] estimate, it would be interesting to see if such a modification would actually produce more accurate mapping of the spatial distribution. Unfortunately the number of $^{36}Cl/Cl$ ratio measurements in precipitation is , at present, insufficient to allow accurate mapping of the spatial variation of $^{36}Cl/Cl$ ratios across the United States.

Reconstruction of the ^{36}Cl Production History via Paleomagnetic Records

Because modulation of the cosmogenic flux occurs primarily in the magnetosphere, production of cosmogenic nuclides should be strongly affected by variations in the earth's virtual dipole moment. Several recent studies have produced reconstructions of the secular variation of the earth's dipole moment (VDM) extending back to as much as four million years [Valet and Meynadier, 1993].

Records of Global Magnetic Field Intensity Variations

Tric *et al.* [1992] present a relatively high resolution record of VDM paleointensity, covering the last ~80 ka, based on sedimentary deposits in the Mediterranean and Tyhrrenian Seas. Prior to development of this record, relatively few archaeomagnetic measurements, primarily from volcanic materials, were available covering the period before ~10 ka. Intensity changes of the geomagnetic field covering the last 10 ka are relatively well-documented based on a wide number of archaeomagnetic of archaeological and volcanic materials [Tric *et al.*, 1992]. The sedimentary record used by Tric *et al.* [1992] is truncated at an upper boundary of ~8 ka B.P. due to disturbance of the tops of the marine cores. Therefore, Tric *et al.* incorporated the data of McElhinny and Senanayake [1982] for reconstruction of the VDM during that period. Comparisons of the record of Tric *et al.*

with the remainder of the McElhinny and Senanayake record and with other volcanic records is excellent [Tric *et al.*, 1992].

Reconstruction of ^{36}Cl Production Record Based on Paleomagnetic Data

In this study, we are constrained to that period of time for which ^{14}C dates may be obtained for the midden samples, approximately the past 40 ka. Thus I have used the paleointensity reconstruction of Tric *et al.* [1992] in order to calculate relative paleo-production rates of ^{36}Cl as a function of time (Figure 1-20). As discussed previously, the time-scale for the Tric *et al.* paleomagnetic reconstruction is based on a number of dating techniques. A number of data points in the first 8 ka of the curve are based on ^{14}C dates [Bard *et al.*, 1990]. Tephra layers, dated by ^{14}C and ^{40}Ar:^{39}Ar methods and comparison with oxygen isotope records were used to constrain older portions of the curve [Paterne *et al.*, 1986]. The relative production rates are calculated based on the production curves given by Blinov [1989].

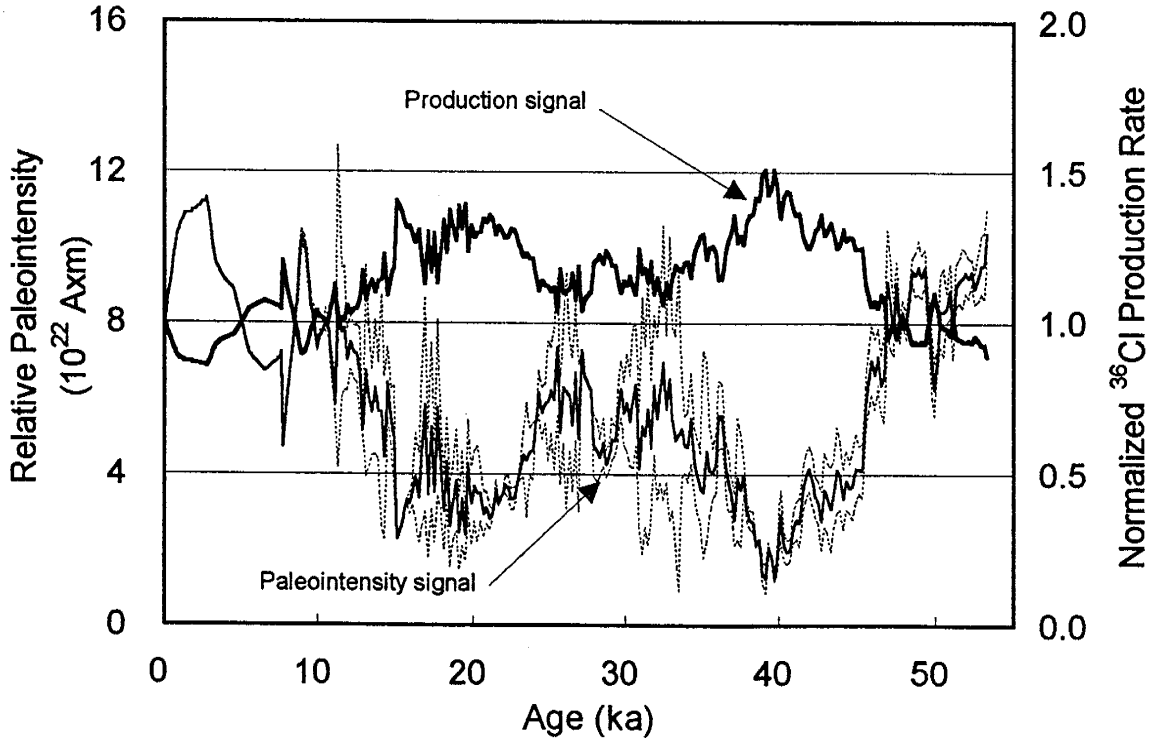

Figure 1-20. Secular ^{36}Cl production signal (upper curve, right axis) based on paleointensity record of Tric et al. [1992] (lower curves, left axis; dotted lines are the paleointensity measurements +/- one σ). Production rate curve is normalized to the modern production rate.

Section Summary

In addition to its importance for calibration of the radiocarbon time-scale, a record of past variations in the production rate of cosmogenic nuclides is of great interest to researchers studying cosmogenic nuclide production and distribution, the relationship between cosmogenic nuclide production and climate, geologic dating via in-situ buildup of cosmogenic nuclides and atmospheric circulation patterns. As a result, there have been many attempts to examine the production history of cosmogenic nuclides at a variety of time-scales. Despite these efforts, the mechanism driving long-term variations in cosmogenic production rates is yet poorly understood. Most of the research in this area, to date, has focused on reconstructing the record of atmospheric ^{14}C activity. Unfortunately, interpretation of the cause of atmospheric ^{14}C activity variations is greatly complicated by exchange processes with other reservoirs of ^{14}C. Detailed archives of other cosmogenic nuclides such as ^{10}Be and ^{36}Cl have not yet been found in locations that would record production variations caused by geomagnetic field intensity variations.

Efforts to calibrate the radiocarbon time-scale demonstrate that atmospheric ^{14}C activity has decreased by approximately 25% during the past ~20 ka. The cause for that decrease has been attributed to several different factors, primarily geomagnetic field intensity variations and/or oceanic venting. The detailed record from Huon Peninsula corals [Edwards et al., 1993] indicates that a large portion of that change occurred between 12.3 and 11.0 ka.

Beryllium-10 measurements in sea-floor sediments suggests that production of ^{10}Be was at least 20% higher during the last glacial maximum than during the Holocene, which is consistent with the atmospheric ^{14}C activity data. Although concentrations of both ^{10}Be and ^{36}Cl in polar ice cores also decreased significantly during the transition from the Pleistocene to the Holocene, evidence suggests that these changes reflect precipitation variations rather than variations in the atmospheric production of those nuclides. Attempts to find geomagnetic modulated production rates in polar ice cores have generally been inconclusive. It is likely, however, that the polar archives of ^{10}Be and ^{36}Cl would not record variations in production caused by geomagnetic field strength variations. Deposition of cosmogenic

nuclides at the poles is dominated by local production, and field strength variations at the poles would have a negligible effect on local production rates.

Beryllium-10 data from polar ice cores convincingly demonstrates the effect of the solar wind on production of that nuclide. Chlorine-36 concentrations in polar ice have not yet been examined in the same detail as have ^{10}Be concentrations but available data suggests that flux of ^{36}Cl at the poles has also varied as a result of solar modulation of production. Detailed ^{10}Be records from several polar locations exhibit ~1,000-yr. long peaks in ^{10}Be concentration at ~35 and 60 ka B.P. Beer et al. [1992] and others contend that these peaks reflect production rate variations rather than precipitation rate variations or changes in atmospheric circulation and it has been suggested that such short-term production peaks may have caused by ancient supernovae.

Archives of cosmogenic nuclides such as ^{36}Cl often do not provide information about independent fluxes of the different isotopes. Changes in ^{36}Cl/Cl ratios, for example, may be caused by variations in the flux of ^{36}Cl or by changes in the flux of stable chloride. Unfortunately, little is know about past variations in stable chloride fallout. Considerable evidence suggests that stable chloride fallout includes a significant component of locally derived salts in some arid areas and may therefore be highly dependent on local climatic effects.

Implications for Further Investigations of ^{36}Cl/Cl Variations

In an analysis of ^{36}Cl data distributed in time, one must consider the possibility of temporal variations in all of the factors that can change the ^{36}Cl/Cl ratio of infiltration. In summary, these include

- Temporal variations in ^{36}Cl production
  - Unknown sources of cosmic radiation
  - Variations in cosmic ray flux incident to the earth's magnetosphere
  - Changes in atmospheric concentrations of target elements (Ar, Cl)
  - Variations in modulating effects

    - Field strength modulation
    - Solar modulation
- Temporal variations in mixing with troposphere
    - Atmospheric circulation and distribution
- Temporal variations in stable chloride concentration in the atmosphere or of stable chloride flux
    - Flux of chloride from the oceans
        - Climatic effects
        - Atmospheric circulation patterns
    - Continental flux of chloride
        - Climatic effects
    - Volcanic emissions and other unaccounted for sources of chloride

Ideally we should like to have estimates of both (1) the magnitude of noise in these different signals as a function of frequency and (2) their pattern of variation due to known climatic changes such as the shift to warmer conditions at the onset of the Holocene. Unfortunately, little data are available concerning the potential variability of most of these factors. Many are highly dependent on local phenomena such as local climatic changes or topographical features. Further discussion of the potential temporal variability of these factors is thus reserved for following sections.

Based on the hypothesis that the most important driving force for long-term variations in ^{36}Cl ratios in chloride fallout is the strength of the earth's magnetic field, suitable temporal records of ancient chloride should display this same record of variation in ^{36}Cl ratio. In the following section, I describe the use of fossil packrat middens to test this hypothesis.

Section Two

Secular Variation of Cosmogenic Isotope Production as Measured in Ancient packrat Urine

Prediction is very difficult, especially of the future.

- Niels Bohr

In this section, I discuss the $^{36}Cl/Cl$ record preserved in ancient packrat middens and its implications regarding long-term changes in cosmogenic production rates. Packrats provide a means of reconstructing the production record of cosmogenic ^{36}Cl production because their middens are preserved for thousands of years in the arid environment of the southwestern United States. These middens are portions of houses that have become indurated into a cohesive mass by impregnation with quick-drying urine [Wells, 1976 in Betancourt and Van Devender, 1990]. The middens therefore contain abundant chloride in which the $^{36}Cl/Cl$ ratio should reflect that of precipitation contemporary with the packrat. Organic carbon, which is also abundant in the midden, allows dating of the sample to provide a temporal scale for the record of $^{36}Cl/Cl$ variation.

packrats

Pack rats (genus neotoma) are relatively large nocturnal rodents that are found in virtually all of the ecosystems of the southwestern United States, from high mountain conifer forests to true desert. Desert-dwelling species of the packrat commonly live in areas where standing water is unavailable. The packrat has adapted to this limitation by deriving its water solely from its food. Unlike other desert rodents such as the kangaroo rat, however, the packrat is unable to obtain a significant portion of its daily water requirement by metabolization of dry food [Schmidt-Nielsen, 1964] and so requires a succulent food source. In the desert, this is generally some type of cactus, commonly cholla or prickly pear, but, where cactus is unavailable, the packrat may consume a considerable amount of creosote bush, juniper or other species. Schmidt-Nielsen [1964] estimate that "on a year-round basis almost half the food of the white-throated wood rat, a southern Arizona species, is made up of cactus

which has a water content of almost 90 per cent. During the driest months the proportion of cactus in the diet increases to nine-tenths of the food bulk."

> *All packrats share two critically important habitat requirements: succulent plant food (plant material with at least 50% water by weight) and adequate shelter, usually in the form of rocks, shrubs, or trees. Although renowned for their ability to live in desert areas that lack drinking water, packrats void copious urine and depend on succulent or moist forage to maintain their water balance. [Vaughan, 1990 in Betancourt and Van Devender, 1990, p. 16 (after Schmidt-Nielsen and Schmidt-Nielsen, 1952)]*

Solute Sampling by packrats

Desert plants of course derive their water from precipitation that has infiltrated to the root zone. Because the plant root system provides preferential flowpaths in the soil, it is likely that water taken up by cacti is essentially contemporary with precipitation. Plants take up water from the soil by osmosis, movement of water being toward the solution of higher concentration. Some of the major constituents of natural water, particularly calcium, magnesium, sulfur, and carbon, are essential for plant growth. Chlorine, also present in natural water, is required for plant growth only in small quantities and sodium is apparently essential to some but not all plants [Hem, 1967]. These solutes, in low concentrations, are transported with the water through the root membranes to supply the nutrient requirements of the plant [Hem, 1967]. As fractionation during such a transport process is negligible, the isotopic species of chlorine in solution in the plant tissues should be present in the same proportion as in the soil moisture. As it obtains water solely from plants, the packrat therefore takes on chloride in essentially the same isotopic proportion. Solutes taken up by the packrat are strongly concentrated by evaporation from the rats body before being voided in the urine. Organic and inorganic solids in the urine then crystallize and, if properly protected from the elements, may be preserved for thousands of years. The crystalline urine, known as 'amberat' is typically translucent and reddish-brown in color.

Fractionating processes occur mainly in chemical reactions such as oxidation and reduction reactions that involve changes in chemical bonds and these are largely absent in the geochemistry of chlorine [Hoering and Parker, 1961]. As with most of the chlorine cycle, the pathway from precipitation to urine involves virtually only the chloride ion, so that

fractionation of chlorine during transport from the soil to the plant and through the rat is negligible. The isotopic ratio of chloride in a packrat midden should therefore be representative of the isotopic ratio of contemporary precipitation to the degree that the soil moisture used by the plants is contemporary. Several processes exist to ensure that the water sampled by the packrat represents a reasonably good average of contemporary precipitation. Mixing of infiltrating water within the root zone and the variable rooting depths of various plant species may average up to several hundred of years of precipitation.

Nesting Habits and Urine Preservation

Unlike most animals, the packrat's nesting habits allow preservation of its urine. The packrat, again being somewhat less well adapted to the desert environment than other more drought- and heat-tolerant species, requires a relatively cool environment to limit water loss. As a means of limiting exposure then, packrats build their nests in shady areas: under bushes or in declivities in cliffs and among boulders.

> *The white-throated packrat (Neotoma albigula), common to the deserts of New Mexico is commonly associated with cacti (especially prickly pear), creosote bush, catclaw acacia, palo verde, and mesquite but also occurs in juniper woodland and shortgrass prairie at the northern edge of its range... Den-building behavior is relatively strongly developed in this species, and, like most packrats, it is partial to rock outcrops, fissures, and boulder piles. In the absence of rocks, dens are built beneath thickets of catclaw or mesquite, or in patches of cactus or yucca [Vaughan, 1990, in Betancourt and Van Devender, 1990, page 18].*

To provide further insulation, the packrat constructs around the nest a pile of plant detritus, dung and other debris and urinates on this accumulation. Due to its concentrated nature, salts and other solutes contained in the urine quickly crystallize within the matrix. This effectively cements the pile together and provides a formidable barrier to predators, particularly since the plant detritus often contains cactus spines. The entire assemblage is known as a midden. This should be distinguished from the nest - a small cavity associated with the midden that is carefully prepared and lined with nesting materials [personal communication, R. Finley, August 1995]. Available information suggests that development of relatively large middens can occur relatively quickly.

> *Indurated middens can develop from one year to the next, as suggested by the inclusion of a dated newspaper in a well-cemented midden from the Great Basin (Thompson, 1985). Erratic representation of plant organs and sisseminules, available to the packrat only seasonally or in mast years, suggests that indurated middens can form during a relatively brief period of a few months to a year..... Because the present evidence is mainly anecdotal, the duration of midden depositional episodes remains unknown. Radiocarbon dating cannot resolve the issue because, at best, the radiocarbon age of a sample merely brackets the time of deposition. [Spaulding et al., 1990, in Betancourt and Van Devender, 1990, p. 63]*
>
> *A single midden may represent portions of a collapsed den and a depositional episode of a few months to a few years. Some midden samples may have accumulated over longer periods, say several decades to several centuries, but this is not determinable given present dating methods. The standard deviation of a sample's radiocarbon date may bracket but does not define the duration of the depositional episode [Spaulding et al., 1990, in Betancourt and Van Devender, 1990, p. 60].*

The midden of a single packrat thus preserves an excellent sample of the vegetation selected by the rat during its lifetime as well as the isotopic composition of Cl in meteoric water. Due to their protected location and composition, these middens are often preserved for extended periods of time and radiocarbon "dead" middens are not uncommon.

> *Saturation by crystallized urine protects plant macrofossils from decay. Extreme dryness suppresses microbial and chemical activity and favors mummification. Urea is hypotonic and mummification of plant fragments is likely accomplished in much the same manner as if they were packed in salt. ..[Spaulding et al., 1990, in Betancourt and Van Devender, 1990, p. 60].*

Development of Composite Middens

Excellent den sites such as caves and rock fissures are usually in short supply and tend to be occupied by packrats discontinuously over very long time spans [Vaughan, 1990, in Betancourt and Van Devender, 1990, p. 18]. Many middens are therefore agglomerations of middens deposited by many packrats and the structure of the resultant strato-midden can be quite complex.

> *Wells (1976) and Thompson (1985) believe that in most cases midden samples represent the accumulations of a few years at most. If true, this means that a midden sequence spanning thousands of years, even if from one large midden, is constructed from discontinuous samples, each representing one to several years. [Spaulding et al., 1990, in Betancourt and Van Devender, 1990, p. 63]*

While packrat middens have been well-studied for the paleobotanical information they contain, the urine that binds the matrix has been largely ignored. Generally, paleobotanists are interested in the fossil plant fragments from which, with the aid of radiocarbon dating, they can deduce changes in the vegetation surrounding the nest and, therefore, to some degree, climatic changes.

Dating Considerations

In order to use packrat middens to determine the relative production rates of cosmogenic ^{36}Cl over time, we must also be able to date the urine sample from which the chloride is extracted. This can be accomplished in one of two ways, (1) by association with the plant detritus contained in the matrix which can be radiocarbon dated, or (2) direct dating of the crystalline urine. We favor the latter method because it avoids the potential problem that the fluidity of the matrix may cause. At the time of the deposition, the urine may flow through older portions of the nest before crystallizing. It is also possible that the amberat may flow as a highly viscous fluid to some degree. In either case, dating the crystalline material itself ensures that the dated portion of the sample is contemporary with the crystalline material processed for ^{36}Cl analysis.

Complications Due to Midden Complexity

While in this case we are concerned with establishing an accurate date for the urine itself, considerable debate has occurred among paleoecologists as to the particular fraction of the midden that should be sampled to accurately date macrofossil collections:

> *The particular fraction of the midden that should be dated has been the subject of considerable debate. King's (1976) systematic excavation and multiple dating of a midden from the Lucerne Valley, California, demonstrate the middens are not always stratigraphically simple (also see Spaulding, 1985). To avoid stratigraphic mixing, Wells (1976) advocates the dating of nonspecific debris (unwashed midden matrix) from a thin, horizontal layer, while Van Devender (1977) suggests dating either a single fragment or a composite sample from a single taxon removed by washing, screening, and sorting the residue from a larger mass. Unfortunately, the large sample size required to secure enough material from a single species for dating increases the risk of stratigraphic mixing. Smaller midden sample size may preclude monospecific dating and may also abbreviate the measurable floral and faunal diversity. [Webb et al., 1990 in Betancourt and Van Devender, 1990, p. 86]*

Complications due to Urine Chemistry

In dating the crystalline urine, one must consider the sources of carbon available to the packrat and how these sources are partitioned in the animal's urine. The chemistry of urine deposits of the species Neotoma cinerea (bushy-tailed woodrat) and Neotoma fuscipes (dusky-footed woodrat) has been studied by Emerson and Howard [1978]. They report that "as much as 45% of the microcrystalline incrustations found at the 'urinating posts' of woodrats in northeastern California consists of calcium oxalates (the dihydrate form, weddelite $[Ca(C_2O_4)*(2+x)H_2O]$ and monohydrate form, whewellite $[Ca(C_2O_3)*H_2O]$). The bulk of the deposits are calcite with, in addition to the oxalates, minor amounts of calcium carbonate monohydrate, a magnesium ammonium phosphate (struvite), amorphous material, and detrital silicates" [Emerson and Howard, 1978]. While not mentioned in their study, it is likely that urea (also known as carbamide, CON_2H_4) also forms a significant percentage of the crystalline material. Urea is the primary means of nitrogenous waste removal and the chief organic constituent in mammalian urine.

Carbon contained in the packrat's urine is derived mainly from the organic carbon in the animal's diet. Due to the nature of that diet, this includes relatively insoluble calcium oxalate, soluble oxalate salts and oxalic acid. Jumping cholla, prickly pear, and mesquite (all major components of the diet of packrats in Arizona) contain relatively high amounts of calcium oxalate. Soluble oxalate species are toxic to many mammals and are an important part of the chemical defenses of many cactus species common in the packrat's diet. In areas where limestone is common, it is also possible that a significant amount of inorganic carbon (as calcium carbonate) may contaminate the rat's food as dust. The possibility that this inorganic carbon may be eliminated in the urine depends on the ability of the rat's digestive system to metabolize inorganic calcium carbonate. While in most mammals that capacity is minor, the packrat has a relatively high capacity for dissolution of $CaCO_3$. Experiments performed by Knut Schmidt-Nielsen indicated that while white rats absorbed only 2.5% of calcium from a test diet containing powdered calcium carbonate, "pack rats , on the other hand, absorbed most of the calcium, for 70 to 79 per cent of that ingested was recovered in the urine. The urine was thick with the precipitate and the calcium concentration went up to values as high as 1150 mEq per liter, virtually all of it in the form of calcium carbonate."

[Schmidt-Nielsen, 1964]. Thus, to accurately date packrat urine, the possibility of significant inorganic carbon content in the urine must be considered. This can be assessed by comparing the $^{13}C/^{12}C$ ratio of the total carbon present (by AMS) to the $^{13}C/^{12}C$ ratio of the carbonate forms. Carbon isotope ratios in organic carbon forms are generally depleted in the heavier isotope compared to inorganic carbon species. This is due to fractionation by the plant in its preferential incorporation of "light" $^{12}CO_2$. A significantly heavier carbon isotope ratio in the carbonate contained in the urine would therefore suggest that a significant portion of the calcium carbonate contained in the urine is produced from metabolization of inorganic carbon.

The process by which the packrat metabolizes oxalates and carbonates is not well understood; if fractionation also occurs in that process, it would complicate matters considerably. In general, because the packrat excretes considerable amounts of carbon in the form of urea and oxalates that are primarily derived from organic carbon, the contribution of inorganic carbon is unlikely to have a significant effect on the radiocarbon ages. Moreover, in areas such as the Painted Hills of Nevada (Mother Midden site) that contain virtually no limestone, the possibility of significant amounts of inorganic carbon being ingested seems remote.

Methods

Sources of Middens used in the Present Study

This study is based predominantly on packrat midden samples obtained from sites in the Painted Hills region of the Virginia Mountains, near Pyramid Lake, Nevada. In particular, 15 of the 20 samples in the Nevada series of samples were obtained from one large midden, termed the "Mother Midden," by Peter E. Wigand of the Desert Research Institute, Reno, Nevada. At this location, a relatively large number of samples were collected from a single locality with ages ranging from several thousand to over 30,000 years. Using a group of samples from the same location limits the potential for possible spatial variation in $^{36}Cl/Cl$ ratios of recharge to interfere with interpretation of temporal variation.

Midden samples were also obtained from the Sierra de Los Pinos area east of Socorro, New Mexico. These samples were generally younger in age, and were obtained in order to examine the spatial variability of $^{36}Cl/Cl$ ratios in essentially contemporary middens. Additional samples were also obtained from the Owens Valley region of California. These samples, provided by Steve Jennings of Texas A&M University, provided a data set from an entirely different locale. Sample locations are shown in Figure 2-1. Ultimately, complete data sets from several locations would be necessary to establish the significance of temporal variations in $^{36}Cl/Cl$ ratios as recorded in fossil packrat middens.

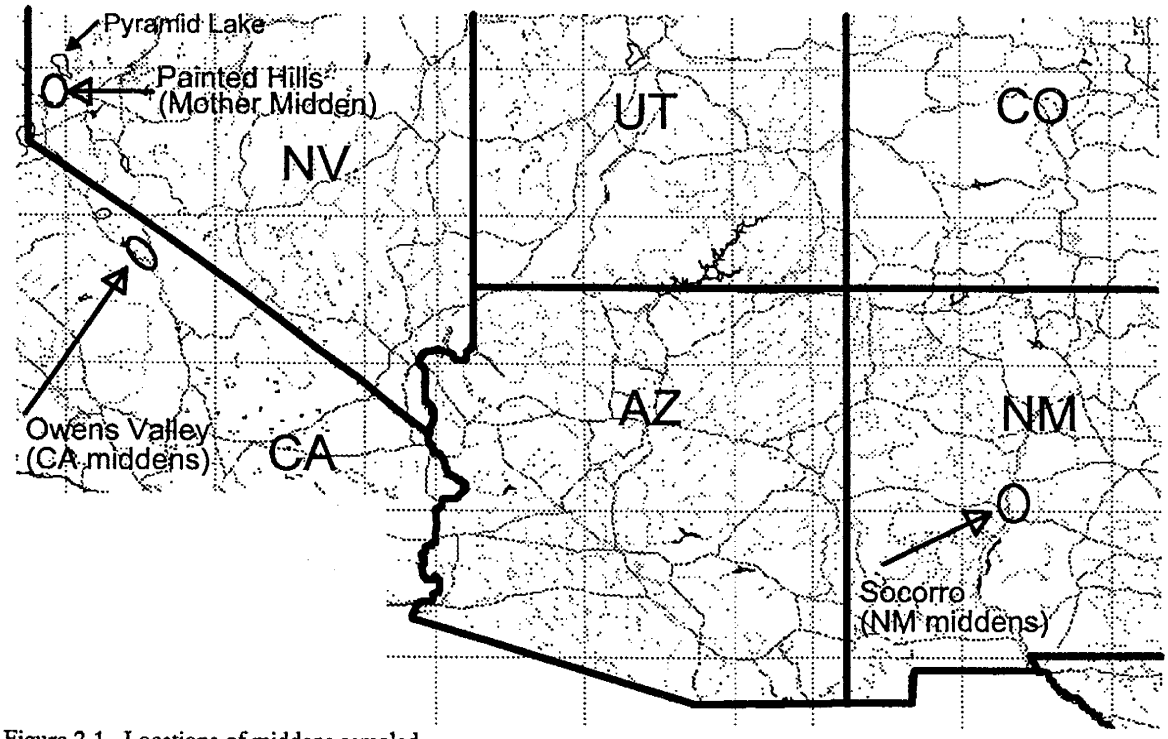

Figure 2-1. Locations of middens sampled.

^{36}Cl Measurements

A total of $^{36}Cl/Cl$ ratio measurements were made on 33 samples of packrat middens from Nevada, New Mexico, and California. Fifteen of these samples were from the Mother Midden from the Painted Hills region of the Virginia Mountains, Nevada and five other samples were from other middens in the same vicinity. Chlorine-36/Cl ratios were also measured for five samples obtained from the Volcanic Tableland north of Bishop, California, and eight samples from an area just east of Socorro, New Mexico. Duplicate

analyses were performed on three of the samples from the Nevada series of midden sections. These duplicate measurements were made to assess the effect of different processing methods on the results.

Midden Processing for ^{36}Cl Ratio Measurements

Sample processing prior to ^{36}Cl analysis was performed at the New Mexico Institute of Mining and Technology. Approximately 10 grams of the midden material was first dissolved in distilled deionized water and the sample shaken for 24 hours. The resulting solution was then filtered through a 0.45-μm filter to remove solids, and the filtrate reserved for further processing. A portion of the filtrate was used to determine Cl concentration of the solution via selective ion electrode measurement of Cl activity. The filtrate was subsequently acidified by addition of HNO_3 to attempt to precipitate urea or other organic compounds. Any precipitate was then removed via centrifugation and decanting and then discarded. $AgNO_3$ was then added to the solution to precipitate Cl as AgCl. This precipitate was also separated by centrifugation and decanting and the supernatant discarded. The AgCl precipitate was then repeatedly dissolved in sodium hydroxide and reprecipitated by addition of nitric acid. Barium nitrate was added to the basic solution at least once to precipitate out unwanted sulfur as $BaSO_4$. The precipitation-dissolution process was continued until the precipitate was visibly free of color impurities. Purification commonly required half a dozen or more repetitions of the solution - dissolution step. The precipitate was then rinsed several times in distilled deionized water and prepared as required by the cooperating AMS facility. A detailed description of the chlorine extraction procedure is included as Appendix A.

Dating Methods

Middens used in this study were selected from samples previously used in paleoecology studies. Dates obtained in the paleoecology studies were used to select samples spanning as wide a range of time as possible. However, because the original dates were obtained via destruction of the sample, the samples obtained for this study were not necessarily of the same midden strata. For this reason, we obtained separate ^{14}C dates for most of the samples in this study.

In addition to the dates provided by the investigators supplying the middens, a total of 18 radiocarbon dates were obtained on the Nevada set of samples. Fourteen of these dates were made on crystalline pieces of amberat and four dates were obtained on plant debris remaining after the completion of processing for ^{36}Cl measurements. Radiocarbon dates for the midden samples from the New Mexico and California series were provided by the paleoecologists supplying the samples. Separate ^{14}C ages were not obtained for those samples because they were generally from single-stratum middens, or from aggregate middens with little variation in age.

Radiocarbon Dating

AMS radiocarbon dates of crystalline urine samples were provided by Krueger Enterprises, Inc., of Cambridge, MA. AMS radiocarbon dates of detrital organic matter remaining after processing were provided by Beta Analytic, Inc., of Miami, Florida.

Midden Processing for Radiocarbon Dating

Radiocarbon measurement of crystalline urine samples determined via AMS was the primary means of dating used in this study. In several cases, we obtained ^{14}C dates on samples of plant detritus left after leaching the chloride from a sample. The latter method was used to attempt to assess whether the plant material was contemporary with the crystalline urine. Crystalline urine samples for AMS ^{14}C dating were selected by crumbling the amberat onto a clean surface and using a microscope to hand-select midden fragments that appeared purely crystalline urine. The crystalline material is easily distinguishable based on color and translucency. The first set of dates obtained via this method were based on urine crystals selected from relatively large samples (~50 - 100 grams). These samples were believed to be representative of the pieces of the sample chosen for ^{36}Cl processing, which were likewise selected from a base sample size of approximately 50-100 grams. Subsequent dating and ^{36}Cl processing were performed on considerably smaller sample sizes, to minimize the risk of sampling across midden strata.

Results of $^{13}C/^{12}C$ analysis performed at NMIMT

Samples of crystalline urine material from four midden samples were analyzed by Andrew Campbell at New Mexico Tech for the $^{13}C/^{12}C$ ratio of the carbonate species. CO_2 was evolved from the samples by addition of phosphoric acid and the gas analyzed by mass spectrometer. Results are shown in Table 1.

Sample ID	$\delta^{13}C$ as provided by DRI	$\delta^{13}C$ from AMS urine sample	$\delta^{13}C$ of evolved CO_2	$\delta^{18}O$ of evolved CO_2	^{14}C age provided by DRI	^{14}C age from AMS of urine	^{14}C age from AMS of residue
PH140889 PEW1(1)	-24.3	-23.0	-4.7	37.8	1,180	2,494	-
PH140889 PEW2(1,2)	-24.5	-23.3	-24.3	29.2	8,560	11,684	12,550
PH211089 PEW1(1,3)	-22.0	-21.9	-23.2	29.2	28,560	25,126	31,155
PH180589 PEW3(2,1)	-23.2	-21.6	-30.6	19.3	16,280	21,731	31,375
PH150990 PEW1(1,6)	-21.8	-22.3	-35.7	6.4	20,784	32,888	31,220

Table 1. Results of $\delta^{13}C$ measurements of amberat samples made at New Mexico Tech and as reported in AMS dating of the urine samples. Samples shown in bold are from the Mother Midden.

Uranium - Thorium Dating

The production record of ^{36}Cl could be better evaluated, and perhaps extended further back in time, if another means of dating the middens could be used. To that end, we attempted to use uranium - thorium dating as an independent means of dating the middens. Uranium and thorium are both present in low concentrations in precipitation. While uranium forms several compounds that are soluble in water, thorium is strongly bound up in insoluble oxides. Water uptake by plants should thus include low concentrations of uranium but virtually no thorium. Because they derive their water solely from plants, packrats should therefore void urine with virtually no thorium After elimination, uranium contained in the crystalline urine would then decay to thorium with half-life of ~2.48×10^5 years. The ratio of ^{234}U to ^{230}Th in a midden sample should thus provide a reliable measure of the age of the midden, independent of the production rate of the cosmogenic nuclides.

To test this hypothesis, T. -L. Ku of the University of Southern California analyzed 6 subsamples of midden sample number PH 150990 PEW 1 (1,6) for uranium and thorium isotope ratios. Three of the subsamples consisted of fossil dung from the sample matrix and three of the subsamples consisted of crystalline urine. Uranium-thorium dating, based

on the hypothesis described above, indicated ages of approximately 240 ka. Several ^{14}C ages have been obtained for this sample, ranging from 21 to 33 ka. The large discrepancy in the two dating methods suggests that the packrats may ingest thorium-bearing particulate matter and that this thorium may then be mobilized in the rat's digestive system, perhaps by acidic conditions in the gut.

^{36}Cl Ratio Measurements

Chlorine-36/Cl ratios were measured by accelerator mass spectrometry at the Rochester Nuclear Research Structure Laboratory at the University of Rochester and at the Purdue Rare Isotope Measurement (PRIME) Laboratory at Purdue University.

Amberat Chemistry

Analyses for urea nitrogen and several inorganic cations and anions were performed on several midden samples to aid in chemical processing and to estimate concentrations of target elements for calculation of in-situ production of ^{36}Cl. Analyses for calcium, magnesium, potassium, sodium, chloride, bromide, HCO_3, fluoride, nitrate nitrogen and sulfate were performed by the New Mexico Bureau of Mines and Mineral Resources (NMBMMR). Analysis for nitrogen as urea was conducted by the Reference Laboratory, Inc., of Albuquerque, NM. Analyses for calcium, magnesium, potassium, sodium, chloride and bromide were also conducted by the Reference Laboratory, Inc. but those results did not agree well with the NMBMMR measurements. The discrepancy is likely due to differences in sample preparation or analytical methods. Full results of the Reference Laboratory, Inc. analyses are given in Appendix B.

Sample	HCO_3	F	Cl	NO_3	SO_4	Na	K	Mg	Ca	N as urea
LSM091282 LP1(1)	4360	4709	31393	11772	17441	2006	593	18313	21801	1221
PH140889 PEW2(1,5)	4425	4786	54539	3251	4605	34313	813	30701	18059	< 300
PH150990 PEW1(1,4)b	12765	2669	13114	638	3946	22049	1625	5919	18568	< 300
PH150990 PEW1(1,6)	18608	5514	6409	648	1309	80635	1654	1792	9649	< 300
PH180589 PEW3(2,1)	10446	4500	16874	3616	5384	24909	1045	9642	15267	482

Table 2. Results of analyses of 5 midden samples for standard water chemistry. Bromide concentrations were not measured because of nitrate interference. Concentrations are mg solute per kilogram midden material. Urea concentrations were measured by the Reference Laboratory, Inc., of Albuquerque, New Mexico. All other analyses were performed by the NMBMMR.

Results and Discussion

Radiocarbon Dates

Radiocarbon ages, chloride concentrations, and $^{36}Cl/Cl$ ratios for the samples are given in Table 3. In several cases, the dates obtained for this study did not agree well with the dates obtained for adjacent samples used in the paleo-ecology research. In many cases the discrepancies appeared to reflect proximity to midden strata boundaries, with the dates obtained for this study representing strata immediately adjacent to that analyzed in the previous paleo-ecology study. Figure 2-2, a field sketch of the Mother Midden and its sampling divisions, illustrates the general complexity which may occur in a composite midden. A large number of samples on the center right in the diagram are dated at ~33 ka. Immediately adjacent portions of the midden have dates ranging from ~3 ka to 26 ka.

Nevada middens	Chloride conc. (mg/Kg)	Macrofossil Uncorrected ^{14}C age (ka)	+/-	Urine Uncorrected ^{14}C age (ka)	+/-	Residue Uncorrected ^{14}C age (ka)	+/-	$^{36}Cl/Cl$ Ratio x 10^{12} Ratio	+/-	Decay-Corrected Ratio
LSM091282LP1(1) PRM..	33,488	1.090	0.070					0.513	0.031	0.514
PH140889PEW1(1)	14,648	1.180	0.080	2.494	0.048			0.679	0.028	0.683
PH270989CLN1(1)	27,285	2.580	0.090					0.463	0.024	0.466
PH140889PEW2(1,1)		3.050	0.090	2.817	0.046			1.082	0.047	1.089
PH211089PEW1(1,1)		4.070	0.090	4.433	0.051			0.608	0.110	0.614
PH120491PEW2(1, A & B)		9.700	0.090	8.469	0.074			0.662	0.044	0.675
PH150990PEW1(1,8)	26,085	8.760	0.170					0.601	0.045	0.613
PH140889PEW2(1,5)		24.580	0.470	11.793	0.102			0.981	0.066	1.008
" - acid		24.580	0.470	11.793	0.102			1.044	0.044	1.073
PH140889PEW2(1,3) "a"	2,543	11.190	0.110					1.428	0.084	1.468
PH140889PEW2(1,2)	2,855	8.560	0.120	11.684	0.105	12.550	0.075	1.227	0.067	1.262
PH140889PEW2(1,4)		11.530	0.160	12.160	0.098			Interf.		
PH140889PEW2(1,3) "b"		12.095	0.060	12.469	0.101			1.354	0.058	1.393
PH211089PEW1(1,5)		23.110	0.410					1.378	0.121	1.453
PH211089PEW1(1,6)	6,491	29.410	0.770					1.139	0.079	1.219
PH211089PEW1(1,3)	6,974	28.560	0.390	25.126	0.372	31.155	0.510	1.162	0.052	1.248
PH211089PEW1(1,2)-base	3,980	29.630	0.590	31.291	0.663			Interf.		
" - acid		29.630	0.590	31.291	0.663			1.096	0.039	1.178
PH180589PEW3(2,1)		16.280	0.160	21.731	0.251	31.375	0.520	1.164	0.082	1.251
" - acid	4,060	16.280	0.160	21.731	0.251	31.375	0.520	1.195	0.046	1.285
PH150990PEW1(1,6) (tp and bt)		20.784	0.245	32.888	0.929	31.220	0.485	1.465	0.064	1.577
PH180589PEW3(2,1)				32.720	0.300			1.330	0.110	1.434
PH150990PEW1(1,4)B				32.870	0.280			1.270	0.080	1.370
California middens										
Chidalgo Flats 2A	6,086	5.110	0.070					1.470	0.040	1.487
Chidalgo Flats 4B	12,492	9.290	0.060					1.150	0.050	1.175
Redrock Canyon 7A	2,559	9.630	0.070					1.480	0.070	1.513
Volcanic Tableland 4E	3,343	12.430	0.100					0.700	0.062	0.720
Volcanic Tableland 5A	12,013	13.050						1.350	0.090	1.391
New Mexico middens										
JLB SLP 41A	9,182	0.510	0.100					0.726	0.027	0.727
JLB SLP 46	6,459	0.680	0.060					0.802	0.045	0.803
JLB SLP 44C		0.840	0.065					0.743	0.019	0.744
JLB SLP39		0.905	0.060					0.913	0.045	0.915
JLB SLP 21	5,401	0.965	0.065					0.945	0.033	0.947
JLB SLP 19		1.230	0.060					0.662	0.008	0.664
JLB OWL CANON 30		1.290						1.360	0.017	1.364
JLB SLP 44A	5,927	1.335	0.065					0.727	0.025	0.729

Table 3. Midden dates, chloride concentrations, and $^{36}Cl/Cl$ ratios.

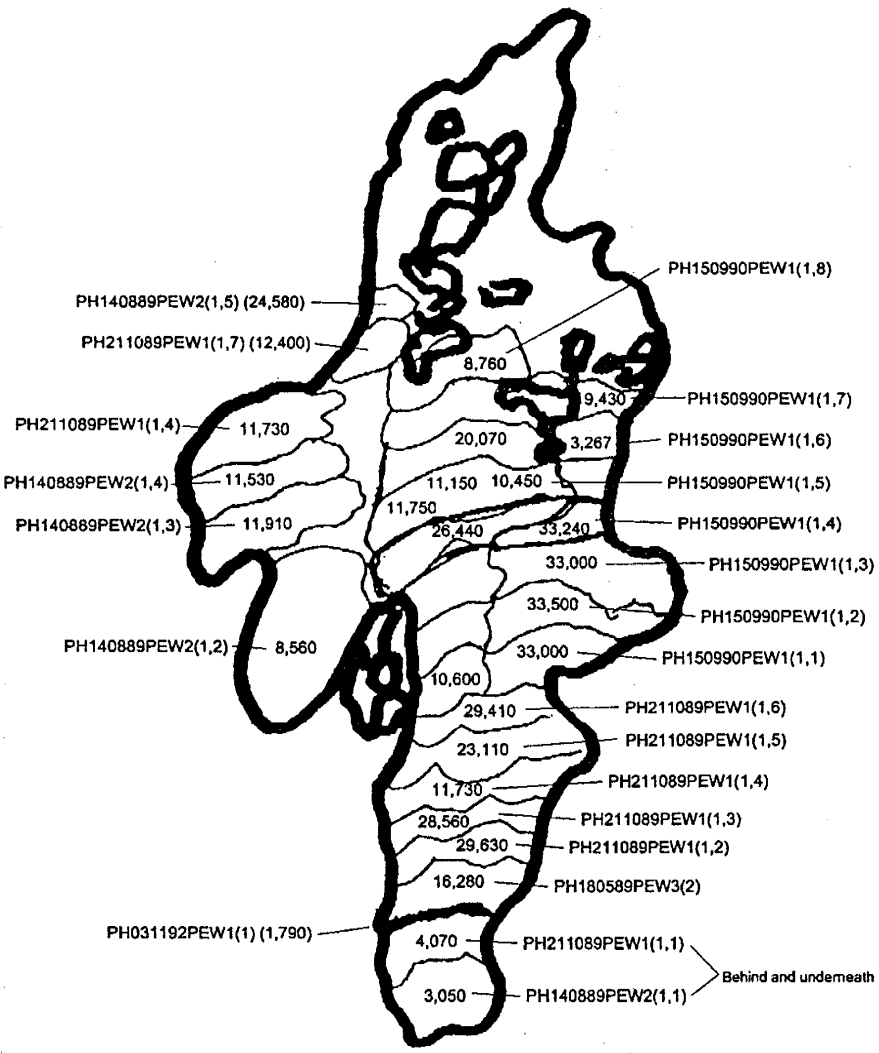

Figure 2-2. Field sketch of front face of the Mother Midden. Sampling divisions and associated dates (ka) are based on paleoecology studies of Peter Wigand of DRI, Reno. Vertical dimension is ~1.5 meters. Redrawn from a sketch provided by Peter Wigand.

Figure 2-3 is a comparison plot of age based on plant material to AMS ages for the crystalline urine. While some of the discrepancies are relatively large, most of these are probably due to unaccounted-for spatial distribution of midden strata within the samples used. In particular, the proximity of many very old samples to samples of a wide variety of ages probably explains the large discrepancies in some of the older samples.

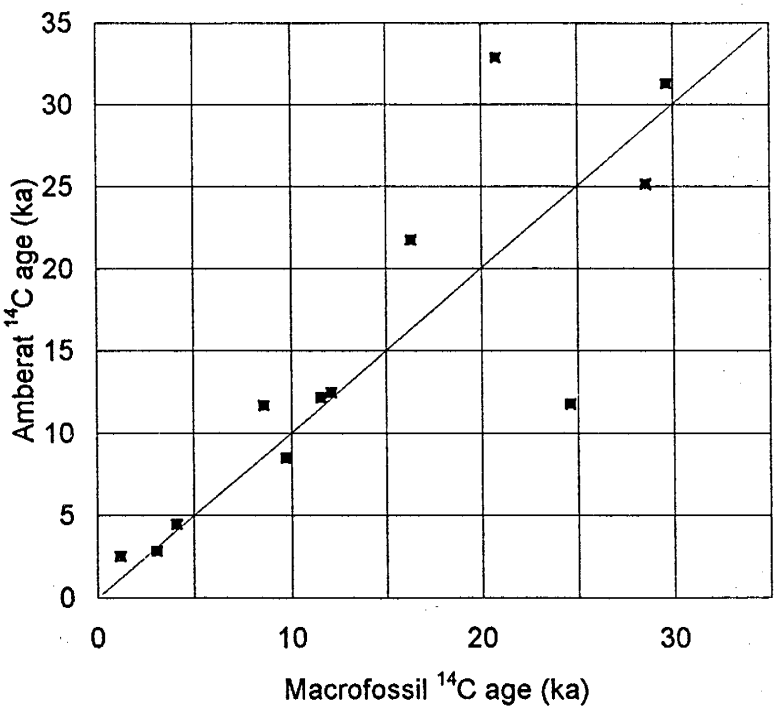

Figure 2-3. Comparison of macrofossil ^{14}C ages with ^{14}C ages of the crystalline urine.

Four of the midden samples were also dated by ^{14}C measurements of the plant debris remaining after processing the samples for ^{36}Cl analysis. In two cases, these dates were dramatically different than the dates obtained from directly dating the urine. In such cases, I contend that the plant material dates are more indicative of the actual age of the sample, because the date is based on the same subsample as the ^{36}Cl measurement. While this invites criticism based on the argument that the urine may have flowed into older portions of the midden, I believe that spatial variations within the midden represent a greater problem for dating than the possibility that the urine has flowed independently of the matrix which it cements.

The variability in the ages obtained for some of the Nevada middens is believed to be due to the proximity of strata of widely differing ages within the Mother Midden. Samples provided to us for this study may have inadvertently included portions of adjacent midden layers that were not included in the original sample used in the paleo-ecology study. It is also possible that the conflicting dates are due to more fundamental problems of establishing dates for portions of composite middens. The midden undergoes rather dramatic changes in the course of becoming an indurated mass, so that a crystalline urine sample might not be contemporary with the plant detritus that it cements. Spaulding *et al.* note [in Betancourt and Van Devender, 1990, p. 63]

We have observed active houses "roofed" with a rind of crystallized urine and pellets. Conceivably, after abandonment the collapsed stick lattice that provides structural support for passageways and chambers combines with urine in the process of rehydration to form middens. We have observed late Pleistocene "houses" in an intermediate stage of collapse in caves on the Colorado Plateau. The loose latticework contained recognizable nest and food chambers subtending an indurated surface. This structure may be inconsistent with the idea that a house "melts" through time to produce a single midden. However, ancient middens frequently have obvious stratigraphy with layers just a few millimeters thick.

Again, some researchers have suggested that, under humid conditions, the highly hydrophilic amberat may flow independently of the plant detritus within the midden:

Packrat middens are composed of soluble and insoluble organic matter, dust, and rocks. Most ancient middens are indurated, and many resemble blocks of asphalt with the consistency and mass of an unfired adobe brick. Crystallized packrat urine, called amberat, saturates plant fragments, pellets, and other debris, encasing them in an amber like matrix... Two kinds of rinds are found on ancient middens: lustrous coats that resemble solidified asphalt or molasses, and lusterless rinds that are frequently convoluted and bear many fine desiccation cracks. The shiny coats develop where recently liquefied amberat has crystallized. A fresh break on the surface of an indurated midden will, over a period of months, become covered with a shiny layer of redeposited amberat. This occurs because amberat is hygroscopic and, during infrequent humid periods, it will rehydrate. It then flows by capillary action to the surface of any fresh break, where it recrystallizes to form a glossy layer. Amberat is hard and smooth to the touch when the air is dry, but sticky and soft when the air is moist. Thin sections show undulating layers (about 0.05 mm thick) of microcrystalline minerals (0.005 mm maximum diameter) and minor amorphous material, with occasionally larger (0.05 mm) detrital inclusions. The coarser microcrystalline material results from recrystallization, which fills desiccation cracks in the weathering rinds (Emerson and Howard, 1978). .... Although the process of rind formation has not been studied, it is likely that dust and organic debris accumulating on glossy surfaces over long periods block the free exchange of moisture between the midden and the atmosphere. Therefore, through the hygroscopic property of amberat, indurated middens appear to be self-sealing (Spaulding, 1985) [Spaulding et al., 1990, in Betancourt and Van Devender, 1990, p. 60].

While it does seem possible that the matrix as a whole may flow, it seems likely that it should do so only as a plastic deformation, more akin to the flow of a glacier transporting bedload than to liquid transport. In the middens I have sampled during this study, it is evident that the crystalline urine acts very much as a cement for the major component of the middens - plant detritus. In these middens, the prospect for flow of small zones of relatively pure crystalline material through the dense fibrous plant material seems very

unlikely. In any case, microscopic examination of numerous midden samples has not revealed any evidence, such as elongated air bubbles, that would suggest that such flow has taken place within the midden. The above descriptions suggest that the more likely problem in relating amberat and plant detritus dates is that the urine may be initially deposited on a non-indurated portion of a previous midden. For this reason, it is clearly preferable to date the amberat itself.

$^{36}Cl/Cl$ Ratios

$^{36}Cl/Cl$ ratios measured in middens from each of the three study areas exhibit considerable variation. Middens in the New Mexico series range in age from about 500 years to 1,400 years and $^{36}Cl/Cl$ ratios range from ~0.9 to 2 times the estimated present-day ratio (~1.3 x 10^{-12}) for precipitation in the area. Middens in the California series range from about 5 ka to 13 ka in age and relative $^{36}Cl/Cl$ ratios range from ~0.5 to 1.2 x 10^{-12}. Nevada middens, most of which were obtained from the large, composite, Mother midden, range from approximately 1 ka to 33 ka in age with $^{36}Cl/Cl$ ratios ranging from ~0.5 to 1.6 x 10^{-12}. Further discussion of each of these data sets follows.

Corrections for Radioactive Decay and In-situ Production of ^{36}Cl

^{36}Cl is produced in the shallow lithosphere as well as in the atmosphere, which makes possible dating of geomorphic surfaces based on the amount of ^{36}Cl produced during their exposure at the surface. The in-situ production is mainly through spallation of ^{35}Cl and via neutron capture of ^{40}Ca and ^{40}K so that this component of production must be evaluated in the packrat middens, where concentrations of these target elements may be relatively high.

To evaluate the contribution of in-situ production to the amount of ^{36}Cl contained in the fossil middens, we estimated spallation and neutron capture rates at the Mother Midden. These estimates account for the effects of elevation, latitude and topographic shielding. The in-situ production rates are highly dependent on concentrations of the target elements. In general, the significance of in-situ production increases as the concentration of Cl decreases and concentrations of the spallation targets (Ca and K) increase. Chlorine-36 production via neutron capture is relatively insignificant because the mass of atmospherically

produced ^{36}Cl also increases as the concentration of the target element (^{35}Cl) increases. We can estimate concentration ratios of the target elements from the results of chemical analyses of the amberat shown in Table 2. The fraction of ^{36}Cl contributed by in-situ production, for a midden with a $^{36}Cl/Cl$ ratio of ~500 x 10^{-15}, is then easily integrated from the production rate for a nuclide produced at a constant rate that undergoes radioactive decay. Results for a range of concentrations of the three target elements are shown in Figure 2-4.

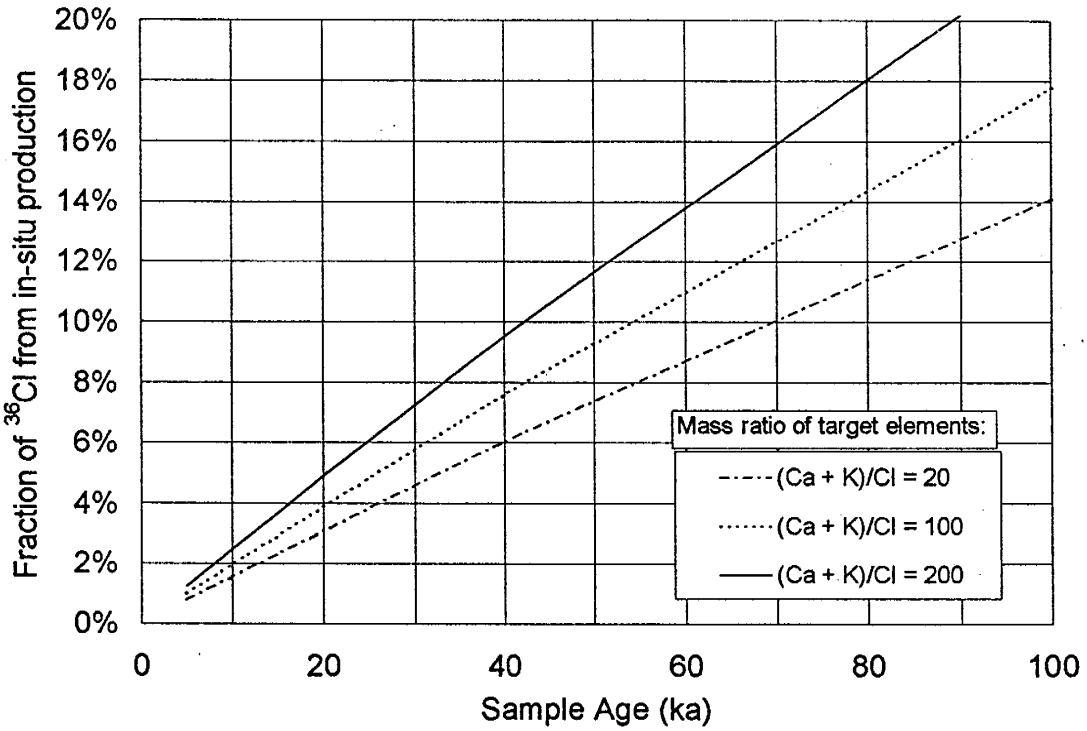

Figure 2-4. Calculated fraction of amberat ^{36}Cl contributed by in-situ production for different ratios of neutron capture target elements (Ca & K) to the spallation target element (Cl). $^{36}Cl/Cl$ Ratio is conservatively assumed to be 0.5 x 10^{-12}.

I conservatively estimate that the concentrations of Ca and K in the amberat may each be as high as 50 times the Cl concentration. The concentrations of the target elements in the urine should be roughly proportional so that it is unlikely that the ratio of Ca + K to Cl would be higher than about 200. For such a ratio, the fraction of in-situ produced ^{36}Cl in the amberat increases approximately linearly to about 8% at ~33 ka. This correction is of approximately the same magnitude as the correction that would be applied to account for

radioactive decay from the initial ratio in the urine. Because these corrections are opposite in direction but similar in magnitude, and because the chemical data are not available for accurate in-situ calculations, I have chosen not to correct for either effect in the following analyses. Ratios discussed below are, therefore, simply the ratios reported by the AMS laboratory.

Duplicate Samples

For each of three samples {PH140889 PEW2 (1,5); PH211089 PEW1 (1,2); and PH180589 PEW3 (2,1)} two samples were submitted for $^{36}Cl/Cl$ ratio measurement. Two of the duplicate samples {PH140889 PEW2 (1,5) and PH180589 PEW3 (2,1)}were obtained from different subsamples of the same midden sample. The other duplicate was obtained by splitting the urine solution during processing to assess the effect of slight variations in the processing method. The latter set of duplicate samples produced only one useful ^{36}Cl measurement. The modified processing method produced a sample insufficiently free of contaminants to allow measurement. The other sets of duplicates yielded $^{36}Cl/Cl$ ratio variations of less than ~6%.

Nevada Middens

The record of $^{36}Cl/Cl$ ratio variation preserved in the Nevada middens (Figure 2-5) is somewhat complicated by differences in dates obtained on several replicate samples. The reasons for some of these discrepancies are discussed later. In general, the dates initially estimated from macrofossil dating of other samples were not reliable. Eliminating these dates yields the record of $^{36}Cl/Cl$ variation shown in Figure 2-6.

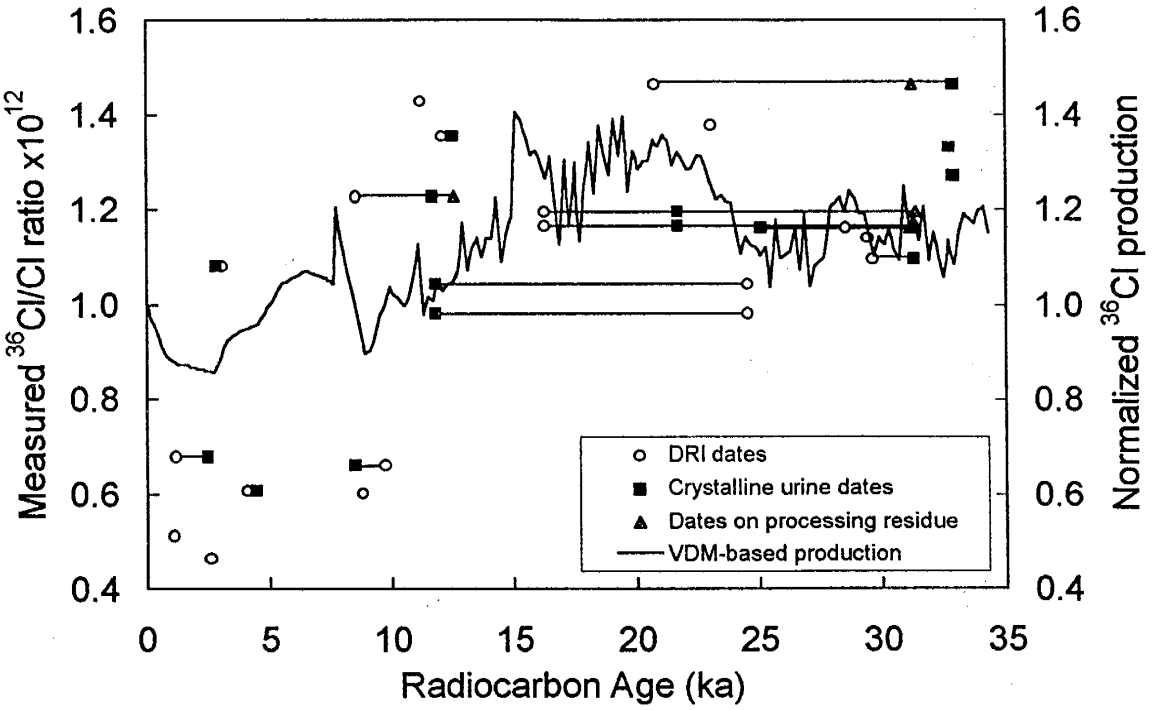

Figure 2-5. Plot of Nevada midden ^{36}Cl/Cl ratios versus age (symbols) and the production variation expected based on the paleointensity (VDM) record of Tric et al. (1992) (solid line). The VDM-based production record is arbitrarily normalized to a ^{36}Cl/Cl ratio of 1.0 x 10^{-12}. Most of the midden samples analyzed for ^{36}Cl have been dated independently of the original DRI dates. Original dates, from similar subsamples dated by DRI, are shown as open circles; crystalline urine dates, based on subsamples of the sample provided to NMIMT, are shown as solid squares; dates based on the plant detritus remaining after processing a sample for ^{36}Cl measurement are shown as shaded triangles. Solid horizontal lines connect points representing different dates on the same sample. Parallel line segments with identical age distributions represent duplicate ^{36}Cl measurements.

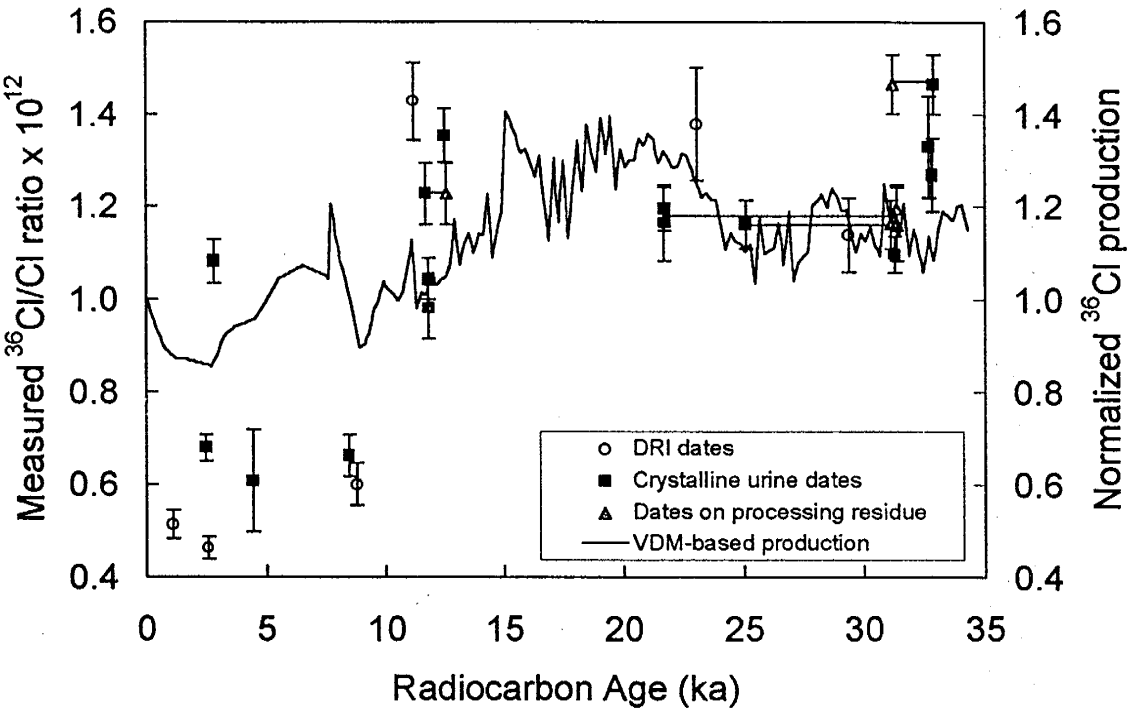

Figure 2-6. VDM-based ^{36}Cl production signal and ^{36}Cl/Cl ratios of midden samples from Nevada. Error bars are for the ^{36}Cl/Cl measurement. Symbols are as described in Figure 2-5. Where other dates are available the DRI dates are not shown. Lines connect multiple dates for the same sample. The VDM-based production record is arbitrarily normalized to a ^{36}Cl/Cl ratio of 1.0 x 10^{-12}.

^{36}Cl/Cl ratios in the middens from western Nevada exhibit considerable temporal variability at a time scale of several hundred to ~2000 years. These short period temporal variations appear however to be superimposed on a larger trend defined by three distinct groups of data points. These are located at approximately 1 to 9 ka, 11.5 to 12.5 ka, and 29 to 33 ka. While the dating uncertainty for some of these points is relatively high, several points within each group are considered relatively well constrained in age. Six of seven samples with ages younger than ~9 ka yielded ^{36}Cl/Cl ratios lightly less than 0.7 x 10^{-12}. This is relatively close to the modern pre-bomb ratio of infiltration of ~0.5 x 10^{-12}, as measured in soil moisture at the Nevada Test Site [Fabryka-Martin, (in press)]. In contrast, all of the ^{36}Cl/Cl ratios of samples older than 11 ka are at least 100% higher than that ratio. In the group of samples dated between ~11.5 and 12.5 ka, all three of the urine-dated samples lie on a line indicating a sharp decrease in ^{36}Cl/Cl ratios from ~11.8 ka to 12.5 ka. The ^{36}Cl/Cl ratios in this group range from ~1 to 1.5 x 10^{-12}. Another data point in that group, dated at ~11.9 ka, does not fit the same trend but also exhibits a relatively high ^{36}Cl/Cl ratio (~1.5 x 10^{-12}). The latter

sample is dated only by correlation with the sample processed by the cooperating paleo-ecologist. Most of the remaining midden samples fall within an age range of ~29 to 33 ka. These samples, and the one sample dated at ~23 ka have relative $^{36}Cl/Cl$ ratios ranging from approximately 1.2 to 1.6 x 10^{-12}.

Some high-frequency variation in the $^{36}Cl/Cl$ ratios is expected. The ^{36}Cl production rate is expected to vary due both to geomagnetic and solar modulation effects. The length of time averaged within each midden sample is unknown but may well be less than 100 years. If so, the midden record may be capable of recording the 200-year periodicity of solar modulation. As shown in Figure 1-6, the sensitivity of ^{36}Cl production to solar activity is only slightly less than for ^{14}C and ^{10}Be at low solar activity and slightly greater at high solar activity. Unfortunately, while the record is theoretically capable of exhibiting those variations, the low sampling frequency effectively eliminates our ability to resolve such variations.

Based on the paleomagnetic record, $^{36}Cl/Cl$ ratios during the past ~30 ka would be expected to vary by about ±30% of the modern ratio, with a peak in production (between 22 ka and 15 ka) approximately 150% greater than the lowest value (at about 3 ka). In the Nevada midden data, $^{36}Cl/Cl$ ratios before ~12 ka appear to be at least 300% greater than ratios during the Holocene, a difference that is two times larger than that calculated from the paleo-intensity record. The abrupt decrease in production between ~11 and 9 ka is consistent with the results of Edwards *et al.* [1993] which also indicate a dramatic decrease (~300 per mille) in atmospheric ^{14}C activity from about 11 ka to 10 ka (^{14}C age) (Figure 1-5). The magnitude of the trend is, however, much greater than the total decrease in ^{14}C seen in the coral studies. As discussed in the previous section, concentrations of ^{36}Cl and ^{10}Be in Greenland ice (Figure 1-11) [Suter *et al.*, 1987] also exhibit a dramatic decrease during the transition from the Pleistocene to the Holocene. That change is, however, generally attributed to a change in the precipitation rate rather than a change in the cosmogenic nuclide production rate.

The high $^{36}Cl/Cl$ ratios of the middens older than ~20ka suggests that the production rate of ^{36}Cl could have been stable at a level about 2.5 times the modern rate up until the end of the Pleistocene. While this trend does not compare favorably with the VDM-based signal, it is consistent with the Bard *et al.* [1990] data which, prior to ~15 ka, exhibit a significant positive discrepancy between measured $\Delta^{14}C$ values and the VDM-based signal for ^{14}C activity [Mazaud et al., 1992].

California Middens

Only five midden samples, ranging from ~5 to 13 ka in age, were obtained from the area north of Bishop, California. With the exception of the ~12.5-ka sample, the $^{36}Cl/Cl$ ratios of these samples (Figure 2-7) are quite high, ranging from ~1.2 to 1.5 x 10^{-12}. The remaining sample has a measured $^{36}Cl/Cl$ ratio of ~0.75 x 10^{-12}. The large variance in the ratios and the few samples available preclude demonstration of a distinct temporal trend in the ratios at this location. The location and climatic situation suggests that the modern, pre-bomb $^{36}Cl/Cl$ ratio here would be similar to that of the Nevada Test Site, approximately 0.5 x 10^{-12}; no clear explanation is apparent for the relatively high measured ratios.

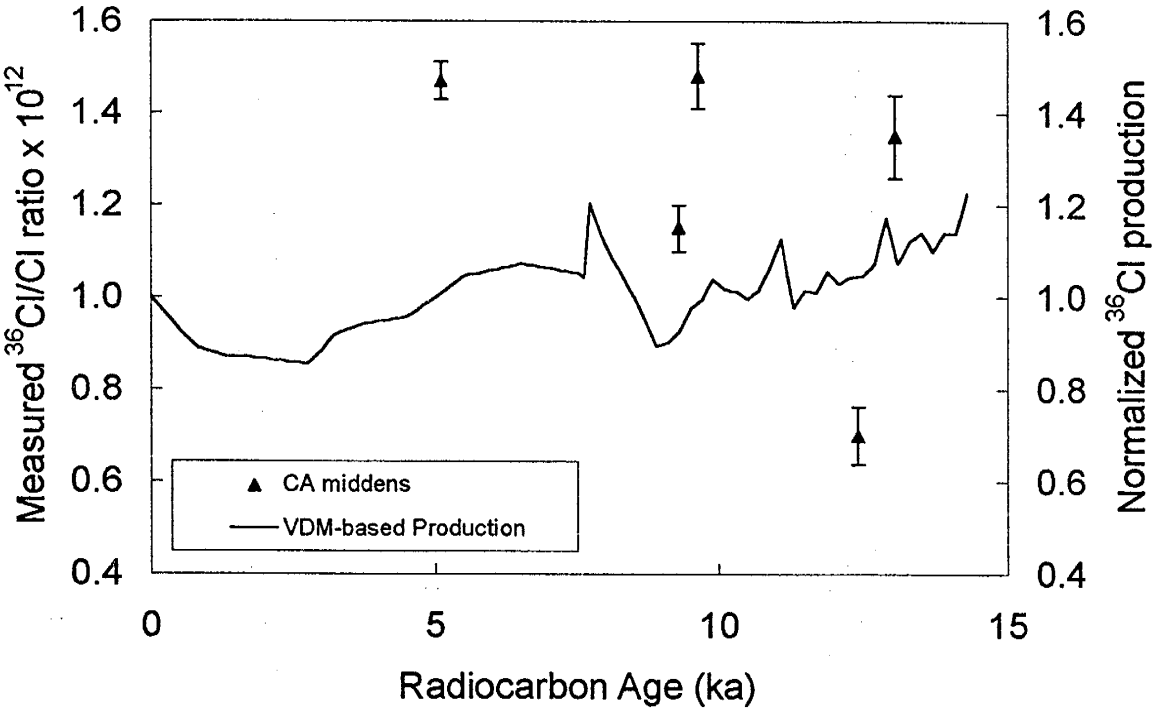

Figure 2-7. Plot of California midden ^{36}Cl/Cl ratios versus age with error bars for the ^{36}Cl measurement. Also plotted is the VDM-based production signal arbitrarily normalized to a ^{36}Cl/Cl ratio of 1.0 x 10^{-12}.

New Mexico Middens

With the exception of one sample dated at ~1.3 ka, ^{36}Cl/Cl ratios of the New Mexico middens range from approximately 0.65 to 0.95 x 10^{-12} (Figure 2-8). Notwithstanding the outlier at ~1.3 ka, this ~45% range is considerably greater than would be expected based on the paleointensity record. The ^{36}Cl/Cl ratio of modern pre-bomb infiltration, as measured in shallow soil moisture samples from an area just north of Socorro, is ~0.7 x 10^{-12} [Phillips et al., 1989].

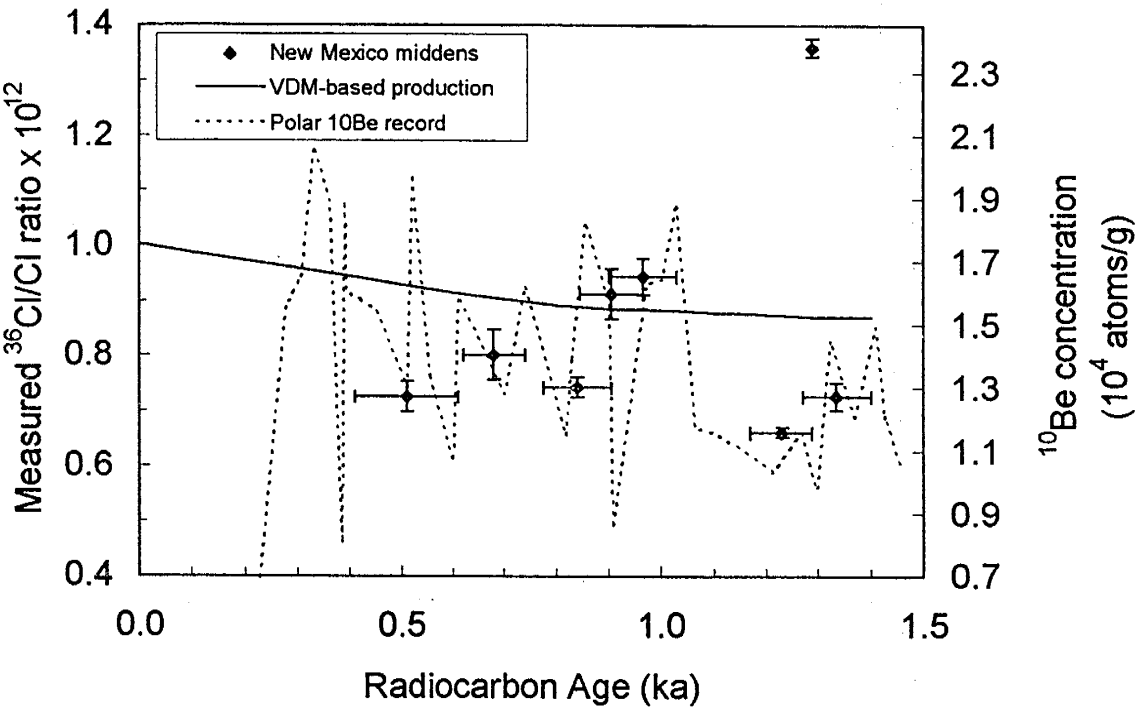

Figure 2-8. Plot of New Mexico midden $^{36}Cl/Cl$ ratios versus age. Also plotted are the VDM-based production signal and the polar ^{10}Be concentration record of Beer et al. (1988) from Camp Century. The VDM-based production signal is arbitrarily normalized to a ratio of 1.0×10^{-12}.

Global dipole field variations for the past ~3 ka are relatively well established [Tauxe, 1993] and these data suggest that relatively little variation has occurred during that time. The sampling interval for paleointensity measurements for that period is, however, relatively large and it is possible that significant variation is not recorded due to that sampling frequency. It is also possible that the sampling frequency of the middens and their temporal averaging allows sampling of the higher frequency effects of solar modulation. The effect of solar modulation on cosmogenic isotope production appears to be well recorded in polar ^{10}Be archives. As described previously, Beer *et al.* [1988] argue that the record of ^{10}Be concentrations in the Camp Century ice core is a proxy for isotope production as modulated by solar activity. If the New Mexico midden data are compared with this record, it is evident that the observed variation is consistent with the degree of variation expected to result from solar modulation. There is little reason to expect, however, that such variability would have occurred only during the past several thousand years. If the observed variation in the NM middens is due to solar modulation of cosmic nuclide production, then

one would expect to see similar variability at all time-scales, which does not appear to be the case for the samples from Nevada.

Alternative Explanations for $^{36}Cl/Cl$ Variations in the Midden Record

Overall, the variability of the $^{36}Cl/Cl$ ratios in the midden records is significantly greater than would be expected based on the Tric *et al.* VDM history. If the $^{36}Cl/Cl$ ratios of the middens accurately reflect atmospheric ^{36}Cl production variations, this implies that the available paleomagnetic data may not be a reliable record of global magnetic field intensity variations or that the production rate variations caused by geomagnetic variations are not well understood. Conversely, factors other than production rate variations may affect the $^{36}Cl/Cl$ ratios preserved the middens, possibly masking the VDM signal. Such factors might include variations in the flux of stable chloride or in the nature of atmospheric mixing of ^{36}Cl with stable chloride. Further discussion of several possible explanations for the observed discrepancy between the midden record and the calculated production signal based on paleointensity data follow.

Non-representative Paleointensity Measurements

Error measurements of one standard deviation above and below the measured paleointensity values are given in the Tric *et al.* [1992] data. While the resultant range exhibits considerable latitude, many of the midden $^{36}Cl/Cl$ ratios from each of the three data sets still fall outside the calculated range. In addition, $\Delta^{14}C$ reconstructions from dendrochronology and Barbados corals seem to suggest that the curve defined by the measured values averages the errors quite well. There is, however, substantial variation among different paleointensity data sets that are believed to represent global changes in the magnetic field. The averaging of these data sets does not necessarily provide the most accurate record of paleo-variations and it is possible that global paleointensity variations are quite different from those described by Tric et al. [1992].

The temporal resolution of the Tric *et al.* paleointensity data is given as less than 400 years, "which is not significantly different from the 200 years averaged over the size of a single sample" [Tric *et al.*, 1992]. The sampling period for any of the packrat midden samples,

which may be extended through averaging of water sources available to the plant species which the rat eats, is, on the other hand, may be considerably less than 100 years. It is possible then that high frequency variations in production may be recorded in the middens which are not recorded in the paleointensity record. While such high-frequency variation may help to explain the variability in the New Mexico and California middens, the Nevada middens appear to indicate a long-term trend in $^{36}Cl/Cl$ ratios independent of smaller time scale variations.

Solar Modulation or Stratosphere-Troposphere Exchange Pattern

Beer *et al.* [1988] argue that variations in ^{10}Be concentrations in the Camp Century and Milcent Station ice cores reflect solar modulation of production. The amplitude of that modulation is comparable to the overall amplitude of the long-term variations anticipated to result from geomagnetic intensity changes. If the ^{10}Be data do indeed reflect solar modulation of production, ^{36}Cl should be similarly affected. This could explain the high-amplitude, high-frequency variations observed in the $^{36}Cl/Cl$ ratios of middens from New Mexico. However, this is not borne out by the ^{36}Cl concentrations measured in polar ice [Elmore *et al.*, 1987; Suter *et al.*, 1987] or in old wines from Germany [Priller *et al.*, 1990]. In addition, the long-term variations in the ^{10}Be concentration data do not support the hypothesis that long-term variations are due to geomagnetic modulation of production. Lal [1987] argued that the ^{10}Be concentration variations observed in the ice cores are too large to be due to solar effects, which should produce variations of ~20% or less. He argues that the ^{10}Be concentration variations are due to climate effects or possibly to changes in the stratosphere-troposphere interaction pattern. If so, ^{36}Cl in ice, wine and packrat middens might be similarly affected. In summary, although the New Mexico middens suggest that large amplitude variations in $^{36}Cl/Cl$ ratios do occur, the data appear insufficient to suggest that the forcing function is solar. Chlorine-36/Cl ratios in the middens from California and Nevada do not in general have sufficient resolution to reflect such high frequency variations.

Stable Chloride Fallout Variability

Some of the observed variation in $^{36}Cl/Cl$ ratios may be due to fluctuations in the rate of stable chloride deposition within the study areas. As discussed in Section One, while the

overall chloride flux from the ocean to the continental interior is presumed to be relatively stable, it is likely that significant variations have occurred in that flux over the time-scale of interest here. It is also likely that other sources of chloride contribute to the stable chloride flux in the study areas. Significant variations in the availability and/or transport of other chloride sources during the period of interest could have a commensurate effect on the $^{36}Cl/Cl$ ratios preserved in packrat middens.

Local Sources of Stable Chloride Variability in Nevada

During the Pleistocene epoch, pluvial lakes existed in the many of the basins in Nevada [Mifflin and Wheat, 1979], including many in the region surrounding the Virginia Mountains. Pyramid Lake and nearby basins are part of a group of seven major basins comprising Lake Lahontan during the late Wisconsin. This includes the Smoke Creek Desert and Black Rock Desert basins to the north of Pyramid Lake, the now dry Winemucca Lake basin east of Pyramid Lake, Carson Sink to the southeast, Cold Springs Valley to the southwest, and a small unnamed basin directly northwest of the Virginia Mountains. With the end of the Pleistocene and change from a relatively humid climate to the present arid conditions, most of these lakes were "eventually evaporated to dryness and the dissolved salts were deposited in the upper part of the sediments, producing modern playas or playa lakes" [Papke, 1976]. In some, salt was present in sufficient quantity to allow its exploitation as a mineral resource. Papke [1976] reports that a small amount of salt was produced from the surface crust of a small playa near Buffalo Springs on the west side of the Smoke Creek Desert: "The area of production is a playa about 1,000 feet in diameter surrounded by low hills. An auger hole 5 feet deep in this playa showed that the clay material contains some soluble salts, principally halite." Salt deposits exploited at White Plains included a "1- or 2-inch-thick crust of impure halite" that covered several hundred acres. Figure 2-9 depicts the extent of playas and saline deposits existing in the region surrounding the Virginia Mountains.

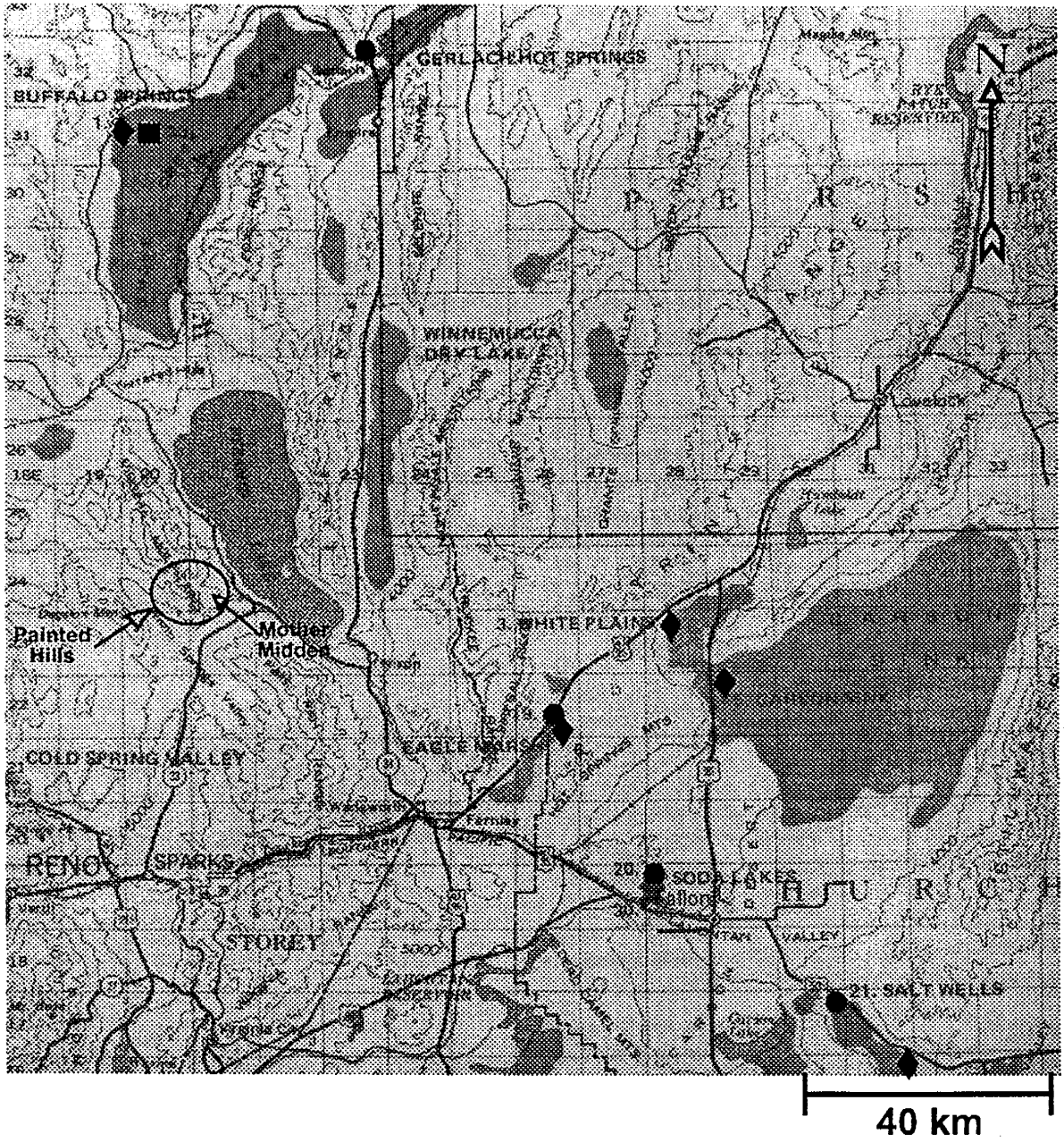

Figure 2-9. Major playas and saline deposits in western Nevada. Darker shaded areas are playas. Diamonds represent halide deposits; circles are borate, x's are sodium carbonate, and squares are sodium sulfate deposits. From Papke, 1976.

Presumably such large sources of chloride would have produced significant amounts of aerosols as the playas began to form. Indeed, in a study of a series of soil profiles in the Lahontan area, Chadwick and Davis [1990] emphasized the importance of eolian dustfall in soil formation in the region, noting that the influx of eolian fines and salts in the soils was concentrated during two brief intervals, one during the Holocene and one during the

previous interpluvial. Thus there may have been a significant increase in eolian deposition of fines and soluble salts in the Virginia Mountains with the onset of the Holocene. This would have substantially reduced $^{36}Cl/Cl$ ratios in infiltration in the area if the dustfall included a substantial amount of chloride salts. Studies of similar playa chloride sources by Phillips *et al.* [1995] indicate that the $^{36}Cl/Cl$ ratio of salts from such basins is generally lower than 0.1×10^{-12}.

The current shoreline of Pyramid Lake is approximately 1160 m above sea level. Studies of paleo lake levels in the Lahontan Basin indicate that the lake reached its 1330-m highstand approximately 13,800 ^{14}C years B.P. and receded to 1310 m by ~13,700 B.P. [Benson, 1993]. ^{14}C ages of deposits which constrain the lake level decline from its highstand are shown in Figure 2-10. A combination of ^{14}C dating of lacustrine carbonates and packrat middens in the basin indicates that further decline in the lake levels occurred relatively rapidly; by ~12,000 B.P. the shoreline was below 1230 m [Thompson *et al.*, 1986]. This suggests that the maximum rate of lake level decline was approximately 5 m/100 yr, which agrees reasonably well with the 6m/100 yr rate proposed for the higher elevation Lake Bonneville [Scott *et al.*, 1983 in Thompson *et al.*, 1986]. The rate of decline below 1230 m is less well constrained but if decline were to have continued at the same rate, the lake would have receded to near its current level before 11,000 yr B.P..

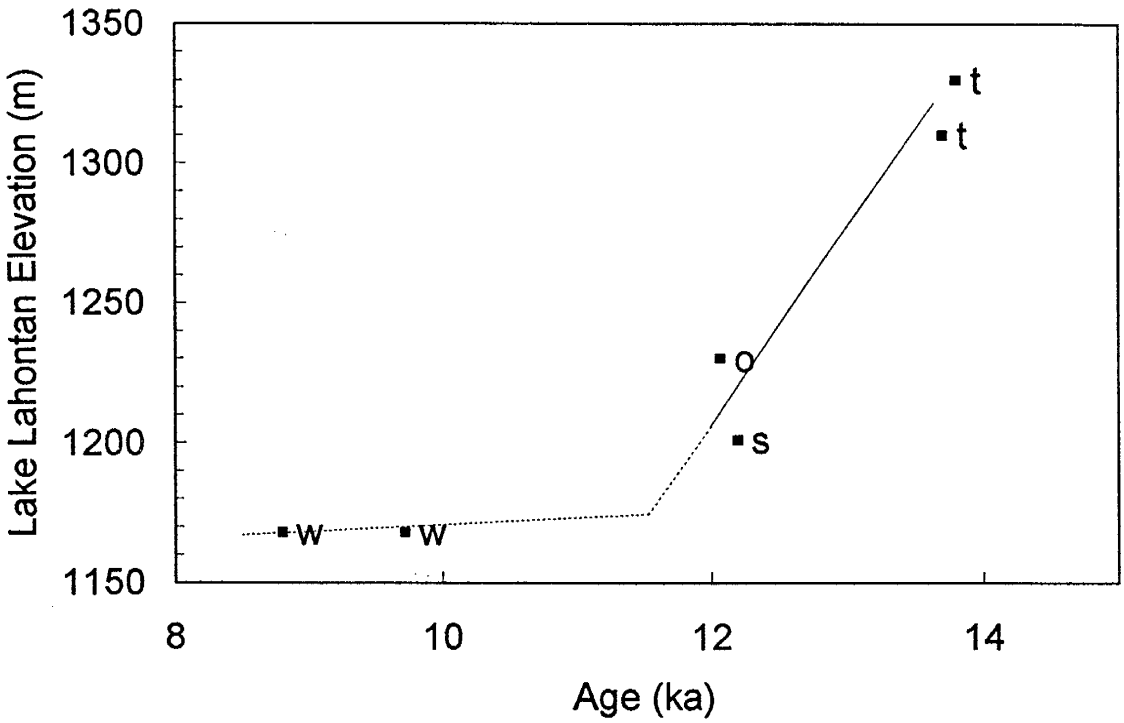

Figure 2-10. Revised chronology for Lake Lahontan from 14 to 8 ka with radiocarbon dates and tephrochronological data from the central Lahontan Basin upon which it is based. Key to symbols for material dated: o = noncarbonate organic material from pack rat middens, w = delta slope wood, t = lithoid tufa, s = ostracods. The line indicates my interpretation of the lake level chronology data; dashed portion indicates area of greater uncertainty. Revised from Thompson et al., 1986 based on corrected tufa ages of Benson et al., 1993.

The available chronology suggests that playas probably began to form and expand rapidly as Lake Lahontan receded into the present day playa basins between 12 and 10 ka B.P. This is generally consistent with the midden data which indicate a rapid decrease in $^{36}Cl/Cl$ ratios between ~12 and 9 ka.

It seems certain that the onset of the Holocene increased the surface area of playas capable of contributing halides to the atmosphere. That these playas actually contributed significant amounts of chloride to the atmosphere, and more specifically, increased the chloride fallout to the Virginia Mountains is considerably less obvious. Based on 29-year average wind directions at stations north and south of Pyramid Lake, the prevailing wind direction in the Pyramid lake area is west[1]. It is possible then that most of the salts removed from paleo-

[1] From "Normal, Means and Extremes" data for Reno and Winnemucca, Nevada, provided by the State Climate Office, Reno, Nevada.

Lake Lahontan playas would have been transported eastward, away from the Virginia Mountains, thereby having a negligible effect on stable chloride fallout in the vicinity of the Nevada middens sampled. On the other hand, large-scale mixing processes in the atmosphere make prediction of the fallout pattern of locally introduced aerosols considerably more complex than that. Further conclusions regarding the potential impact of aerosols removed from these playas would require further knowledge of atmospheric transport and distribution of continental aerosols. As discussed in Section One, the impact of continental aerosols on chloride concentrations in recharge is poorly understood at present.

Longer Time-Scale Sources of Stable Chloride Variability

While the proximity of large sources of dry chloride suggests that a local phenomenon may explain the Nevada data, it is also possible that significant long-term variations may occur in the flux of stable chloride from the oceans to the continental interior. The Mayewski *et al.* [1993] record of stable Cl flux in the GISP 2 core (Figure 1-14) and the data of Legrand *et al.* [1988] from the Vostok ice core (Figure 1-15) both indicate a substantial decrease in both chloride flux and flux variability at the termination of the Younger-Dryas. If a similar decrease in stable chloride flux occurred at that time in western Nevada, we might anticipate generally greater $^{36}Cl/Cl$ ratios during the Holocene, opposite the trend actually seen in the Nevada midden data.

NADP Data & High-Frequency Temporal Variations in Modern Precipitation Chemistry

Since approximately 1978, a number of cooperating US agencies and universities under the leadership of the USGS have maintained a large precipitation chemistry sampling network within the United States. This network, known as the National Atmospheric Deposition Program (NADP), was developed as part of an effort to establish a long-term data base of precipitation chemistry for studies of acid rain. The network consists of approximately 200 sites at which weekly measurements of several ionic constituents including chloride were performed starting about 1978. Collection sites in the arid portion of the southwest included four sites in Nevada, ten in California and five in New Mexico (Figure 2-11).

Sampling began at most of these sites in 1984. Precipitation-weighted chloride concentration data from these sites provide an excellent means of assessing very short-term temporal variability of chloride flux. The short duration of the program, however, does not allow evaluation of longer-term (decadal to centennial scale) trends such as might be represented in the packrat middens.

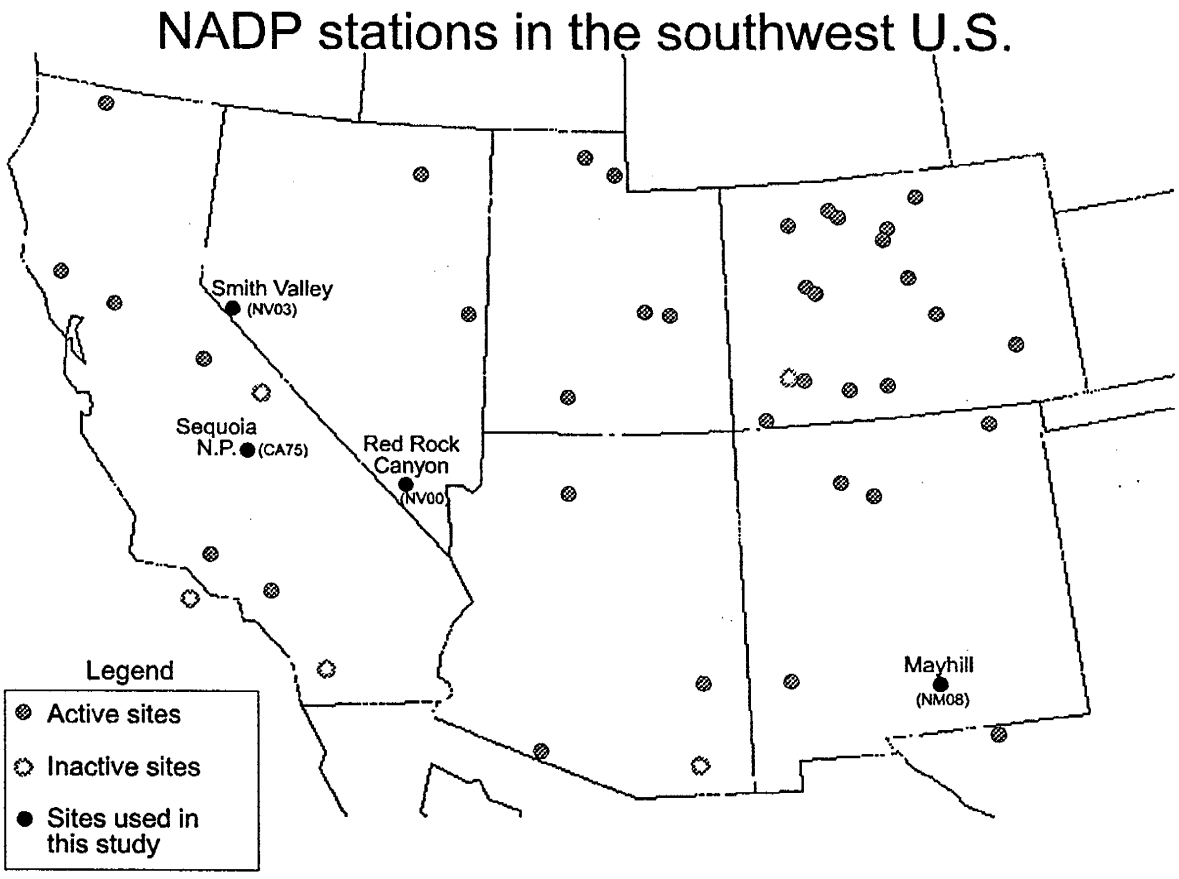

Figure 2-11. NADP stations in the southwest United States (gray circles); locations for which temporal records were examined for this study are shown in black.

While the NADP records do not provide temporal concentration data on the time scale of interest, they do provide some information about regional sources of chloride in precipitation. Figure 2-12 displays plots of annual average chloride concentration and precipitation for several of the stations displayed in Figure 2-11. The Smith Valley and Sequoia N.P. stations are the closest stations to the Painted Hills, NV, and Volcanic

Tableland, CA, midden sites, respectively. Multiplying concentration by precipitation rate provides an estimate of the average annual chloride flux for wet deposition (Figure 2-13).

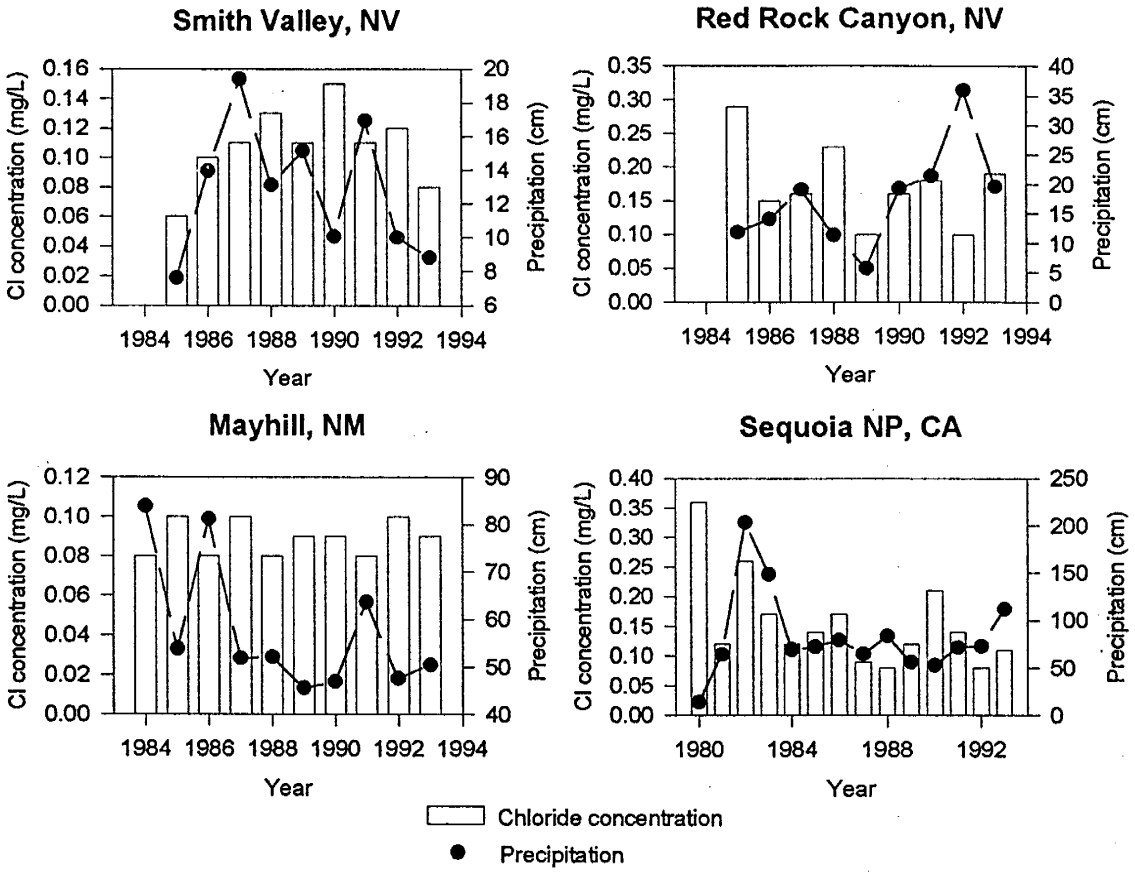

Figure 2-12. Average annual chloride concentrations and precipitation at four NADP sites in Nevada, California, and New Mexico.

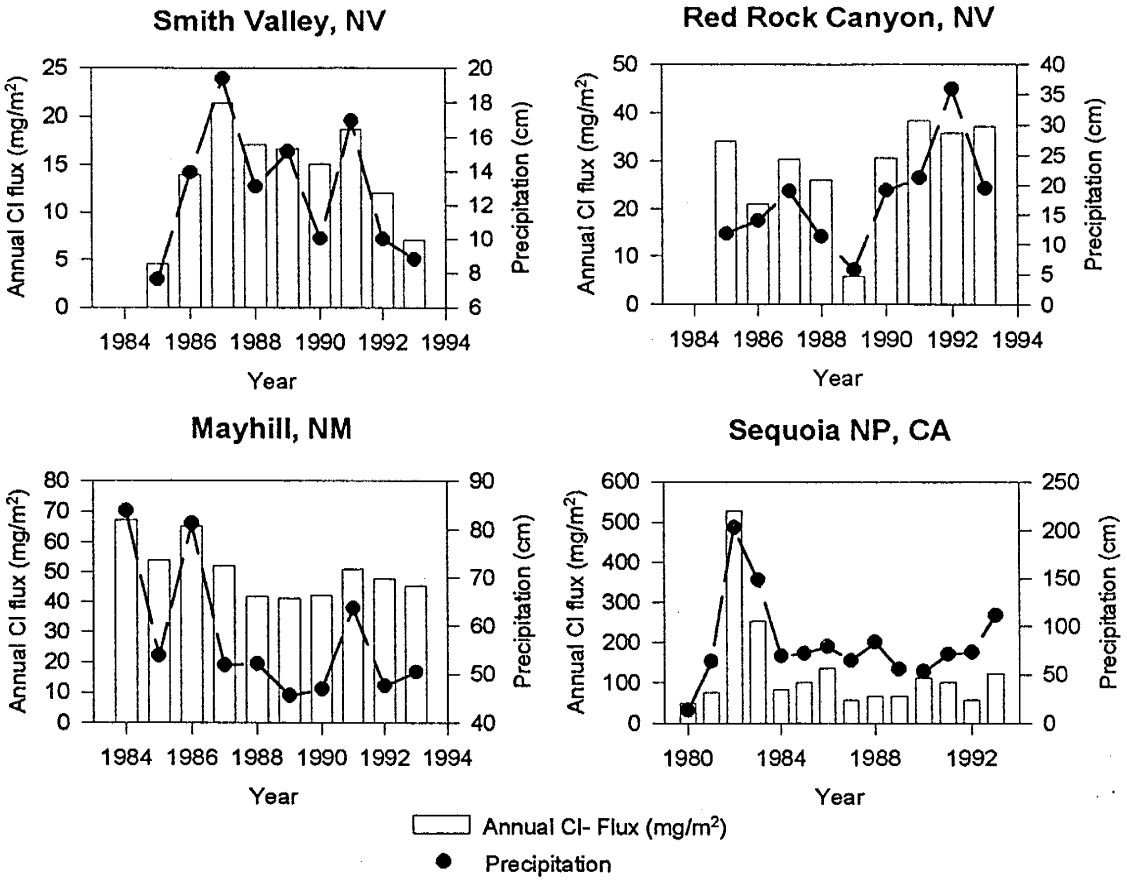

Figure 2-13. Average annual chloride flux (based on wet deposition measurements) at four NADP sites in Nevada, California, and New Mexico.

Correlation coefficients between average annual Cl concentrations and precipitation rates and between Cl fluxes and precipitation rates are given in Table 4 for the sites shown in Figure 2-11 as well as a station at Hopland, CA, approximately 40 km from the coast.

	ρ Avg. annual Cl concentration with precipitation rate	ρ Avg. annual Cl flux with precipitation rate
Hopland, CA	0.45	0.87
Sequoia N.P., CA	0.02	0.67
Smith Valley, NV	0.15	0.50
Red Rock Canyon, NV	-0.26	0.46
Mayhill, NM	-0.58	0.21

Table 4. Correlation coefficients for several NADP stations, between average annual Cl concentration and precipitation and between average annual Cl flux and precipitation.

Chloride flux is generally more correlated with precipitation for sites nearest the coast, where chloride concentration is relatively uncorrelated with precipitation rate. Further inland, such as at the Mayhill, NM, station, Cl flux and precipitation are only slightly correlated. This reflects the increasingly stronger inverse correlation between chloride concentration and precipitation rate with increasing distance from the coast. The observed relationship between chloride flux and precipitation rate is related to the source of chloride washed out by precipitation. The major source of precipitation near the coasts is eastward moving frontal systems originating in the Pacific. These systems carry chloride as well as moisture, so if years of heavy precipitation are largely due to an increased number of these fronts, there is likely to be a corresponding increase in chloride flux. The situation seems to be quite different in areas where precipitation is dominated by convective activity. Convective storms such as those that dominate the monsoon season in New Mexico wash out only the chloride that has reached that distance inland due to larger-scale transfer processes (i.e. not directly related to coastal storms). The chloride concentration of precipitation is therefore generally inversely related to the amount of precipitation in such areas. It should be noted that dry deposition data are not available for the NADP stations discussed above. Dry deposition is probably inversely correlated with precipitation, possibly counterbalancing, to some degree, the trends in correlation between chloride flux and precipitation discussed here.

Precipitation chemistry at the Nevada midden site is probably similar to that of nearby NADP stations, where chloride flux is weakly correlated with precipitation. Knowing the likely source of chloride for that area gives us some basis for estimating what effect the dramatic climate change at the Pleistocene - Holocene boundary would have had on the local chloride flux. It seems reasonable to assume that during the wetter Pleistocene, there would have been both a greater number of chloride-bearing frontal storm systems moving eastward and higher precipitation rates that would remove that chloride from the atmosphere. This suggests that the onset of more arid conditions at the end of the Pleistocene would have reduced stable chloride fallout to the midden sampling sites in Nevada and California. This clearly does not explain the decrease in $^{36}Cl/Cl$ ratios observed at that period in time.

The above-described model assumes that the higher precipitation rates that existed during the last ice-age would have caused greater chloride flux in the areas just east of the Sierra Nevada. While this is reasonable and consistent with the available precipitation chemistry data, it is also possible that the other factors may be important when considering the effect of major climate change on chloride flux and washout by precipitation. It is possible, for instance, that Pacific frontal systems were not any more frequent during the Pleistocene. There may have, however, been increased orographic activity in that climate and an attendant increase in chloride removal in mountainous areas, thereby decreasing chloride flux to areas in the rain shadow of the Sierra Nevada. While the latter explanation is consistent with the observed decrease in $^{36}Cl/Cl$ ratios in packrat middens at the climate transition, there is no evidence to suggest that both chloride deposition rates were actually lower in western Nevada before the Holocene.

Whatever the sources of variability in stable chloride fallout, it is possible that the ^{36}Cl production signal in the $^{36}Cl/Cl$ ratio of the middens is swamped by variability in stable chloride flux. Variations in the former are predicted to be on the order of 0.5 to 1.5 times the current ratio while variation in the stable chloride flux may be several times that, depending on the time scale of the sampling. The effect of short-term variations in stable chloride flux is minimized if the temporal averaging of the middens is large. Pack rats sample the chloride in plants over a relatively short period of time, typically only a few years. Uptake of infiltration by plants likely extends the averaging of a midden sample considerably, so that the period represented in a midden sample may be many decades to hundreds of years. If that period is not sufficiently long to damp out the high amplitude, high frequency, variations that can occur in the stable chloride flux, significant variations in the $^{36}Cl/Cl$ ratios measured in packrat midden samples may result.

Summary and Conclusions

The preserved urine in fossil packrat middens preserves the chlorine isotope ratio of ancient infiltration because packrats obtain water solely from their plant diet. The middens are readily dated using via AMS or conventional radiocarbon technique. Middens examined in this study were dated primarily via AMS ^{14}C measurements of the crystalline urine, as it is

evident that care must be taken to date a portion of the midden as closely related to that portion used for ^{36}Cl analysis as is possible. Although significant discrepancies in dates for some replicate samples from the Mother Midden have been observed, I believe that these are likely due to inaccurate separation of strata from vastly different ages, not to problems with crystalline urine "flowing" through the midden.

$^{36}Cl/Cl$ data from the three regions considered in this study are shown collectively in Figure 2-14. The middens from western Nevada provide a reasonably detailed record of long-term changes in the $^{36}Cl/Cl$ ratio of chloride in infiltration, at least in that region. Data from the other two regions is generally too scattered and the number of samples too small to permit any meaningful conclusions regarding temporal variations in those $^{36}Cl/Cl$ ratios.

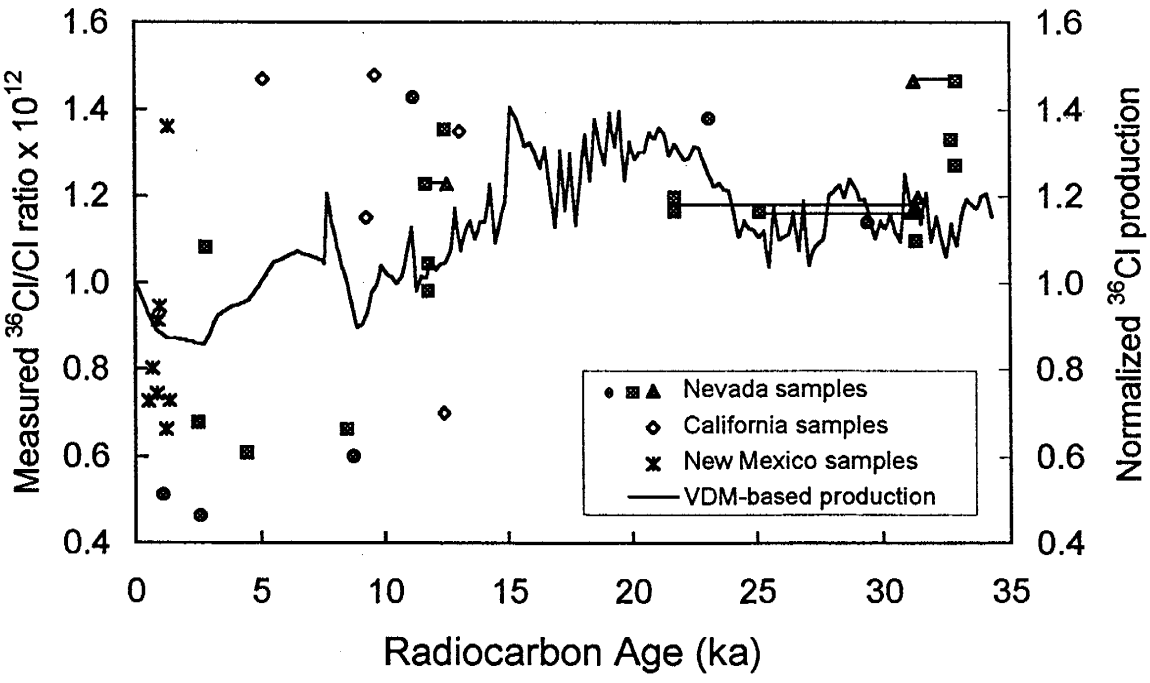

Figure 2-14. Combined $^{36}Cl/Cl$ data from midden samples collected from western Nevada, eastern California and central New Mexico.

Based on the Nevada samples, $^{36}Cl/Cl$ ratios of chloride fallout in western Nevada decreased abruptly approximately 10,000 years ago. The observed decrease may be due either to a change in the atmospheric production rate of ^{36}Cl or to a change in the stable

chloride flux to the area caused by local or large-scale regional climate variations. If the decrease in $^{36}Cl/Cl$ ratios is due to increased stable chloride flux in vicinity of the middens, it is probably attributable to an increase in chloride-bearing aerosols reaching the study site from saline intermontane playas forming at the onset of the Holocene. The primary cause of the observed $^{36}Cl/Cl$ variations might also have been changes in the atmospheric production rate of ^{36}Cl, although the large decrease at ~10 ka is much larger than the change expected based on the available global paleo-intensity data. This suggests that either there are important but as yet unknown factors affecting cosmogenic production rates or that the available paleomagnetic records are a poor record of global magnetic field strength variations during the past ~30 ka.

The primary purpose of this study was to test the hypothesis that the strength of the earth's dipole field is the dominant long-term control on the continental flux of cosmogenic nuclides. While our results are not inconsistent with that hypothesis, the data are insufficient either to strongly support or to refute that mechanism. However, even if the large decrease in $^{36}Cl/Cl$ ratios in the Navada middens at ~10 ka was caused by variations in stable chloride flux, $^{36}Cl/Cl$ record of the middens could still prove valuable. If a reliable record of the production and flux of cosmogenic nuclides at the mid-latitudes is ultimately established, then the midden record could be used to estimate past variations in stable chloride flux. Even if such a record does not become available, the $^{36}Cl/Cl$ record of the middens in western Nevada provides at least a regional tracer of the long-term input function of the chlorine isotope ratio of infiltration .

Through further chemical analysis of the middens, it may be possible to determine whether the change in ratios at ~10 ka is due to variations in the flux of stable chloride or of ^{36}Cl. If the decrease was caused by an increase in stable chloride flux, then this increase should also be reflected in the $^{36}Cl/Br$ ratios of the samples. Although an attempt was made to measure Br concentrations in several samples, the analyses were unsuccessful due to interference from other species. This problem may be avoided with a different analytical treatment and further analyses should be attempted to try to resolve variations in the $^{36}Cl/Br$ ratio.

The conclusions of this study are based on data from only one location in western Nevada. Interpretation of the $^{36}Cl/Cl$ record at that location would be more meaningful if similar records were obtained from other regions of the southwest. The addition of a detailed midden record from an area further inland and well-removed from saline playas would provide a good basis for interpretation of the $^{36}Cl/Cl$ record preserved in middens across the southwest.

Section Three

Potential Application of the ^{36}Cl Production Record as a Tracer for Solute Transport in the Vadose Zone

Natura non facit saltura.

- Linnaeus, Philosophia Botanica

Due in part to national interest in developing low-risk natural containment for radioactive wastes, there is currently a great deal of interest in examining the nature of recharge in arid regions of the country. Several field studies performed in desert soils conclude that recharge in much of the desert southwest is nearly negligible and has been so for many thousands of years [Phillips, 1994; Conrad *et al.*, 1993]. Other studies have noted that diffuse recharge through unvegetated desert soils, as demonstrated by lysimetry studies, may indeed be significant. Clearly, the development of an additional tool with which ancient recharge rates may be estimated would be of great benefit in furthering our understanding of the hydrogeology of arid regions.

^{36}Cl Data From Other Investigators

Several field studies have used the bomb pulse of ^{36}Cl and tritium to trace the movement of soil moisture in the vadose zone. These isotopes are excellent tracers because of their generally conservative behavior in soil moisture transport and because the temporal and spatial pattern of "bomb" radionuclide fallout has been relatively well studied. As the bomb pulse was produced only about 40 years ago however, its use as a natural tracer is limited to studies of recently infiltrated water. For very long term studies, a signal of much greater age is required. This appears to be available as a result of the varying Cl deposition rate and/or production rate of ^{36}Cl in the atmosphere. In this section, I discuss how this variation in the $^{36}Cl/Cl$ signal may be used as a tracer for the movement of soil moisture in areas of severely limited recharge. Section Four discusses the application of this signal as a groundwater tracer.

A Soil Moisture Study at the Sevilleta National Wildlife Refuge

Use of the hypothetical ^{36}Cl production signal as a soil moisture tracer requires measurement of $^{36}Cl/Cl$ ratios in a soil profile for which an independent record of soil moisture age can be identified and which spans a suitably long period of time over which the production variation of ^{36}Cl has been assessed. The vadose zone of the Sevilleta Wildlife Refuge near Socorro, NM, where previous studies have suggested that residual flux is extremely low, appears to fulfill this requirement. We have therefore measured the concentrations of chloride, ^{36}Cl, and stable isotopic composition of an approximately 12-m deep soil boring at that site. The tracers used provide approximate ages for the soil moisture contained in the profile and also allow estimation of variations in residual flux to the profile.

Tracer Methods

In summary, chloride mass balance was used to estimate soil moisture sample ages in the vertical profile. These ages and the associated chloride concentrations in the soil solution were then used to determine approximate residual fluxes and advective transport velocities within the profile. The ^{36}Cl secular variation production record was then compared to the $^{36}Cl/Cl$ ratios obtained for the soil samples. Stable isotope ratios of the soil moisture were also measured to provide information about paleo-infiltration temperatures and climate conditions. Discussion of the various techniques applied in this study to obtain information about residual fluxes follows. Much of the information reported here is taken from a previous report entitled "A Stable Isotope Study of Soil Water, Sevilleta Refuge, New Mexico" prepared by Russel J. Vanlandingham and Andrew R. Campbell at New Mexico Tech.

Chlorine-36

As discussed previously, natural ^{36}Cl is produced in the earth's stratosphere by cosmic ray interactions with atmospheric argon. The cosmogenically produced chloride and stable chloride from the ocean are rapidly washed out of the atmosphere by precipitation or removed by dry fallout. The ratio of natural ^{36}Cl to stable chloride in atmospheric deposition over the study area has been estimated to be about 700×10^{-15} [Bentley *et al.*,

1986]. Chlorine-36 was produced in much higher ratios during thermonuculear weapons tests by neutron activation of ^{35}Cl in sea water. The peak bomb ^{36}Cl fallout occurred in about 1955 as a result of oceanic weapons testing on Pacific atolls. Previous investigations at the Sevilleta have demonstrated that the bomb pulse had penetrated to a depth of about 1.5 meters in 1987 [Phillips *et al.*, 1988]. This study focuses on soil moisture from depths below the estimated maximum penetration depth of the bomb pulse, in order to examine only natural variations in the $^{36}Cl/Cl$ ratio of infiltrating water.

If the flux of stable chloride to the study area is essentially constant, then the initial $^{36}Cl/Cl$ ratio of moisture entering the soil profile should directly reflect the ^{36}Cl production rate in the earth's stratosphere. Thus the production variation record shown in Figure 1-20 may be considered to represent a tracer input signal. If numerous samples spanning a long period of time are available (and the signal input has sufficiently distinct characteristics for different periods of time), the location of this input signal within the subsurface may be used to estimate solute migration rates and other transport characteristics of the soil.

Chloride Mass Balance

Chloride is deposited at the earth's surface both as dry fallout and in precipitation. If the soil itself does not initially contain a significant amount of chloride, then chloride accumulates in the soil only via infiltrating meteoric water. If the rate of chloride deposition and precipitation are generally constant over time, and if the chloride moves downward predominantly by piston flow, then the mass of chloride in the soil profile can be used to determine the infiltration time to a given depth by chloride mass balance (CMB). The CMB equation for infiltration time to depth z is then

$$t_{infiltration} = \sum_i \frac{C_i z_i}{C_o P}$$

where: C_i = chloride mass per unit volume of soil measured in depth interval z_i

z_i = depth at interval i

C_o = chloride concentration of precipitation

P = annual volume of precipitation per unit area

i.e., the time, $t_{infiltration}$, required to accumulate the chloride in a specified thickness of soil is given by the inventory of chloride per unit area in that thickness divided by the average chloride accumulation rate per unit area. Solution velocities may then be estimated by dividing the distance of solute travel by the travel time determined from the CMB method. This approach has been used by Matthias *et al.* [1986] for estimating the transport rates under irrigated fields and by Phillips *et al.* [1988] for estimation of bomb pulse (^{36}Cl and tritium) travel times.

Residual flux is inversely proportional to the ratio of soil moisture chloride concentration to infiltration chloride concentration and can be determined from the chloride concentration data by the relation

$$\text{residual flux} = \frac{Cl_o}{\sum Cl \sum H_2O} P$$

where: ΣCl = Cumulative chloride to depth

ΣH_2O = Cumulative water volume to depth

$Cl_o = d_{Cl}/d_{H2O}$

d_{Cl} = Average annual chloride deposition per unit area

d_{H2O} = Average annual precipitation per unit area

P = Mean annual precipitation

In the southwest, the long-term mean chloride input, including both precipitation and dry fallout, is estimated at approximately 0.375 mg/liter [Phillips *et al.*, 1988].

Oxygen-18

Hydrogen (^1H) and ^{16}O are preferentially evaporated from sea water in a kinetic fractionation process that thereby produces a water vapor enriched in those isotopes. During subsequent precipitation, the fractionation effect produces isotopically heavy condensate and an increasingly light vapor mass. This increasing depletion of the vapor mass by continued preferential removal of the heavier isotope in condensation/precipitation is known as Rayleigh distillation. Because the vapor mass

becomes increasingly depleted by the distillation process, the later precipitation events occurring within a given vapor mass tend themselves to be more depleted in the heavier isotopes. Precipitation thus tends to be isotopically similar to SMOW (though slightly depleted by evaporative fractionation from the ocean) near the oceans and increasingly lighter with distance inland.

Because fractionation of oxygen and hydrogen is coupled, precipitation throughout the world, plotted on a graph of $\delta^{18}O$ vs. δD, tends to follow a straight line known as the meteoric water line ($\delta D = 8*\delta^{18}O + 10$) [Craig, 1961]. Thus in any part of the continental interiors, the ratio of ^{18}O to ^{16}O tends to be relatively constant when several years of data are averaged. The distillation effect is greater when the temperature gradient between the oceans and the continents is larger because the temperature gradient drives the precipitation events that cause the distillation process. Thus, winter precipitation tends to be more depleted in the heavier isotopes than summer precipitation because the pool of water vapor from which the condensate is drawn is more depleted by previous precipitation events [Dansgaard, 1964]. Similarly, global climate changes may alter the mean $\delta^{18}O$ and δD ratios by changing the temperature gradients.

Field Area

The Sevilleta LTER (Long-term ecological research) site is located in the Sevilleta Wildlife Refuge, 24 km north of Socorro (Figure 3-1). Average annual precipitation is about 20 cm and average annual lake evaporation is about 180 cm. Maximum temperatures in summer approach 40° C, while winter minimums below 0° C are common [Stephens and Knowlton, 1986].

Test boring LTER-1 was located west of highway I-25, north of San Acacia, on a bench adjacent to the Rio Salado. The area was sparsely vegetated with grasses, low shrubs and some small cacti. Test boring LTER-2 was located east of I-25, south of Turitutu, on a piedmont above the flood plain of the Rio Grande river where vegetative cover consisted of scattered clumps of grasses.

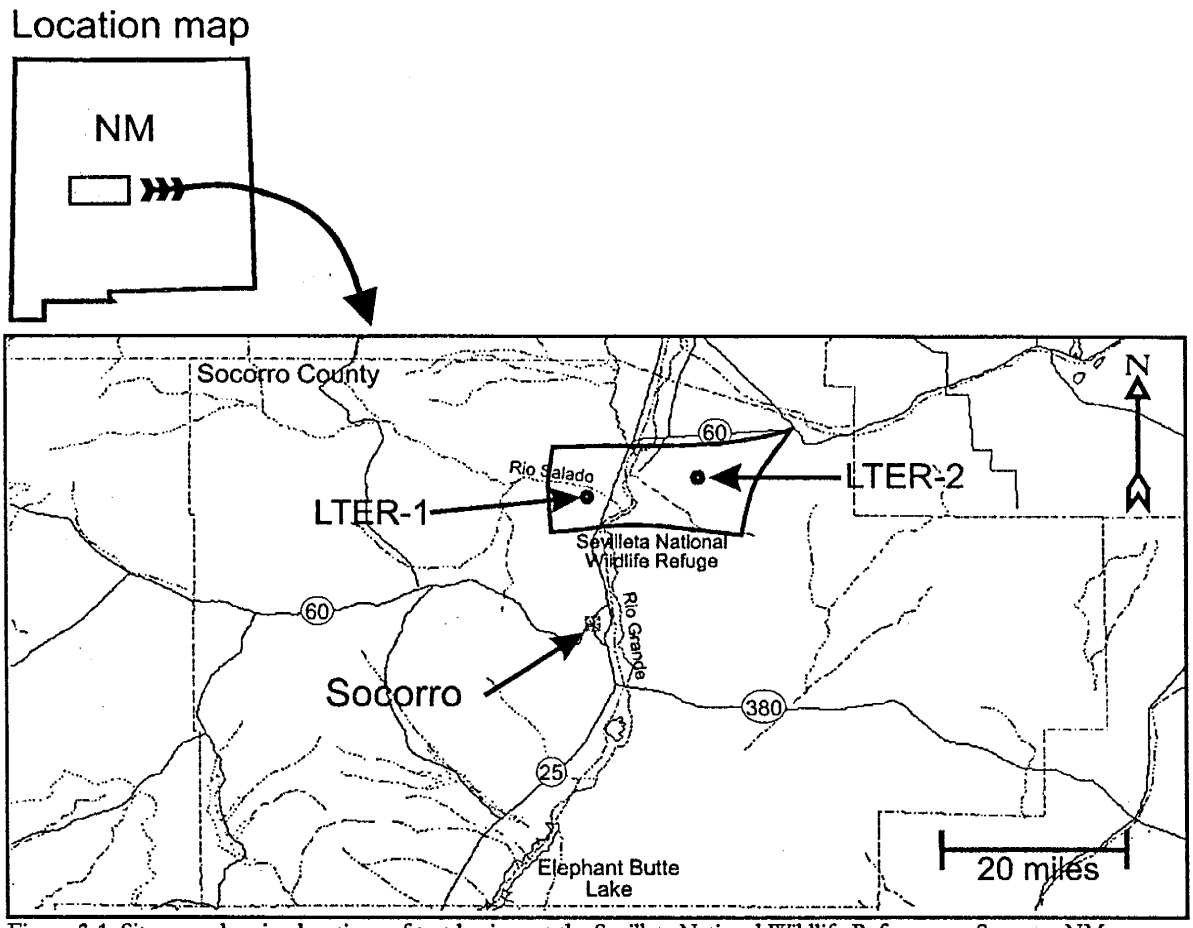

Figure 3-1. Site map showing locations of test borings at the Sevilleta National Wildlife Refuge near Socorro, NM.

Experimental Methods

Moisture content measurements, chloride concentrations and $\delta^{18}O$ measurements were made on samples from both test boring LTER-1 and LTER-2. In addition, $^{36}Cl/Cl$ ratios were determined for many of the samples obtained from test boring LTER-1.

Soil samples were collected from the test borings using a hollow-stem auger and split-spoon sampler. Sub samples, sealed in the field, were used for moisture content, chloride content, and $\delta^{18}O$ measurements. Water for ^{18}O analyses was extracted from the soil samples by a non-azeotropic vacuum distillation technique developed by Knowlton *et al.* [1989]. After extraction, analyses for $\delta^{18}O$ were performed. The oxygen analysis was a standard CO_2-H_2O equilibration technique developed by Roether [1970]. Analyses were calibrated by running SMOW, GISP, and SLAP as standards. Isotope ratios for oxygen-18 are reported in the standard per mille notation relative to standard mean ocean water (SMOW).

Chloride concentrations in the soil were determined using the methods outlined by Sharma and Hughes [1985]. Several hundred grams of soil were leached with an approximately equal mass of deionized water for several days in a rotating shaker. Leachate concentrations were then measured with a selective ion electrode. Chloride for ^{36}Cl analysis was extracted by leaching several hundred grams of soil with distilled, deionized water and precipitating the chloride as AgCl. The AgCl was purified of sulfur as described by Bentley *et al.* [1986] and analyzed for ^{36}Cl at Lawrence Livermore National Laboratory by tandem accelerator mass spectrometry [Elmore *et al.*, 1979]. Further details of the Cl extraction procedure are included as Appendix C.

Results and Discussion

Tabulated data from analyses and measurements of samples from borings LTER-1 and LTER-2 are given in Appendix D. The following discussions focus on data from LTER-1, where $^{36}Cl/Cl$ ratios were measured. Where appropriate, data from LTER-2 is used to lend support to data interpretation.

Stratigraphy and Moisture Content Variations

Boring LTER-1 was augured to a depth of 12.9 meters and 32 samples were recovered. Intervals between samples ranged from approximately a few centimeters in the upper portion to about 1/2-meter in the lower portion of the boring. The samples generally consisted of interlayered clays and sands with a few gravely horizons and a layer of caliche. Roots were observed to a depth of about one meter. Figure 3-2a illustrates the stratigraphy of LTER-1. A total of 23 samples were obtained from boring LTER-2 which was terminated at a depth of 9.2 meters. Samples were similar to those found in LTER-1 though only one fine-grained layer was encountered. This silt and clayey-silt layer was located immediately beneath the caliche horizon, at a depth of approximately 2.3 to 2.7 meters.

Volumetric water content varied from about 4 to 38% in LTER-1 (Figure 3-2b) and from about 2 to 25% in LTER-2 (Figure 3-3). In both borings, water content appears to

correspond closely to soil type, with highest water contents in the finer, silty or clayey layers. The water content of the sand layers was relatively constant at about 5 to 10 percent.

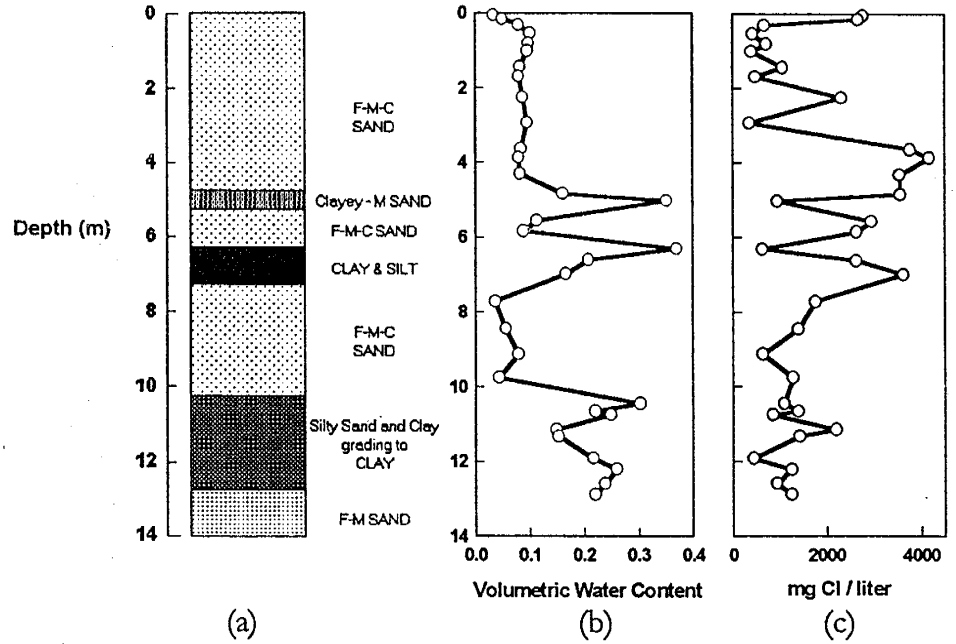

Figure 3-2. LTER-1; (a) stratigraphy, (b) water content profile and (c) Cl- concentration profile. 'F-M-C Sand' indicates fine to coarse sand; 'clayey-M Sand' indicates clayey sand to medium sand; 'F-M Sand' indicates fine to medium sand.

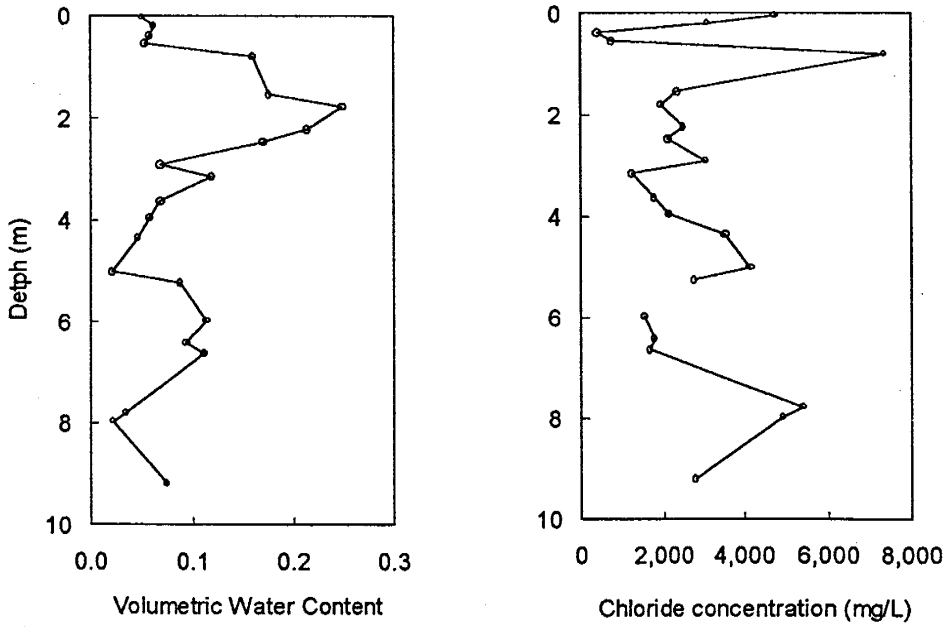

Figure 3-3. LTER-2; soil moisture contents and solution chloride concentrations vs. depth.

CHLORIDE

Solution chloride concentrations in LTER-1 (Figure 3-2c) range from about 500 to 1500 mg/liter in the upper 4 and lower 4 meters of the profile. Low concentrations in the upper portion of the profile are believed to reflect the greater infiltration that occurs above the root zone. Above the root zone, precipitation infiltrates relatively quickly, carrying chloride deeper into the root zone until the chloride is eventually concentrated by transpiration. A bulge in the chloride concentration profile is observed in the middle, 4 to 8 meter zone of the profile, where concentrations range from about 1000 to 4000 mg/liter. In the middle portion of the profile, chloride concentration appears to be negatively correlated with water content and average grain size. Water content peaks there correspond to the two clayey layers which are separated by fine-to-coarse sand. The chloride profile is also relatively "spiky," exhibiting significantly steeper concentration gradients than the smooth profiles typical of advective-dispersive transport. The chloride concentration profile of LTER-2 (Figure 3-3) is similar to that of LTER-1 but the changes in concentrations do not appear to correspond as closely to soil texture changes or water content variations.

AGE BY CHLORIDE MASS BALANCE

CMB ages of the profiles are plotted against depth in Figure 3-4. Steep slopes in this plot represent areas of lower chloride accumulation and , therefore, greater residual flux. The CMB age in LTER-1 (i.e. the total infiltration time for dissolved chloride to reach a given depth) is about 35 ka at 13 m. In LTER-2, CMB age at the bottom of the profile, ~9 m, is about 28 ka. While CMB ages between the two profiles are quite different in the upper few meters, both profiles yield a CMB age of approximately 26 ka at

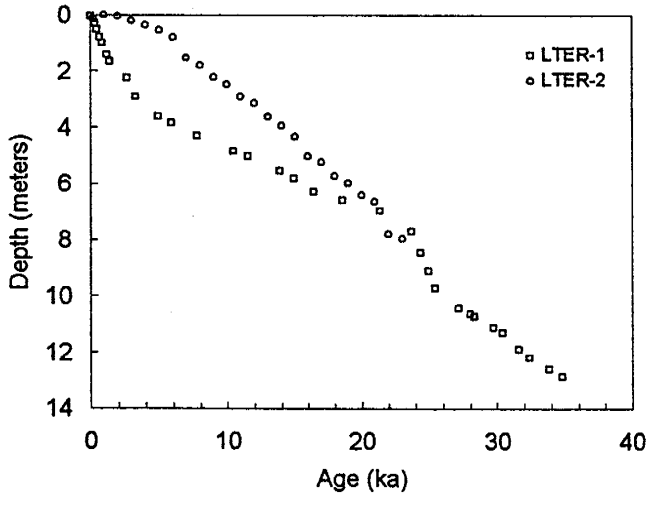

Figure 3-4. in LTER-1 and LTER-2; depth vs. chloride mass balance age.

~8 m. The difference between the profiles suggests that while chloride has been transported at different rates at the two locations, the overall mass of chloride in each is similar when integrated over a depth sufficient to average out such variations.

Residual Flux Estimates

Figure 3-5 is a plot of cumulative soil water versus cumulative Cl- in LTER-1. The variations in slope of a series of linear regressions through the data points indicates how the residual flux has varied over the past 35 ka. The data suggest that there have been several different periods of relatively stable residual flux, varying from approximately 0.02 to 0.07 mm/yr.

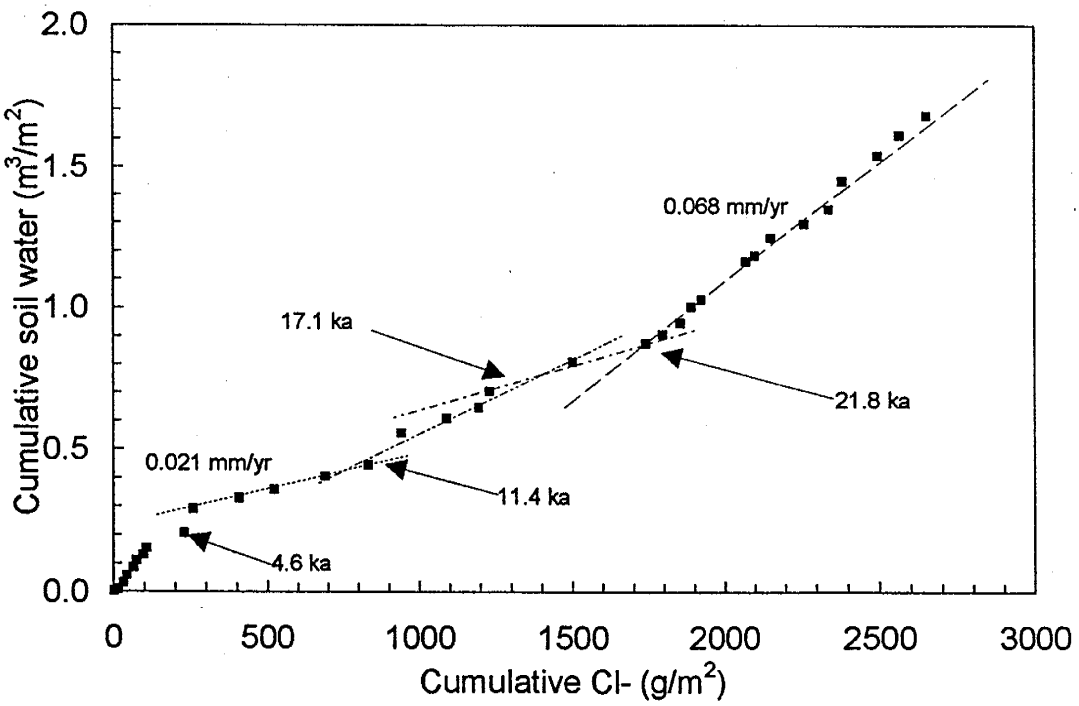

Figure 3-5. LTER-1; cumulative soil water content plotted against cumulative chloride to illustrate changes in residual flux by trends in slope. Dotted lines are regressions of data subsets and corresponding net infiltration estimates are given for two of these ranges. Ages are shown in the figure are for significant breaks in slope. Steeper slopes, corresponding to lower chloride concentrations indicate higher residual flux. The points in the upper portion (~0 - 2 meters) of the soil profile (lower left hand corner) are affected by preferential flow in the root zone and as such are an unreliable estimator of long-term .

A major change in residual flux at the site is evident at ~21 ka and several smaller changes are evident in the period from ~4 ka to 17 ka. Prior to 22 ka, residual flux appears to have

been approximately 0.07 mm/yr. That flux appears to have been reduced at ~21 ka to about 0.025mm/yr and then slightly increased at ~16 ka, to approximately .05 mm/yr. The decrease in residual flux that occurs at ~10 ka, from ~0.05 mm/yr to ~0.02 mm/yr is roughly coincident with the Pleistocene/Holocene boundary, representing the end of the last ice-age and a substantial reduction in infiltration due to greatly increased evapotranspiration. The line connecting the points from 3.3 ka to 10.4 ka appears to represent the present residual flux. The slope of this line indicates a flux of approximately .021 mm per year, which compares favorably with the rate estimated for this area from Phillips *et al.* [1988], approximately 0.03 mm per year. The samples obtained from nearest the surface also fall along a nearly straight line that could be used to determine another residual flux. Because these samples correspond to the root zone, where water is also being removed by plants, they are considered an unreliable estimator of deep soil moisture flux.

Cumulative water vs. cumulative chloride in LTER-2 (Figure 3-6) presents a largely different history than LTER-1. Virtually all of the points lie on a consistent slope that indicates a net infiltration rate of approximately 0.024 mm/yr.

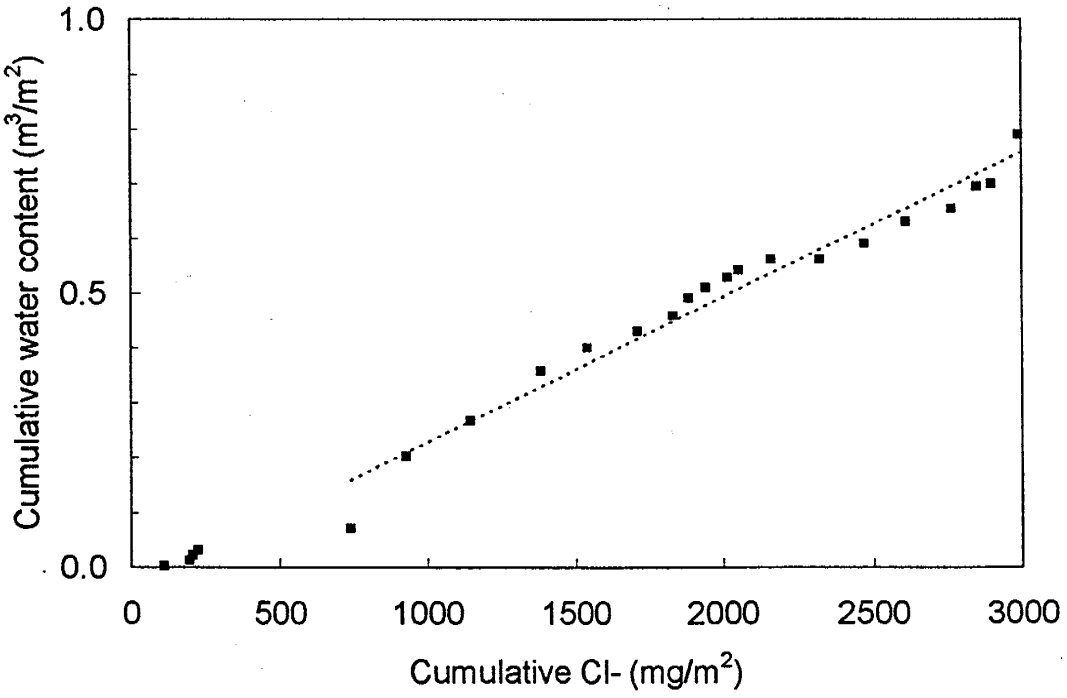

Figure 3-6. LTER-2; cumulative soil water content versus cumulative chloride. Dotted line is a regression through the samples below ~0.5 meters.

$^{36}Cl/Cl$ ratios

Results of ^{36}Cl analyses of twenty-four samples from LTER-1 are shown in Figure 3-7. Chlorine-36 measurements of shallow soil moisture in the Sevilleta [Phillips et al., 1989] indicate that the modern pre-bomb ratio in the area is about 700 x 10^{-15}. Anomalously high $^{36}Cl/Cl$ ratios at depths of 2 and 6 meters indicate the presence of bomb ^{36}Cl. While the former sample likely represents the normal penetration of the bomb pulse, the latter may be either due to contamination during the sampling process or to preferential, "bypass," flow of bomb ^{36}Cl to that depth. The ratio in the 7.7-m sample is also relatively high. If the bomb pulse at ~6 m is due to preferential flow, it is possible that this sample also contains some bomb ^{36}Cl. The ratio itself is not unambiguously indicative of the bomb pulse and it therefore seems justified to retain it in further analysis.

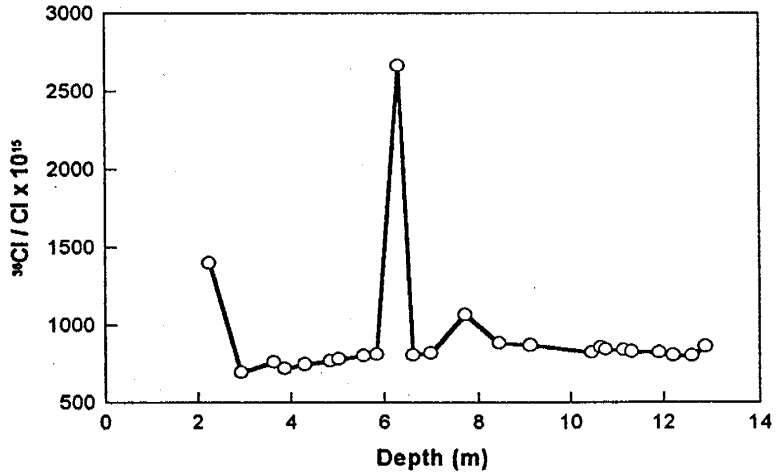

Figure 3-7. LTER-1; $^{36}Cl/Cl$ ratios of samples. Peaks at approximately 2 and 6 meters depths likely represent bomb-pulse chloride.

If the bomb peaks are removed from the plot, the $^{36}Cl/Cl$ profile exhibits the curve illustrated in Figure 3-8c, which also compares the ^{36}Cl concentrations in the soil water to the stable chloride concentrations and $^{36}Cl/Cl$ ratios in the profile.

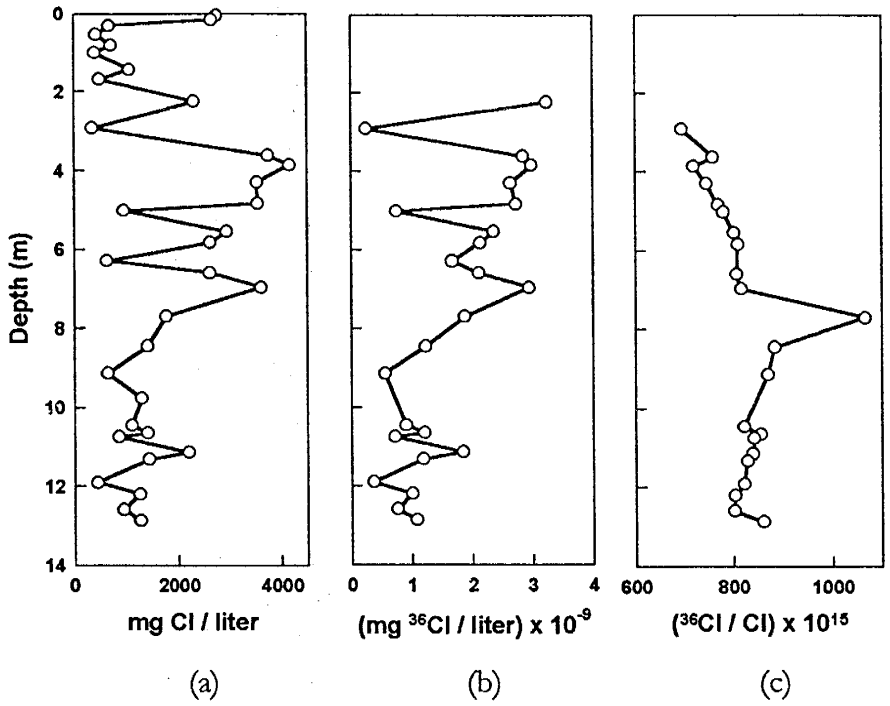

Figure 3-8. LTER-1; (a) chloride concentrations, (b) ^{36}Cl concentrations and (c) $^{36}Cl/Cl$ ratios.

If chloride flux to the site is constant and solute transport is simply via piston-type flow, the $^{36}Cl/Cl$ ratio at any depth, or CMB age, should reflect the flux of ^{36}Cl to the site. Figure 3-9 compares the measured $^{36}Cl/Cl$ ratios, plotted against CMB age, to the VDM-based production signal. Observed ratios increase from $800x10^{-15}$ to ~$900x10^{-15}$ between ~33 and 24 ka and then steadily decline toward the present day value of ~$700x10^{-15}$. While the $^{36}Cl/Cl$ ratio variations are generally smooth, a peak occurs in the record at ~24 ka (7.7 m) that is ~25% higher than adjacent values. The location of the peak is consistent with the overall trend in the data but its magnitude is somewhat anomalous; the maximum change between adjacent samples in the remaining data is ~8%. With the exception of the peak at ~24 ka, the pattern in the observed data is much smoother than the VDM-based production signal. If the magnitude of variations are neglected, there are some similarities between the two curves. Both curves generally decline from maximums that occur before 15 ka and some of the peaks in the observed data roughly correspond to similar variations in the paleomagnetic record.

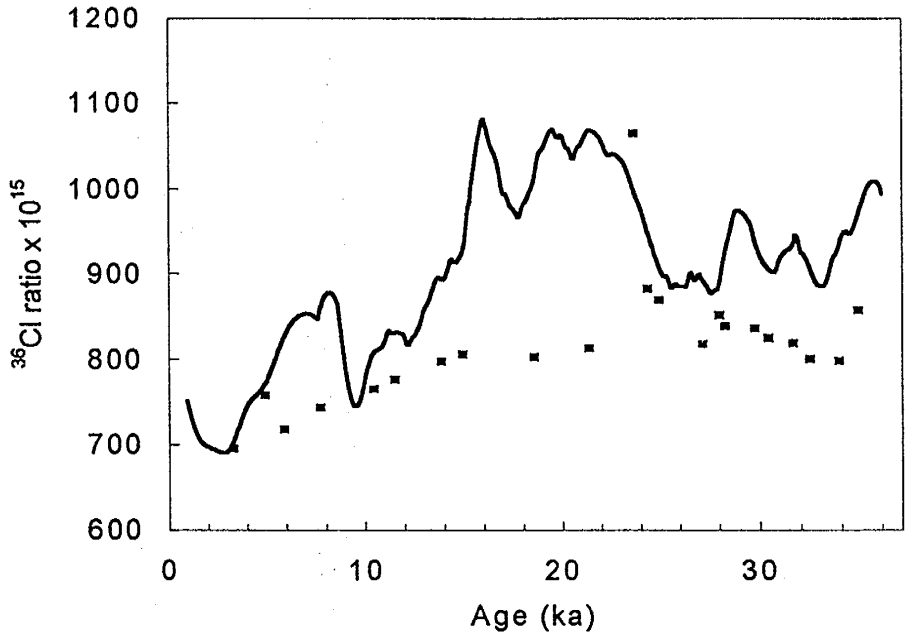

Figure 3-9. LTER-1; $^{36}Cl/Cl$ ratios plotted vs. age (solid squares) and 10-point moving average of the VDM-based production variation signal (curve). The VDM-based signal is arbitrarily normalized to an estimated present-day $^{36}Cl/Cl$ ratio of 800 x 10^{-15}.

Some of the discrepancies (e.g. the timing of major trends) between the profile predicted by piston flow transport and the observed data may be due to inaccuracies in the chloride mass balance, which is based on chloride data from discrete rather than continuous soil samples. The difference in the magnitude of variation and smoothness however is undoubtedly a result of dispersive transport properties not accounted for in the piston flow model. There is little doubt that dispersion has a significant effect on the slow transport of solutes in the vadose zone. Water contents, particularly in LTER-1, are seldom below 5% and thus generally high enough that water should form a continuous film throughout the profile. It is possible that steady state water contents in the profile were lower at some time in the past. If so, portions of the soil might have been dry enough to present an effective barrier to solute transport. In that the present climate is considerably warmer and drier than the preceding glacial period, it seems unlikely that water contents would have been much lower than at present.

We can estimate the effect of dispersion on chloride transport in LTER-1 from a 1-D analytical solution of the advection-dispersion equation (ADE). The ADE for transport of a non-volatile conservative solute through a porous media with variable water content is

$$\frac{\partial}{\partial t}(\theta C) = \frac{\partial}{\partial z}\left(D_h \frac{\partial C}{\partial z}\right) - \frac{\partial}{\partial z}(qC).$$

where: θ = volumetric water content

C = solute concentration in solution

q = flux of solution through the profile

D_h = hydrodynamic dispersion coefficient, $D_h = \alpha v + \xi(\theta) D_m$

where: α = dispersivity

v = seepage velocity

ξ = tortuosity factor, a function of water content and pore characteristics

D_m = molecular diffusion coefficient, for solute in free liquid

In this model, I assume that θ is a function of depth but not time and, again, that the flux below the root zone is constant. The equation can therefore be rewritten as

$$\theta \frac{\partial C}{\partial t} = \frac{\partial}{\partial z}\left(D_h \frac{\partial C}{\partial z}\right) - q \frac{\partial C}{\partial z}$$

or, in standard form,

$$\frac{\partial C}{\partial t} = \frac{\partial}{\partial z}\left(\frac{D_h}{\theta} \frac{\partial C}{\partial z}\right) - \frac{q}{\theta} \frac{\partial C}{\partial z}.$$

For an analytical solution to the equation, I have assumed constant values for q and θ so that the coefficient of the first spatial derivative is simply the advective velocity. Calculation of the hydrodynamic dispersion coefficient requires some empirical form for the tortuosity factor. Wilson and Gelhar [1974] suggest the following formulation for the D_h.

$$D_h = \alpha v + \frac{1}{3}\left(\frac{\theta}{\theta_T}\right)^2 D_m$$

where: θ_T = total porosity

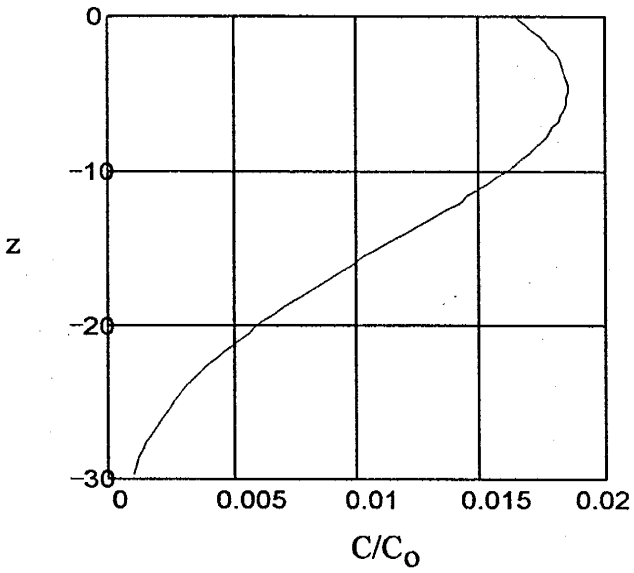

Figure 3-10. Analytical solution for a 1 ka slug after 10 ka.

Figure 3-10 depicts the results of solute transport in a homogenous profile after approximately 10 ka assuming an input slug of concentration C_o = 1 injected over a 1 ka period. The analytical solution is for a third type upper boundary condition and second type lower boundary at some infinite distance. Seepage velocity is estimated based on CMB solute travel time of ~25 ka to 8 meters. Estimated hydraulic and solute characteristics are given in Table 3-1.

Parameter	Estimated value
Dm	1 E-09 m^2/sec
v	0.32 m/ka
α	0.01 m
θ	0.05
θ_T	0.30

Table 3-1. Estimated hydraulic parameters and solute characteristics.

The peak concentration after 10 ka is located at about 4 m depth but its value is only ~1/50 of its initial value and the peak has spread so that the concentration even at ~17 m is half of the maximum concentration. Even if the dispersion coefficient is reduced to 1/10 of the minimum likely value, dispersion is still quite significant (Figure 3-11). After 10 ka, the

maximum peak is again at about 3 meters, half of the maximum is present at about 8 meters and the tail of the distribution extends beyond 10 meters.

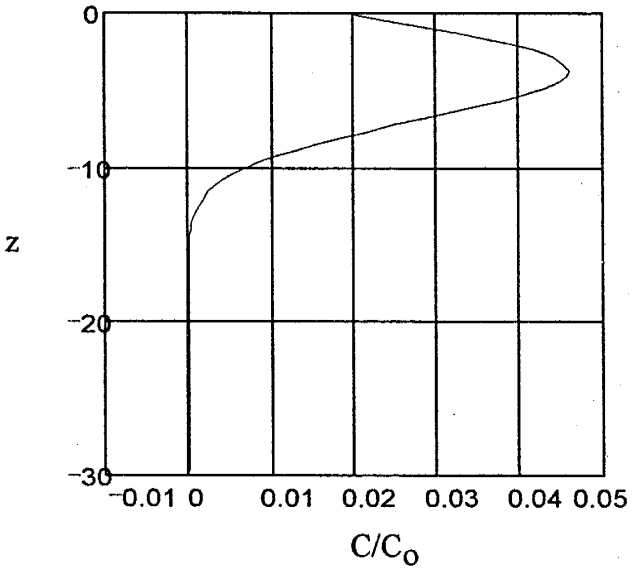

Figure 3-11. Analytical solution for a 1 ka slug after 10 ka.

While analytical solutions provide insight into the magnitude of the processes at work, a distributed parameter model is required to model the varying input concentration and how its transport is affected by varying soil moisture content. Accordingly, I developed a simple finite difference model of the system in order to simulate transport of the hypothetical ^{36}Cl production signal into the vadose zone. The model assumes a constant vertical flux through the vadose zone with a variable advective velocity determined by the volumetric water content. Transport of ^{36}Cl is modeled with ^{36}Cl concentration as the independent variable. The upper boundary for the transport equation is a variable concentration boundary; the lower boundary is also a Dirichlet boundary with a concentration fixed arbitrarily at one. The initial concentration throughout the modeled portion of the profile is assumed to be approximately zero. The model solves the 1-D advection dispersion equation (ADE) using block-centered finite differences, with discrete tables of data for volumetric water content and the varying concentration upper boundary. The hydrodynamic dispersion coefficient is calculated using the Wilson and Gelhar [1974] model described above. While the model is helpful in predicting the distribution of solutes for a complicated input signal, its utility is severely limited due to our restricted knowledge of the input function.

The actual flux of ^{36}Cl atoms into the soil is dependent not only on its production rate in the atmosphere but also on the evaporative concentration which occurs before the soil solution moves below the root zone. While the production rate variation can be estimated

from paleomagnetic reconstructions, it is not nearly so easy to reconstruct the past variations in evaporation patterns in the vadose zone. That pattern of variation appears to be well preserved in the vadose zone profile (Figure 3-8), with both Cl concentrations and ^{36}Cl concentrations in the soil exhibiting large fluctuations over small changes in depth. This is atypical of advective transport and suggests that other factors may be controlling the concentration distribution in the soil. Similarly perplexing ^{36}Cl profiles have been observed by Phillips *et al.* [1988] in a shallow profile from another location on the Sevilleta National Wildlife Refuge and from a boring in the New Mexico Stage University Ranch Site near Las Cruces. Norris *et al.* [1987] observed a "similar "spiky" ^{36}Cl profile in an arid site in southern Nevada. If these spiky profiles actually reflect large fluctuations in input, then the ^{36}Cl input signal is essentially a minor variation superimposed on the highly variable stable chloride input concentration. In order to model transport of ^{36}Cl then, I would first have to model the variable evaporative effect that produces the spiky input signal. It is apparent simply from the analytical solutions that, unless dispersion is dramatically less than would be expected given the observed water contents, such spiky profiles could only result from unrealistically large variations in salt concentration of the residual flux.

Oxygen-18

$\delta^{18}O$ in both profiles exhibits the typical enriched zone near the surface, indicative of evaporative enrichment in the root zone. Stable isotope variations below the evaporation front are considered representative of variations in meteoric composition, with some modification by local climatic effects. To examine variations in the isotopic composition of infiltration, the profiles have been rescaled to highlight the variations below the evaporation front. These profiles are shown in Figure 3-12 and Figure 3-13 with attendant moisture content profiles.

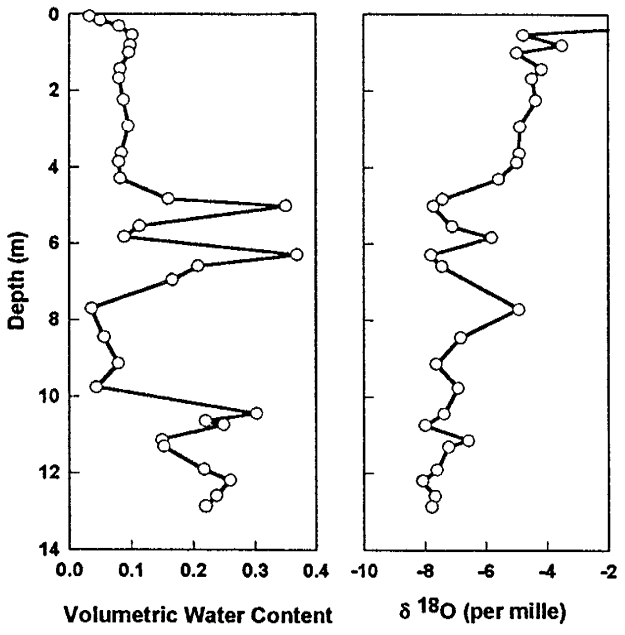

Figure 3-12. LTER-1: (a) volumetric water content and (b) $\delta^{18}O$

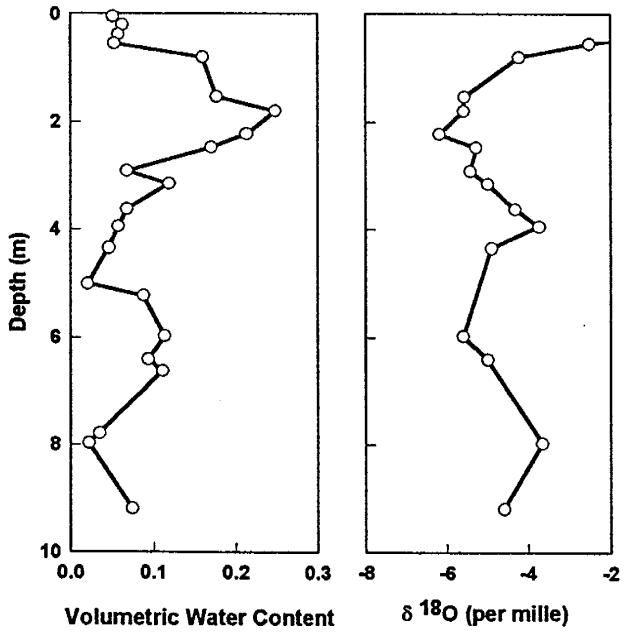

Figure 3-13. LTER-2: (a) volumetric water content and (b)$\delta^{18}O$.

In LTER-1, soil moisture appears to be increasingly depleted in ^{18}O with increasing depth but two prominent depleted regions in the profile correspond closely to peaks in water content. There also appears to be weak negative correlation between $\delta^{18}O$ and water content in LTER-2. As mentioned earlier, chloride concentrations appear to be negatively correlated with water content. If these correlations are more than coincidental, it may be that preferential flow or unknown transport processes play an important role in the subsurface at LTER-1. Although the relationship between chloride concentration variations, oxygen isotope variations and water content might suggest that evaporation is significant in the sand between the clay layers, this seems unlikely given the depth of the peaks and the distance from LTER-1 to the bank of the Rio Salado where the soil layers might become exposed to evaporation.

While this apparent negative correlation suggests that the depleted regions at ~5 and 6.3 meters in LTER-1 are related to soil characteristics, it is possible that the $\delta^{18}O$ variations reflect the changing composition of precipitation due to large scale climate shifts over the last 30 ka or to dramatic changes in the manner in which precipitation is modified during infiltration. Figure 3-14 shows the $\delta^{18}O$ data for both borings plotted against CMB age. Examination of this plot indicates that two prominent peaks in ^{18}O occur in LTER-1 at approximately 15 and 24 ka and that similar peaks occur in LTER-2 at ~14 and 23 ka. If these peaks in the two profiles are caused by the same process, it seems unlikely that this would be related to geologic heterogeneities which are quite different at the two locations. Even if the peaks are related, it would be difficult to determine whether the changes are due to isolated events, or processes, that led to infiltration enriched in the heavy isotopes at ~15 and 23 ka or to processes that led to depleted infiltration between ~7 and 15 and before 24 ka.

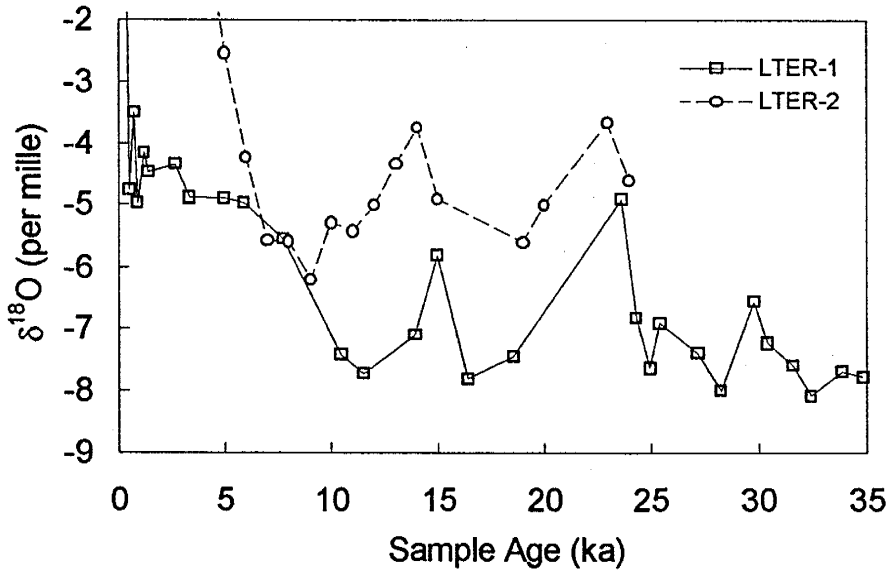

Figure 3-14. $\delta^{18}O$ as a function of CMB age in LTER-1 and LTER-2.

Other than the two peaks in ^{18}O, the isotope profiles from the two borings show few consistent and remarkable features. While the LTER-1 $\delta^{18}O$ vs. age shows a distinct increase in ^{18}O between ~11 and 7 ka, a corresponding change in LTER-2 plainly appears to be related to near-surface evapo-transpirative effects. If this shift toward lighter soil

moisture in LTER-1 between 4 and 5 meters actually records changes in the composition of infiltration, then the deeper soil moisture may reflect isotopically lighter Pleistocene infiltration. Phillips [1986] showed a similar shift at about 10 ka (of about 3 - 4 per mille $\delta^{18}O$) in ground water samples from the Central San Juan Basin, New Mexico. On the whole, the stable isotope data support the premise that preferential flow or other processes have a significant effect on flow and transport in the vadose zone as revealed in LTER-1.

Summary

Stable chloride, $^{36}Cl/Cl$ ratios, and stable isotopes of oxygen were examined in two soil profiles in the Sevilleta Wildlife Refuge near Socorro, New Mexico. If steady state plug flow is assumed, chloride mass balance analysis suggests that the age of the soil moisture at the base of the profile is approximately 35 ka. This implies that net infiltration at that location has been nearly negligible for at least that period of time. Stable isotope data in LTER-1 appear to indicate lighter isotopic composition with increasing depth but large variations across short distances in the profile make interpretation of the timing of that shift ambiguous. Chlorine-36/Cl ratios dated via CMB suggest that $^{36}Cl/Cl$ ratios of infiltration were higher in the past, though it should be noted that preferential flow within the profile may have allowed bomb pulse ^{36}Cl to impact more than the one sample discarded for that reason. While the trend in the $^{36}Cl/Cl$ ratios follows the general trend predicted by the hypothesized geomagnetic control, the overall magnitude of variation is quite different. Overall, interpretation of the data is highly equivocal due to a number of inconsistencies which complicate the analysis. These include

- larger Cl and ^{36}Cl and $\delta^{18}O$ gradients in the profile than would be expected after several thousand years of diffusive-dominated flow;
- apparent correlation of chloride concentration and oxygen isotope ratios with water content which, in turn, corresponds closely to changes in soil type and
- a prominent bomb-level ratio of ^{36}Cl in a sample obtained from a depth of six meters, near the middle of the profile.

Preferential flow is a possible explanation for the observed inconsistencies. Preferential flow paths may dominate transport in the finer-grained units of the profile, perhaps through soil cracks in these zones. This would tend to preserve very old water in the primary porosity of the finer-grained units, as flow would not displace interstitial water as rapidly as it would under strictly piston-flow conditions. Other scenarios involving strong lateral flow patterns within the profile are possible as well.

Unpublished $^{36}Cl/Cl$ Data from Other Sites

Tyler *et al.* [in press] have measured $^{36}Cl/Cl$ ratios in the deep vadose zone of the Nevada Test Site (NTS). They report $^{36}Cl/Cl$ ratios of 33 core samples from PW series and ST series boreholes at Area 5 of the NTS. Samples were collected from depths of up to approximately 210 meters with most from a range of 5 to 70 meters. Depth to the water table at that the NTS site is typically greater than 300 meters. Chlorine-36/Cl ratios from PW-1 were supplemented with six samples from the nearby shallow borehole ST-1. Based on Cl mass balance, sample ages were reported as ranging between ~25 and 120 ka. Chlorine-36/Cl ratios, plotted against CMB ages are shown in Figure 3-15. The estimated modern $^{36}Cl/Cl$ ratio for infiltration is 0.5×10^{-12}.

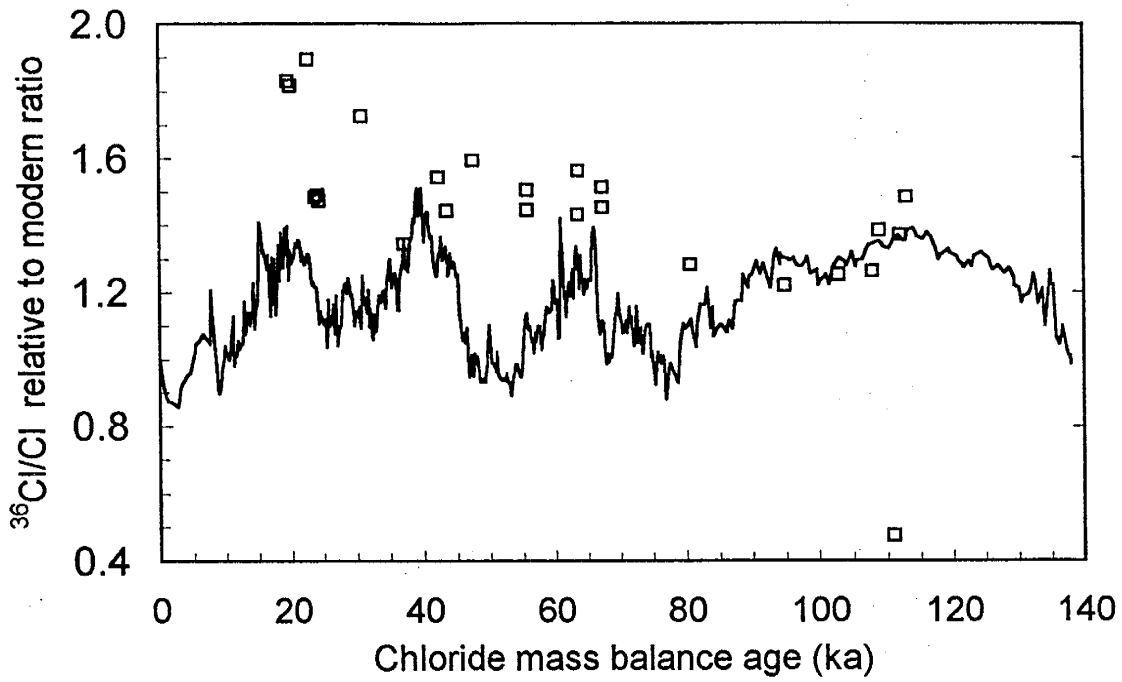

Figure 3-15. ^{36}Cl/Cl ratios of samples from the Nevada Test Site (squares) plotted against chloride mass balance age. Ratios are decay-corrected based on the estimated ages. Solid line is the hypothetical ^{36}Cl production signal based on the paleomagnetic reconstructions of Tric et al. [1992] and Meynadier et al. [1992]. After Tyler et al. [in press].

With the exception of one sample, the ratios are between 1.2 to ~2 times the estimated modern ratio of 0.5×10^{-12}. The ratios also decrease substantially with age, a trend that would be even more prominent were the ratios not corrected for decay. Neither the pattern of variation nor its range agrees very well with the VDM-based signal.

Section Summary

Interpretation of trends in the ^{36}Cl/Cl ratio of soil moisture at LTER and the Nevada Test Site is difficult and the data lend little support to the hypothesis that geomagnetic field strength variations are the primary control on cosmogenic nuclide production. Both data sets indicate that ratios were significantly higher in the past but the magnitude and timing of actual changes is not consistent between the records. For example, a ^{36}Cl/Cl peak of ~2500×10^{-15} in LTER-1 appears to indicate the presence of bomb ^{36}Cl as other ratios in the profile range to only 140% of the modern pre-bomb ratio. Ratios of similar magnitude (in relation to estimated present-day ratios) dominate the NTS profile of Tyler et al. [in

press] yet it is difficult to attribute this either to sample contamination by bomb pulse or to deep penetration of the bomb signal.

Because ages have been calculated using chloride mass balance, the vadose zone data examined in this study do not provide a means of determining whether the observed $^{36}Cl/Cl$ ratio variations are due to changes in production of ^{36}Cl or changes in stable chloride flux. If the observed trends in the LTER and NTS data are not due primarily to changes in the composition of infiltration, then it would appear that deep mixing in thick vadose zones may be a more significant process than is often assumed.

^{36}Cl ratios in this set of data exhibit a general increase with time. Unfortunately there are no samples from the period before ~25 ka to allow comparison with trends in the LTER data. The trend in this data set does not appear to be correlated with the VDM-based production signal.

Section Four

Potential Application of the ^{36}Cl Production Signal as a Groundwater Tracer

> *"Water generally flows downhill in this area."*
>
> *- Bob Bennett, WDIV News 4, Detroit, reporting on a flood that destroyed some suburban basement apartments.*

While previous studies have reported temporal variations in $^{36}Cl/Cl$ ratios in groundwater [Phillips *et al.*, 1986; Torgersen *et al.*, 1992], most have focused on the radioactive decay of that radionuclide to provide groundwater ages for very old groundwater. In a few cases, researchers have measured both $^{36}Cl/Cl$ ratios and chloride concentrations to reconstruct past climatic variations (e.g. Magaritz, 1990). Variations in $^{36}Cl/Cl$ ratios measured in the Carrizo aquifer [Bentley *et al.*, 1986] were interpreted as the result of ion filtration. In this section, I discuss variations in $^{36}Cl/Cl$ ratios measured in groundwater samples from two systems and the possible mechanisms for those variations. As discussed in Sections One and Two, the $^{36}Cl/Cl$ ratio of soil moisture recharge should vary as a function of the flux of stable chlorine and production and distribution of atmospheric ^{36}Cl. If this temporal variation is predictable at any given location and preserved in the groundwater, it could have important application as a long-term tracer signal.

Temporal variations preserved in groundwater are likely quite different from those seen in an archive such as fossil packrat middens. The slow recharge and mixing characteristics of groundwater systems act as a low-pass filter to high-frequency variations in the $^{36}Cl/Cl$ ratio that may occur due to solar modulation of cosmic ray flux or other factors. On the other hand, long-term variations in the $^{36}Cl/Cl$ ratio of recharge, such as may result from geomagnetic field variations, long-term variations in solar modulation or stable chloride flux, should be preserved and groundwater samples taken along a flow path should reflect these variations if travel times are sufficiently long.

Use of groundwater as an archive of variations in atmospheric ^{36}Cl production must take into account other sources of variation for that radionuclide in the subsurface, such as radioactive production and decay, mixing of water from different aquifers and geochemical changes that may introduce additional chloride. While the $^{36}Cl/Cl$ ratios discussed herein have been corrected for radioactive decay, its effect is actually quite minor. For the oldest samples considered in this study (approximately 35 ka), radioactive decay of ^{36}Cl decreases the initial ratio only by about 8%, which is approximately equal to the analytical error of measurement. In addition to the ^{36}Cl that enters the groundwater in recharge, ^{36}Cl is also produced in the aquifer. This in-situ production is dominated by the thermal neutron capture reaction $^{35}Cl(n,\gamma)^{36}Cl$ and occurs in both the aquifer matrix and groundwater [Andrews *et al.*, 1991]. The equilibrium $^{36}Cl/Cl$ ratio for a typical sandstone is about 0.010×10^{-12} [Andrews *et al.*, 1991], approximately two orders of magnitude less than the ratios observed in the groundwater samples obtained for this study. Thus, Cl leached from the rock should effectively dilute the groundwater ratios rather than provide a significant source of additional ^{36}Cl. Production of ^{36}Cl in the groundwater would be expected to reach the same equilibrium ratio only if its residence time in the aquifer considerably exceeds the 301 ka half life of ^{36}Cl [Stute *et al.*, 1993]. As the average age of waters considered in this study is less than approximately 35 ka, production in the groundwater itself is negligible, particularly considering the much higher ratios that exist in the groundwater recharge.

Assuming that in-situ production and decay of ^{36}Cl are negligible and that, during transport, Cl- is not introduced or removed, $^{36}Cl/Cl$ ratios in groundwater should be a function only of the relative fluxes of ^{36}Cl and stable chloride to the recharge area. The flux of ^{36}Cl is believed to be primarily a function of the rate of production in the atmosphere. The flux of stable chloride may vary due to atmospheric distribution patterns of both marine and continental sources of chloride. Stable chloride flux may be related to precipitation rates, as in coastal areas where storms transfer large amounts of chloride inland, or may be dominated by deposition of continental aerosols unrelated to precipitation rates. Other things being constant, variations in the flux of stable chloride should produce a strong negative correlation between chloride concentrations and $^{36}Cl/Cl$ ratios in groundwater.

However, chloride concentrations in groundwater are also a function of the extent of evapotranspiration prior to infiltration. In some situations, then, changes in stable chloride flux may be masked by changes in the flux of water to the system. For example, if the stable chloride flux doubles and the recharge rate increases by roughly the same factor, $^{36}Cl/Cl$ ratios would decrease but Cl- concentrations would remain essentially the same. These coupled effects may be separated by comparing $^{36}Cl/Cl$ ratios to the flux of chloride rather than to chloride concentrations. That flux can be estimated from chloride concentration distribution and distance between isochrons in the aquifer. This, of course, requires sufficiently accurate knowledge of the spatial distribution of chloride, aquifer thickness and groundwater age distribution, which is not always available.

To test the hypothesis that the production variation of ^{36}Cl may be recorded in groundwater samples, we measured $^{36}Cl/Cl$ ratios in samples of varying ages from two different aquifers in the southwestern United States --the San Juan Basin in northern New Mexico and the Carrizo aquifer in the gulf coastal plain of southern Texas. The patterns of $^{36}Cl/Cl$ ratio variation observed in these sample sets are discussed below.

Work performed for this study included only the measurement and analysis of chloride, bromide and $^{36}Cl/Cl$ ratios in groundwater. The hydrogeology of both the San Juan Basin in New Mexico and the Carrizo aquifer in Texas have been studied in considerable detail by a number of previous investigators. To familiarize the reader with the basic geography and essential hydrogeologic characteristics the San Juan Basin, I have included excerpts from a previous paper by Phillips *et al.* [1989] entitled "An isotopic investigation of groundwater in the central San Juan Basin, New Mexico: carbon-14 dating as a basis for numerical flow modeling." Relevant information concerning the Carrizo aquifer is drawn from Stute *et al.* [1992] and from a preprint of an IAEA paper by Stute *et al.* entitled "Paleoclimatic information derived from the groundwater archive: Cl-, ^{36}Cl, and noble gases, Carrizo Aquifer, Texas."

San Juan Basin

Twenty-four groundwater samples were obtained from a region overlapping parts of San Juan, Rio Arriba, Sandoval, and McKinley Counties, New Mexico. The location of the study area is shown in Figure 4-1. The samples were obtained from domestic water supply wells tapping the Ojo Alamo sandstone and the Nacimiento Formation of the San Juan Basin. Phillips *et al.* [1989] describe the geography and hydrogeology of the basin as follows.

Geography

> *The San Juan Basin lies within the Colorado Plateau physiographic province, a large, relatively flat upland region south and east of the Rocky Mountains. The area has a continental, semiarid climate with a mean annual temperature of about 9.5 C and mean summer maximum and winter minimum f 31 C and -10C respectively. The mean annual precipitation is about 220 mm. Precipitation is divided approximately evenly between summer convective storms originating in the Gulf of Mexico and winter frontal storms from the Pacific Ocean.*
>
> *Approximately 4/5 of the area drains north to the San Juan River and the other 1/5 south to the Rio Grande. The elevation of the recharge areas ranges from 1950 m to 2100 m, while the ultimate discharge point, the San Juan River, lies at about 1850 m. Most of the study area is covered by low vegetation consisting of saltbush, sagebrush, and bunch grass. Mesa tops at slightly higher elevation, which are the primary recharge areas for the aquifers, support a pygmy forest of one-seed juniper and pinyon pine.*

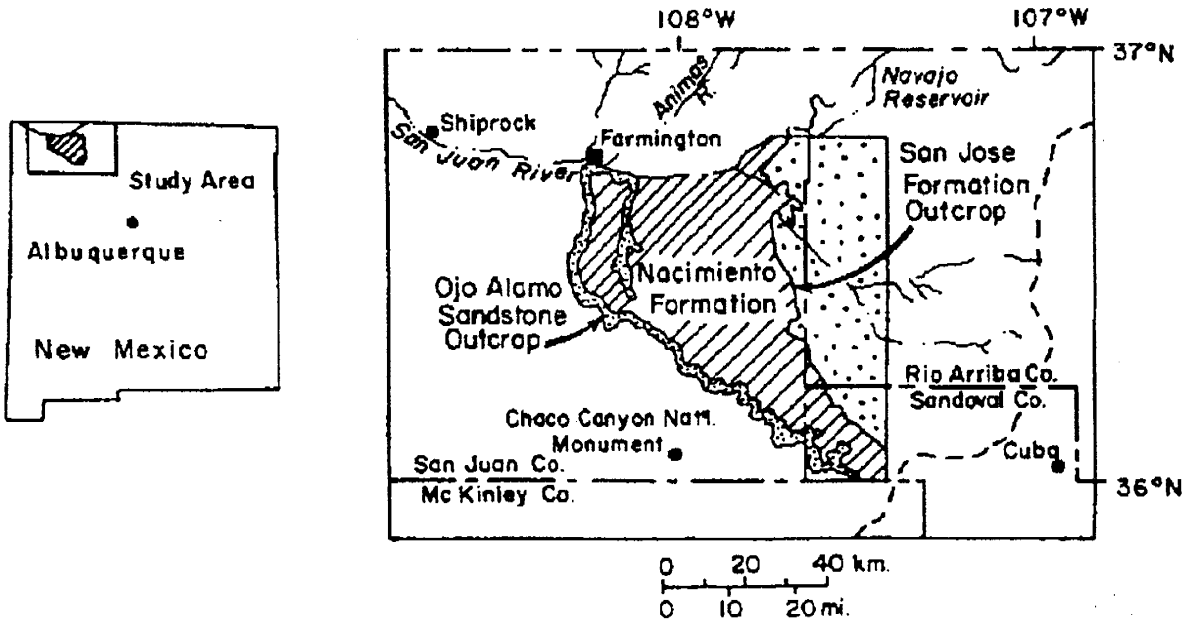

Figure 4-1. Location map of study area. From Phillips et al., 1989.

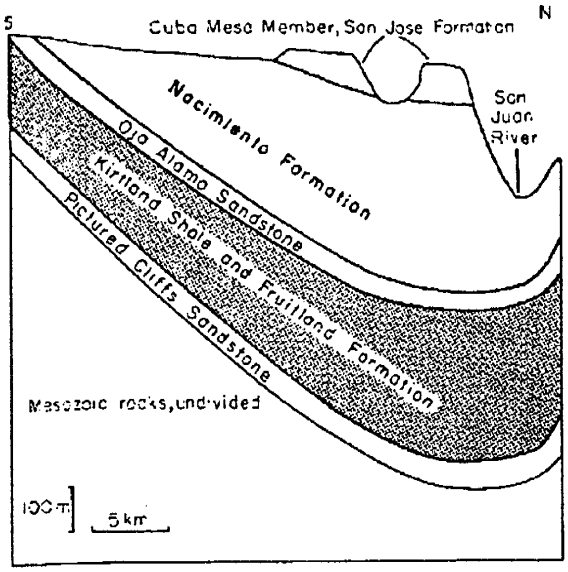

Figure 4-2. North-south generalized cross section of Tertiary and upper Mesozoic rocks in the study area. North is on the right. Vertical exaggeration is 75 x horizontal scale From Phillips et al., 1989.

Hydrogeology

The San Juan Basin is a structural depression in northwestern New Mexico and southwestern Colorado which contains sedimentary rocks ranging in age from Cambrian to Tertiary. The basin outline is nearly circular in plan view, covering approximately 77,000 km². However, the basin is asymmetric in cross section and contains a maximum of about 4400 m of sediments at the basin axis, close to the San Juan River, which is near the northern margin of the basin (Figure 4-2). Tertiary sediments are restricted to the central part of the basin.

The Ojo Alamo sandstone marks the Cretaceous-Tertiary boundary. The sandstone is a fine- to coarse-grained alluvial deposit varying from 20 to 100 m in thickness. The Ojo Alamo aquifer is confined below by the Fruitland Formation and Kirtland shale. The Kirtland shale contains minor interbedded siltstone and sandstone, while the Fruitland Formation is distinguished from it by coal beds. The combined thickness of the two formations is about 700 m, but the transmissivity of the combined units is thought to be less than 10^{-5} m²/s (Stone et al., 1983). The significantly more permeable Pictured Cliffs sandstone beneath the Fruitland Formation tends to act as a drain for the Tertiary aquifers.

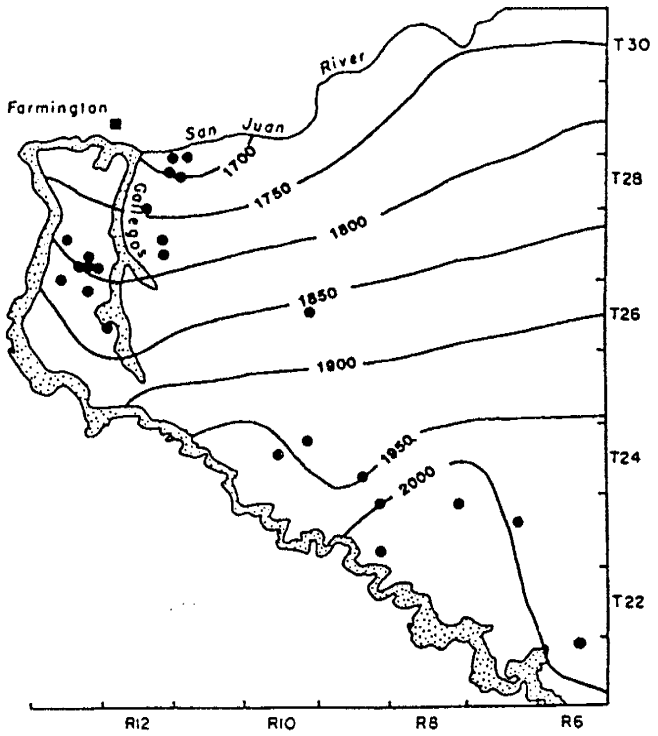

Figure 4-3. Potentiometric map of the Ojo Alamo sandstone aquifer. From Phillips et al., 1989.

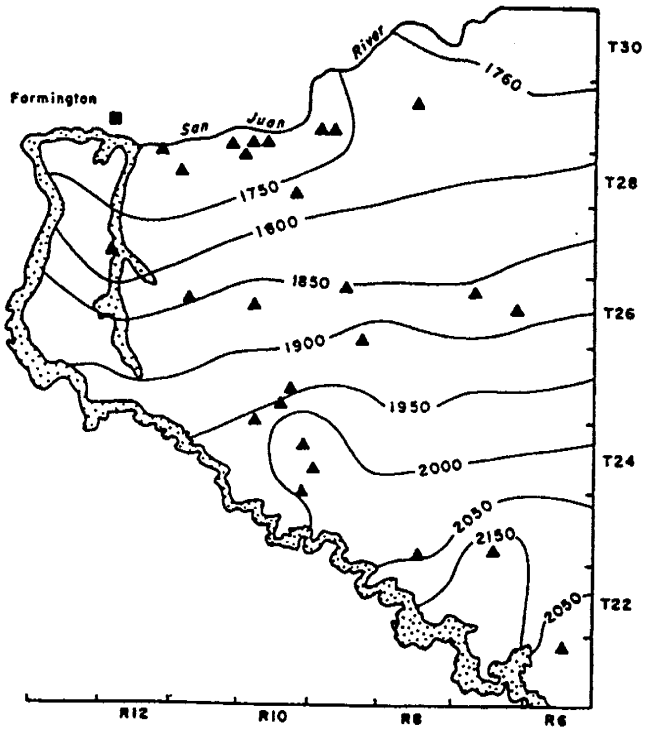

Figure 4-4. Potentiometric map of the Nacimiento Formation aquifer. From Phillips et al., 1989.

The Nacimiento Formation of Paleocene age forms the upper confining layer on the Ojo Alamo. The Nacimiento Formation consists largely of shale and siltstone with thin interbedded sandstones at regular intervals. The sandstone units within the Nacimiento Formation, although less permeable than the Ojo Alamo sandstone, are of greater aggregate thickness and thus form an aquifer of comparable transmissivity. The average total thickness of the Nacimiento Formation is about 300 m. The Eocene San Jose Formation is the youngest Tertiary unit in the San Juan Basin. The lowermost unit of the formation, the Cuba Mesa Member, is the only one present in the study area. The Cuba Mesa Member is composed predominantly of coarse-grained sandstone but intertongues with less permeable units of the San Jose Formation. The thickness varies from 50 to 250 m.

The general directions of flow in the Ojo Alamo and Nacimiento aquifers are indicated by the potentiometric contours depicted in Figure 4-4 and Figure 4-3.

Sample Collection and Measurements

Groundwater samples were obtained on in November 1991 by Martin Stute of the Lamont-Doherty Earth Observatory (L-DEO). Samples from 24 locations were initially collected major and trace ion chemistry, noble gases, stable isotopes (^{18}O, D), carbon isotopes (^{13}C, ^{14}C), tritium and ^{36}Cl. Temperature, pH, alkalinity, electrical conductivity, and oxygen content of the water samples were determined in the field. Details of the sampling procedures are described in Stute *et al.* [1995]. Locations of the wells sampled (excluding wells NM-12, -12, -19 and -24) are shown in Figure 4-5.

Of the initial 24 samples, ^{14}C dates and $^{36}Cl/Cl$ ratios were obtained for all but four samples, those from well numbers NM-12, NM-14, NM-19 and NM-24. Samples from those four locations are therefore not included in the following discussions. Both ^{14}C and ^{36}Cl measurements were thus obtained on a total of 20 groundwater samples from the Ojo Alamo and Nacimiento aquifers. It is worth noting that three of the initial samples, NM-15, NM-19, and NM-24 are located near the southern edge of the region shown in Figure 4-5 and are likely part of a different flow regime than that of the remaining samples. While Stute *et al.* [1995] therefore excluded those samples in their paleotemperature study, sample NM-15 is included in this analysis because its ^{14}C age seems reasonable for its location considering the overall flow velocities in the basin.

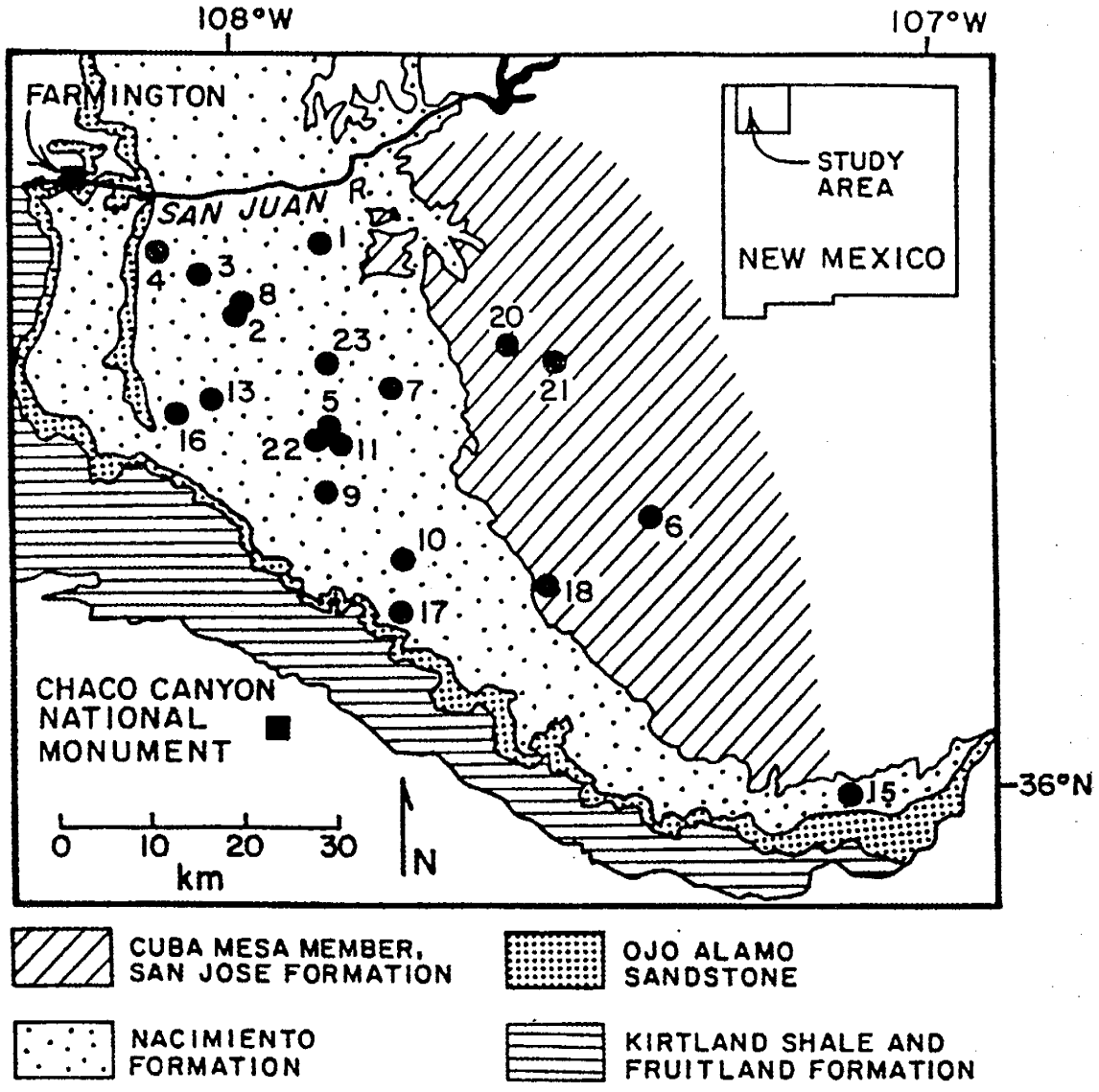

Figure 4-5. Locations of domestic wells sampled in the San Juan Basin. From Stute et al., 1995.

Cl- and Br- Measurements

Cl- concentrations were measured both at the New Mexico Bureau of Mines and Mineral Resources (NMBMMR) by ion chromatography and at L-DEO by ion chromatography. The initial analysis by the NMBMMR included some repeated measurements to explain anomalously high readings in two of the samples. Additional measurements of Cl- concentrations were later made by the NMBMMR in May 1995 with corresponding Br- determinations to obtain Cl-/Br- ratios. Data from the previous Phillips *et al.* [1989] study (for which analyses were also performed by the NMBMMR) provided an additional check on the Cl- concentrations determined during the present study. The available Cl- and Cl:Br-

data are shown in Table 4-1. Average Cl- concentrations shown in the table incorporate all measurements made for the present study with the exception of the indicated anomalous readings.

L-DEO ID	L-DEO Cl- measurements		NM-BMMR ion chromatograph Cl- measurements *				Average Cl- conc. (meq/L)	Average Cl- conc. (mg/L)	NM-BMMR Br- (ug/L)	Cl/Br ratio (by wt.)
	Cl-ometer (meq/L)	Dionex (meq/L)	1 (meq/L)	2 (meq/L)	3 (meq/L)	4 (meq/L)				
NM-1	0.36	0.30	0.41	0.18	0.19	0.22	0.25	8.9	69	129
NM-2	0.09	0.12	0.12	0.08		0.08	0.09	3.3	32	103
NM-3	0.15	0.17		0.10	0.07	0.12	0.12	4.3	28	153
NM-4	0.13	0.17		0.18		0.11	0.15	5.2	35	149
NM-5	0.19	0.24		0.09	0.18	0.16	0.17	6.1	88	70
NM-6	0.26	0.26		0.26		0.22	0.25	8.8	102	86
NM-7	0.10	0.14		0.10		0.10	0.11	3.8	19	201
NM-8	0.08	0.08		0.06		0.07	0.07	2.6	30	88
NM-9	0.09	0.13	0.10	0.08		0.09	0.10	3.5	59	60
NM-10	0.08	0.08		0.07		0.08	0.08	2.7	13	211
NM-11	0.11	0.11	0.24	***2.09***	0.06	0.10	0.10	3.4	23	148
NM-12	0.23	0.22		0.21		0.22	0.22	7.8	40	195
NM-13	0.21	0.20	0.49	0.20		0.20	0.20	7.2	80	89
NM-14	0.17	0.16		0.15		0.16	0.16	5.7	51	111
NM-15	0.16	0.14		0.14		0.25	0.17	6.1	51	120
NM-16	0.17	0.17		0.14		***0.56***	0.16	5.7	160	36
NM-17	0.14	0.13	0.18	0.11		0.14	0.13	4.6	91	51
NM-18	0.18	0.17	0.21	***0.37***	0.14	0.17	0.16	5.8	49	119
NM-19	0.14	0.13	0.08							
NM-20	0.19	0.17	0.24	0.14		0.16	0.16	5.8	2400†	2
NM-21	0.12	0.09		0.08		0.08	0.09	3.3	53	62
NM-22	0.33	0.31		0.19	***0.51***	0.27	0.28	9.7	61	160
NM-23	0.07	0.08	0.17	0.09		0.08	0.08	2.8	26	109
NM-24	0.30	0.29	0.24	0.29		0.29	0.29	10.4	101	102

NOTES:

*: NMBMMR Cl measurements numbered 1 - 4 are identified below:

1 - Measurements made for Phillips *et al.*, 1989 study.

2 - Measurements made for present study in August, 1992.

3 - Measurements made for present study in March, 1994 to assess anomalies in earlier measurements.

4 - Measurements made for present study in May, 1995.

Bold italics indicate anomalous readings not included in Cl concentration averages.

†: Repeat measurements made on same date to confirm high concentration of bromide.

Table 4-1. Anion concentrations in San Juan groundwater samples.

^{36}Cl Processing and Ratio Determination

Preparation of samples for ^{36}Cl/Cl ratio determination was performed at New Mexico Tech. The samples were first acidified with nitric acid and $AgNO_3$ was then added to precipitate

AgCl. The precipitate was then purified by repeatedly dissolving the samples in NH_4OH and reprecipitating AgCl by addition of nitric acid. $Ba(NO_3)_2$ was added during one or more of the dissolution steps to remove sulfate. Satisfactory purification was based on visual observation of the precipitate, and the final precipitate was rinsed several times in distilled deionized water before preparing for shipment. In several cases, it was necessary to add 'dead' chloride carrier to the samples to provide sufficient Cl- for the isotopic ratio measurements. These dilutions were then accounted for in the calculation of actual sample $^{36}Cl/Cl$ ratios. Details of the processing method are included as Appendix C and details of the measurements and correction factors are included in Appendix D.

$^{36}Cl/Cl$ ratios were measured by tandem accelerator mass spectrometry at Purdue University according to techniques developed by Elmore and others [1979]. Chlorine-36/Cl ratios were measured for 23 groundwater samples as listed in Table 4-2. A total of 20 ^{36}Cl measurements with corresponding ^{14}C dates are thus available for this study. A sample age was not obtained for NM-12 but the $^{36}Cl/Cl$ ratio of that sample clearly suggests that it contains some bomb pulse water.

^{14}C Dating

L-DEO made radiocarbon age determinations on 21 of the samples (radiocarbon dates were not obtained for sample numbers NM-12, NM-14, and NM-24). A discussion of these dates and how they were obtained is included in Stute *et al.* [1995].

SAMPLE	Age given by Phillips et al. [1989] (ka)	L-DEO Sample Age (ka)	Decay-Corrected ^{36}Cl Ratio (x 10^{-12})	^{36}Cl Ratio +/- (x 10^{-12})	Cl/Br ratio (mg/mg)	Aquifer
NM-1	30.0	32.395	0.690	0.033	129	Tn
NM-2	16.3	23.901	1.162	0.032	103	Tkoa
NM-3		26.310	0.645	0.017	153	Tkoa?
NM-4		21.121	0.762	0.029	149	Tkoa
NM-5	14.0	15.127	1.293	0.027	70	Tn
NM-6	33.0	32.612	1.088	0.031	86	Tn
NM-7	18.0	19.469	1.112	0.013	201	Tn
NM-8	16.3	23.400	1.262	0.011	88	Tn
NM-9	7.3	9.677	1.004	0.004	60	Tkoa
NM-10	17.0	3.207	1.009	0.005	211	Tkoa
NM-11	19.0	19.285	0.989	0.031	148	Tkoa/Tn
NM-12			2.256	0.024	195	
NM-13		19.847	0.907	0.010	89	Tkoa/Tn
NM-14			0.735	0.017	111	
NM-15		4.430	0.730	0.011	120	Tkoa
NM-16		17.764	0.912	0.010	36	Tkoa
NM-17	2.0	2.075	0.765	0.010	51	Tkoa
NM-18	19.0	20.364	0.705	0.007	119	Tkoa
NM-19	2.5	20.689		0.000		
NM-20		33.972	1.084	0.011	2	Tn
NM-21	35.0	31.024	1.190	0.013	62	Tn
NM-22		9.809	1.082	0.013	160	Tn
NM-23	23.0	19.021	1.169	0.010	109	Tkoa/Tn?
NM-24			0.906	0.011	102	

Toa - Ojo Alamo sandstone
Tn - Nacimiento Formation
'?' indicates uncertainty as to the formation(s) tapped

Table 4-2. $^{36}Cl/Cl$ ratios, ^{14}C ages and aquifer tapped for the wells selected for this study.

Results and Discussion

Radiocarbon dates

Radiocarbon dates obtained by Stute *et al.* [1995] generally agreed quite well with dates previously obtained by Phillips *et al.* [1989] for samples from the same well (Figure 4-6). Age deviations for samples NM-2, NM-8 and NM-23 were slightly greater, though within 15%. Stute *et al.* suggest that these wells may tap water from variable sources. The date

obtained for sample NM-10 deviated greatly from a Phillips *et al.* date obtained for a nearby well, suggesting that the two wells tap different sources. While there appears to be some discrepancy in the date for NM-21, the Phillips *et al.* date for that well was a minimum age; the slightly higher age given by Stute *et al.* is thus in good agreement there. For consistency, I have used the dates determined from the Stute *et al.* measurements in considering the variation of $^{36}Cl/Cl$ within the aquifers.

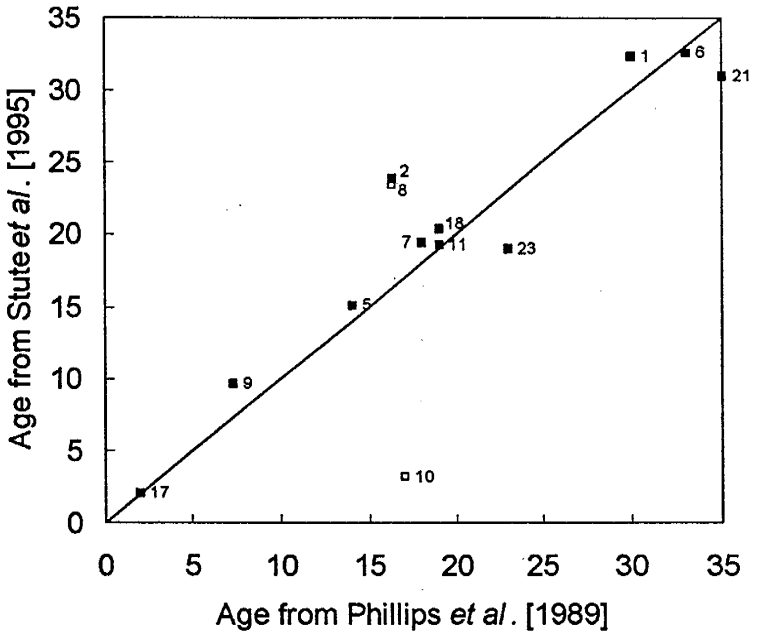

Figure 4-6. Comparison of ^{14}C ages determined by Stute et al. [1995] with those of Phillips et al. [1989]. Open squares compare dates for samples for nearby wells. Solid squares compare dates obtained from different samples from the same well. Well numbers of Stute et al. [1995] are shown next to data points.

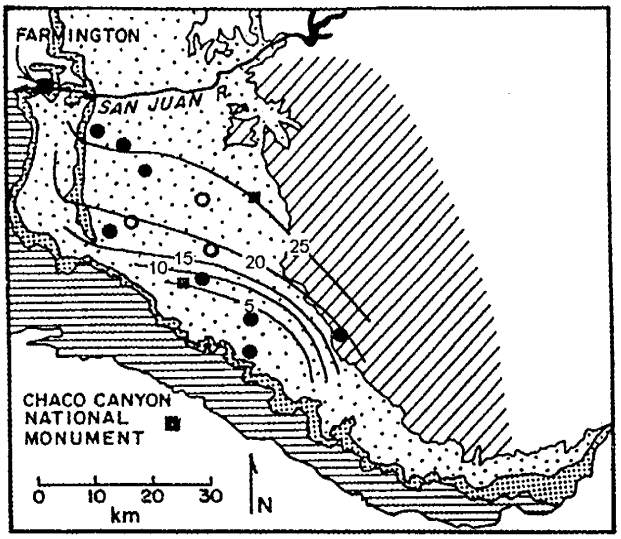

Figure 4-7. Isochrons of ^{14}C age for water in the Ojo Alamo aquifer. Solid circles represent wells sampled by Stute et al. that tap the Ojo Alamo sandstone. Open circles represent wells which may tap both the Ojo Alamo and Nacimiento aquifers. Solid squares represent wells sampled by Phillips et al. [1989].

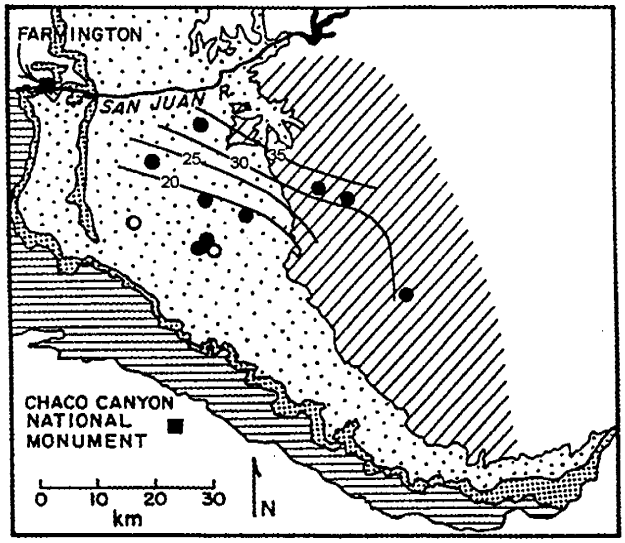

Figure 4-8. Isochrons of ^{14}C age for water in the Nacimiento Formation. Solid circles represent wells sampled by Stute et al. that tap the Nacimiento Formation. Open circles represent wells which may tap both the Ojo Alamo and Nacimiento aquifers.

The ^{14}C dates calculated by Stute *et al.* together with supplemental data from Phillips *et al.* [1989] allow generation of isochron maps for the Ojo Alamo and Nacimiento aquifers (Figure 4-7 and Figure 4-8). In the Nacimiento aquifer, sufficient detail for contouring is available only in the 20 to 30 ka range.

In discussing the distribution of solutes in groundwater along a flowpath it is important to consider the transport processes involved. If, for example, mixing processes are dominant, the input signal of ^{36}Cl in recharge will be considerably damped out during transport. One would then expect to find a rather flat profile of ^{36}Cl as a function of groundwater age. Conversely, if mixing processes are minor compared to the advective transport rate, one would expect the $^{36}Cl/Cl$ ratios along a flowpath to mirror the input signal quite closely. Phillips *et al.* [1989] addressed this issue in their analysis of the physical phenomena affecting the distribution of ^{14}C in the system. They concluded that macroscopic longitudinal dispersion exerts at most a minor influence on the ^{14}C distribution. To analyze inter-aquifer mixing effects they used a mixing-cell ^{14}C transport model to model transport along a two dimensional cross section of

the aquifer. They observed that, despite significant vertical flow components, the mixing cell model yielded groundwater ages in good agreement with a piston flow model of the system. This suggests "that the two aquifers are acting as a single, unified, three-dimensional regional flow system rather than as discrete hydrologic entities influenced by interaquifer leakage" [Phillips *et al.*, 1989].

Distribution of Cl-, Cl/Br and ^{36}Cl in the San Juan Aquifer

^{36}Cl variations

^{36}Cl/Cl ratios for the 20 samples from the Ojo Alamo and Nacimiento aquifers are plotted versus age in

Figure 4-9. The ratios exhibit considerably greater variability than anticipated if variations in the production of ^{36}Cl are the sole source of variability. In addition, a large number of samples in the period between about 17 and 27 ka exhibit much lower ratios than anticipated. While the data seem to indicate a poor match to the anticipated variation signal, it is likely that some of the ratios may be affected by mixing processes that would alter the meteoric ^{36}Cl input signal. To attempt to remove such artifacts from the data, we have also analyzed variations in Cl/Br ratios within the aquifers. It should be noted that the possibility of bomb pulse effects on the samples was addressed by Phillips et al. [1989]. All samples except those taken from springs in recharge areas had "tritium contents indistinguishable from zero."

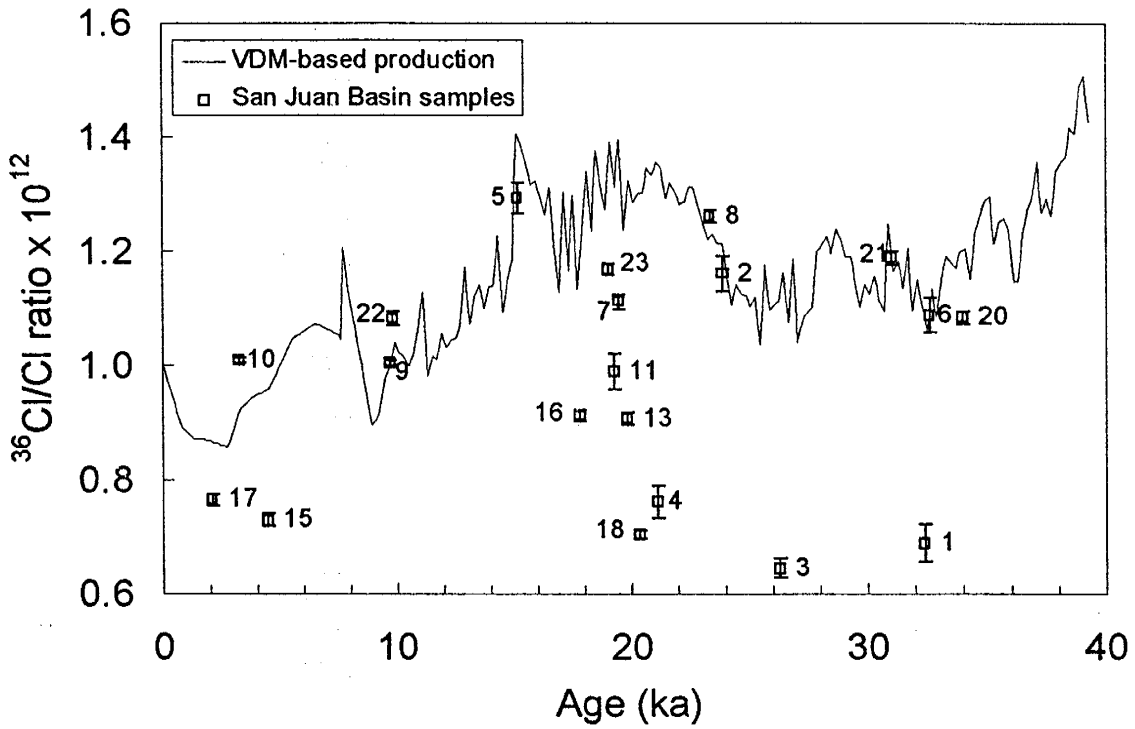

Figure 4-9. $^{36}Cl/Cl$ ratios (corrected for radioactive decay) of groundwater samples from the San Juan Basin (solid squares) vs. the uncorrected ^{14}C ages determined by Stute et al. [1995]. Well numbers are shown next to data points. Solid line represents the production variation of ^{36}C that would be expected based on variations of the earth's dipole moment as seen in the paleointensity record of Tric et al., [1992]. The VDM-based production signal is arbitrarily normalized to a $^{36}Cl/Cl$ ratio of 1 x 10^{-12}.

Variations in the $^{36}Cl/Cl$ ratio of groundwater may be attributed to several possible causes. Because the flux of stable chloride may vary independently of the flux of ^{36}Cl, climatic shifts, variable continental sources of salt, or other factors may alter the $^{36}Cl/Cl$ ratio of recharge over time. Similarly, mixing between aquifers may alter $^{36}Cl/Cl$ ratios during transport. The latter variations should however be evident in the evolution of chloride concentrations and $^{36}Cl/Cl$ ratios along a flowpath. Mixing with older water of higher chloride concentration, for example, should both increase chloride concentrations along the flowpath and decrease the $^{36}Cl/Cl$ ratio.

Chloride Concentration Variations

Initially, the primary source of input for chloride is precipitation, which is then concentrated to some degree by evapotranspiration before recharging the aquifer. Precipitation chemistry measurements recorded at the nearest NADP site (Cuba, NM), indicate that the average

chloride concentration for the period from 1982 to 1993 is 0.10 mg/L. The average chloride concentration of groundwater samples collected for this study is approximately 5 mg/L, consistent with an anticipated evaporative concentration increase of about one order of magnitude.

Information concerning the temporal variability of chloride concentration in recharge is scarce. While available NADP data for nearby Cuba, NM (Figure 4-10) indicate that chloride concentrations in precipitation have been relatively consistent during the past approximately 10 years, this clearly does not reflect the potential variations that may occur due to large-scale climatic shifts or other factors that may affect the flux of stable chloride. Such sources of chloride concentration variation could cause significant variations in $^{36}Cl/Cl$ ratios of recharging soil moisture. There is, however, little evidence to suggest that such variations may have occurred in the San Juan Basin. There are no significant sources of dry chloride in the surrounding region as there are in the region from which the middens discussed in Section Two were obtained. Marine sources of salt are remote and only major changes in atmospheric weather patterns would be expected to alter the annual flux of chloride from these sources. Most of the precipitation that occurs in the region is due to convective activity during the summer monsoons rather than from coastal storms that carry with them a lot of chloride and other aerosols.

The greatest variation in the Cl- concentration of recharge is almost certainly due to variations in evapotranspirative concentration in the soil root zone. These variations would be highly sensitive to climate. However, because the concentration would affect all of the chloride in the soil moisture recharge, this should not affect the $^{36}Cl/Cl$ ratio of the recharging water. It is also worth noting that more concentrated recharge waters are in a sense buffered against variations in Cl/Br ratio and isotopic Cl/Cl ratios due to mixing with water from other sources. Thus, one might expect that an aquifer recharged in a material that promotes evaporative concentration would be relatively insensitive to mixing with water from an aquifer where recharge conditions produce significantly more dilute groundwater. Unfortunately it is generally difficult to distinguish whether the source of salt

in waters of greater salt concentration is evaporative concentration or greater flux of stable chloride in precipitation and dry fallout.

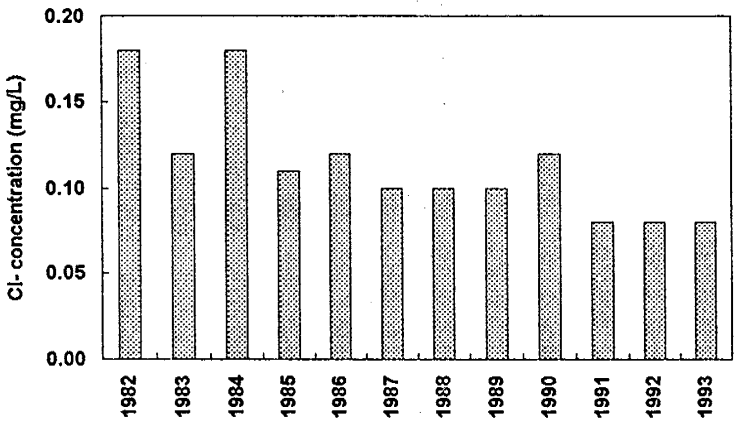

Figure 4-10. Average annual Cl- concentrations in precipitation at Cuba, NM for the period between 1982 and 1993. Data from the National Atmospheric Deposition Program (NADP).

CHLORIDE - BROMIDE RATIOS

Cl/Br ratios can be a useful tool in analyzing mixing evolution. Because both chloride and bromide in the atmosphere are derived mainly from the oceans, the ratio of these two ions over time is not expected to vary significantly even if significant variations in the flux of sea-derived salt to the recharge area occur. Variations in the Cl/Br ratio of local fallout may however be caused by varying sources of continental salt, such as the formation of saline playas during a climatic shift toward a warmer climate. Variations in the Cl/Br ratio of groundwater may also be caused by mixing of water from aquifers of differing ion chemistry. Such effects should be evident in the evolution of Cl- concentrations and Cl/Br ratios along a flowpath.

In general, the Cl/Br ratio of the groundwater should be essentially the same as that of precipitation in the recharge area. Several measurements of Cl/Br ratios in precipitation have been made in the Socorro area between 1978 and 1979 (Table 4-3). Weight ratios of Cl/Br in these samples ranged between approximately 40 and 90, with a mean of 63. The weight ratio of these ions in seawater is approximately 290 [Petersen, 1994; Hem, 1985]. Unfortunately, bromide concentrations are not included in most studies of precipitation chemistry. Cl/Br ratios are therefore not obtainable from NADP records. Several modern studies conducted in the southwest have measured Cl/Br ratios however and these data give an indication of the possible spatial variation of Cl/Br ratios in the region.

Sample ID	Cl (mg/L)	Br (mg/L)	Cl/Br weight ratio
R192	2.56	0.0487	53
10-14-94	0.718	0.0111	65
R&DD Roof Date 08-21-78	4.18	0.0498	84
R&DD Roof Date 09-22-78	0.2315	0.0051	45
R235	7.44	0.0981	76
R237	17.5	0.3150	56

Table 4-3. Cl/Br ratios of rainwater samples collected in Socorro, NM between 1978 and 1994. Samples 10-14-94 was collected by R.S. Bowman, using G. Gross's collection funnel on the roof of Workman Center. All other samples are from G. Gross's archives, collected at various times in 1978 and 1979 using the same apparatus. Analyses were performed by Scott Wightman at Los Alamos National Laboratory under the direction of June Fabryka-Martin.

Chloride and bromide data from Yucca Mountain, Nevada[2] indicates that precipitation in southern Nevada has a Cl/Br ratio of 67 (geometric mean of 92 samples collected during Spring 1995). Turin [personal communication, June, 1995] has measured chloride and bromide concentrations in a series of pools in Lechuguilla cave in southeastern New Mexico. Cl/Br weight ratios of the 22 samples analyzed ranged from 57 to 322 with a mean of 106 and standard deviation of 56. It is possible that the water in those pools may be affected by some unknown process that could alter the initial Cl/Br ratios of the recharge represented. It seems more likely however that the mean Cl/Br ratio of those samples is generally representative of the Cl/Br ratio of precipitation in that region. The Cl/Br ratio of groundwater in the Carrizo aquifer of south central Texas is approximately 210 [Stute *et al.*, 1993]. The trend in the data reported for the three different regions discussed above suggests a decreasing Cl/Br ratio with distance from an oceanic source. Such a trend has not been established in the few atmospheric chemistry studies that have included measurements of both chloride and bromide [Duce *et al.*, 1963, 1965, 1965a; Lininger *et al.*, 1966]. There is some evidence however that Cl/Br ratios in precipitation can be quite variable. Duce *et al.* [1965a] measured Br/Cl ratios up to 30 times the sea water ratio in aerosols collected in Barrow, Alaska and concluded that the behavior of bromide, as well as iodine, in atmospheric transport is somewhat different than that of chloride.

[2] Fabryka-Martin J.T., S.J. Wightman, B.A. Robinson, and E.W. Vestal (in press). Infiltration processes at Yucca Mountain inferred from chloride and chlorine-36 distributions, Los Alamos National Laboratory, Report LA-12970-MS.

It must also be noted that all of the measured Cl/Br ratios in the desert southwest which are discussed above are quite recent and could reflect anthropogenic effects. Lininger *et al.* [1966] noted a strong correlation between concentrations of bromine and lead in aerosols in Boston, MA and Washington, DC. Duce *et al.* [1965] also attributed lower Cl/Br ratios in aerosols over Hawaii than over the sea to pollution from automobile exhaust. It seems unlikely that such pollution would have a substantial effect on precipitation chemistry in either Socorro or Carlsbad Caverns National Park, where Lechuguilla cave is located.

In Figure 4-11, Cl/Br ratios (ordinate axis) of the San Juan basin water samples are plotted against Cl- concentrations (abscissa) with $^{36}Cl/Cl$ ratios depicted by dimensions of the bubble defining the point. While no general trends are obvious in the data, it is likely that variations due to spatial heterogeneities would mask the subtle variations that might occur along one or more flow paths.

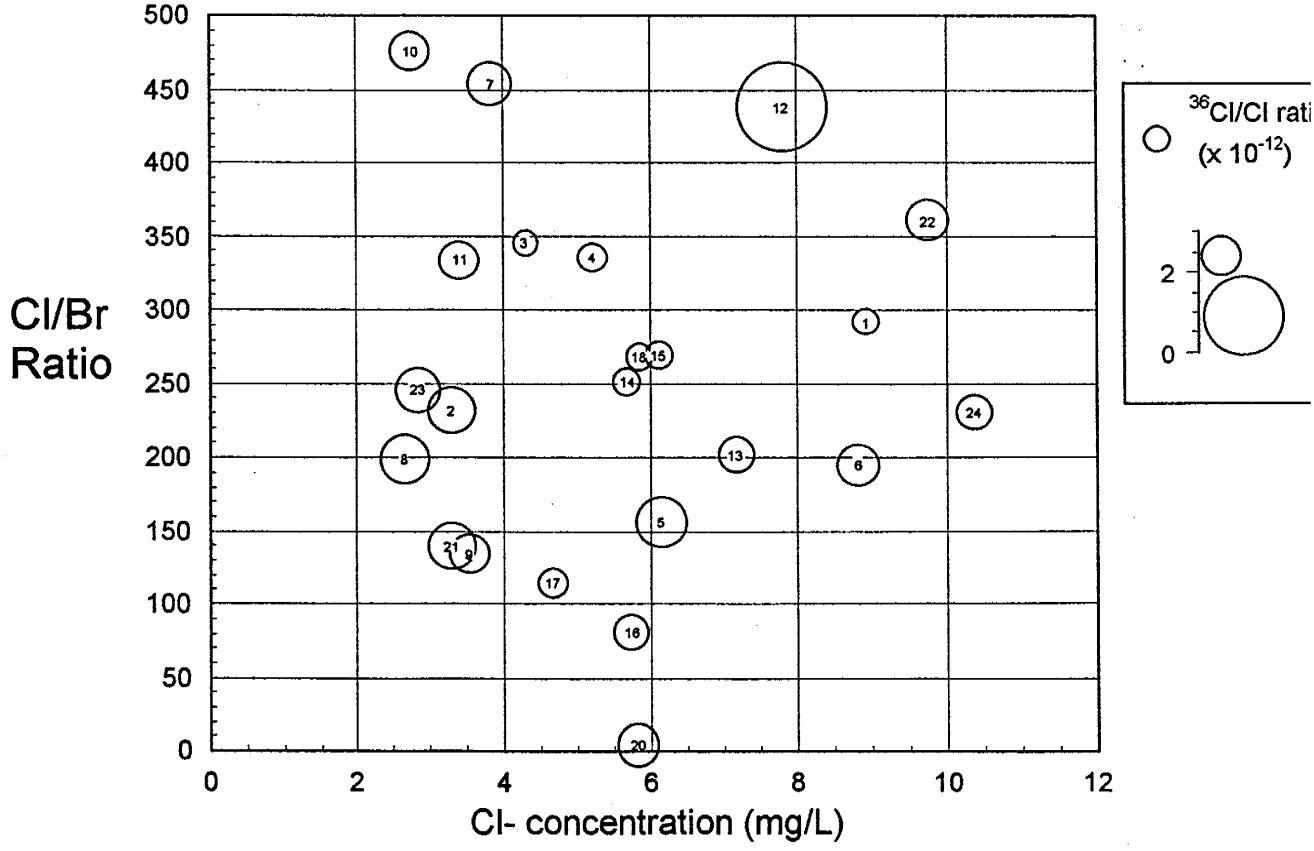

Figure 4-11. Groundwater samples from the San Juan Basin. Cl- concentration vs. Cl/Br concentration with $^{36}Cl/Cl$ ratios (x 10^{13}) shown by dimensions of bubbles. Sample numbers are shown in bubbles.

Several trends are apparent within subgroups of the data. These trends and their implications for evaluation of the temporal variation pattern of ^{36}Cl in recharge to the aquifers are summarized below.

- Cl/Br ratios of samples NM-7, NM-10 and NM-12 are much greater (~200+) than expected based on available data concerning modern variations in Cl/Br ratios and Cl- concentration. While this suggests mixing with water with a non-meteoric source of chloride, the $^{36}Cl/Cl$ ratios are not correspondingly low and the combination of high Cl/Br ratios and average $^{36}Cl/Cl$ ratios is difficult to explain.

- Samples NM-1, NM-3 and NM-4 all exhibit relatively high Cl/Br ratios (~130 - 150) and very low $^{36}Cl/Cl$ ratios. These wells are all located in the northernmost portion of the area shown in Figure 4-5, nearest the San Juan river. It therefore seems likely that the higher Cl/Br ratios in those wells are due to mixing with upwardly discharging water from underlying formations. Samples from NM-2 and NM-8, the closest upgradient wells, have both lower Cl/Br ratios and higher $^{36}Cl/Cl$ ratios, again suggesting that decreasing $^{36}Cl/Cl$ ratios with proximity to the river are due to in-situ mixing effects rather than variations in the $^{36}Cl/Cl$ ratio of ancient recharge. Stute *et al.* [1995] note that NM-1 is "characterized by an unusually high Mg^{2+} and Ca^{2+} content ... possibly representing a mixture with water from another aquifer."

- The anomalously high $^{36}Cl/Cl$ ratio of sample NM-12 is a strong indication that it contains modern water containing bomb pulse ^{36}Cl. No ^{14}C date is available for that sample.

- Cl/Br ratios of samples NM-15 and NM-18 are 120 and 118 respectively. These ratios are considered slightly above the range expected for meteoric water and their $^{36}Cl/Cl$ ratios are correspondingly low.

- Sample NM-11 also exhibits an elevated Cl/Br ratio suggesting mixing with water from other hydrogeologic units in the basin. Stute *et al.* note that both NM-11 and NM-13 tap both the Nacimiento and Ojo Alamo units.

- The Cl/Br ratios of three samples, NM-16, NM-17, and NM-20 are below 50, considerably lower than the range expected for meteoric water in the region. The bromide concentration of sample NM-20 (2400 mg/L) is anomalously high for natural water. Petersen [1994] indicates that 10% of the bromine mined in the USA is for well drilling fluids. The anomalously high Br concentration in that sample may thus reflect sample handling contamination or perhaps contamination of the well by drilling fluids during well installation.

Implications for Analysis of ^{36}Cl Variations

Based on the above observations, it appears that samples NM- 1, 3, 4, 7, 10, 11, 15, 16, 17, 18, and 20 exhibit the effects of mixing with non-meteoric sources of chloride. Based on present day measurements of precipitation chemistry, the Cl/Br ratio of meteoric water in the San Juan Basin should be between approximately 40 and 90, with an average of ~60. The Cl/Br ratio of all of the above-listed samples is outside that range and variations in the Cl/Br ratio along certain flowpaths in the aquifer also suggests mixing with other sources of chloride. The high Cl/Br ratios in many of these samples could be due to a varying amount of continentally derived aerosols in water recharging the aquifer. Continental sources of chloride typically have much higher Cl/Br ratios than that of seawater. The intermontane playas mentioned in Section Two are an example of such a source. Climate fluctuations could vary both the degree to which such sources are exposed to erosion and the rate of removal and distribution of the resultant aerosols. No such sources are known to exist near the basin however and it seems more likely that they are due to geochemical evolution of the groundwater within the basin itself. In order to consider the variations in the ^{36}Cl/Cl ratio of recharge due only to variations in the flux of stable marine chloride and production and distribution of ^{36}Cl, I have eliminated these points from further evaluation of the temporal variation of ^{36}Cl. The remaining data points are plotted against age in Figure 4-12.

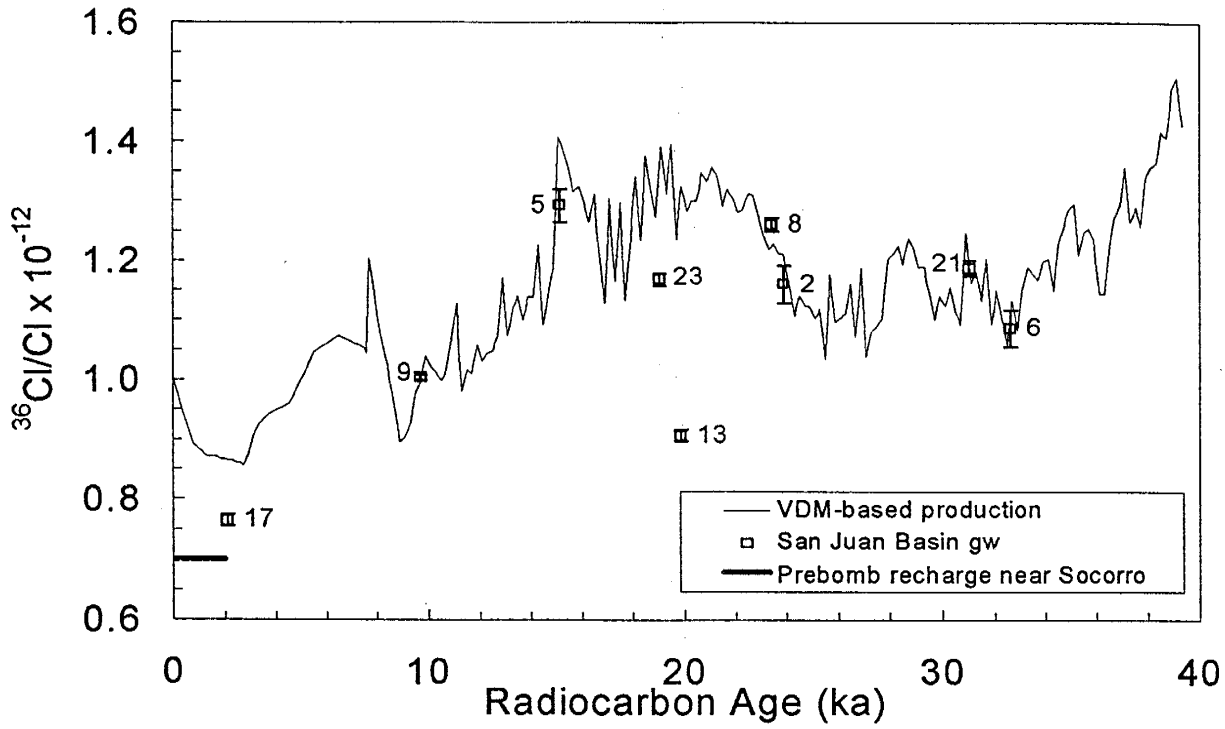

Figure 4-12. ^{36}Cl/Cl ratios of groundwater samples from the San Juan Basin (solid squares) vs. the uncorrected ^{14}C ages determined by Stute et al. [1995]. Some sample data is excluded for reasons stated in the text. Solid line represents the production variation of ^{36}C that would be expected based on variations of the earth's dipole moment as seen in the paleointensity record of Tric et al., [1992]. The production record is arbitrarily normalized to a ^{36}Cl/Cl ratio of 1 x 10^{-12}.

Except for NM-13, the temporal variation of ^{36}Cl/Cl ratios displayed in the remaining samples fits the VDM-based production curve remarkably well. It is worth noting that sample NM-13 taps both the Ojo Alamo sandstone and the Nacimiento Formation. Even if the sample represents a mixture of water from the two aquifers, the ratio is lower than predicted by the production variation based on changes in the geomagnetic field strength. The ^{14}C ages of groundwater from well NM-13 and nearby NM-16 are 19.8 and 17.7 ka, respectively. The VDM-based production record indicates that ratios as low as that observed in NM-13 would only have been produced in the last approximately 10 ka.

If ^{36}Cl/Cl variations are primarily due to changes in the flux of stable chloride to the region, then the ^{36}Cl/Cl ratio should be inversely correlated to the total mass of chloride present in the aquifer per unit time. I have examined this relationship along a flowpath in the Ojo Alamo sandstone, using estimated Cl- concentration contours, distance between adjacent

isochrons (Figure 4-7), and aquifer thickness (based on isopach maps developed by Tansey [1984]) to estimate chloride mass between isochrons. Comparing these temporal variations with the variations in $^{36}Cl/Cl$ seen in the Ojo Alamo and Nacimiento aquifers (Figure 4-13) suggests that, at least along the flow line for which the greatest amount of data is available, $^{36}Cl/Cl$ ratios and Cl- input fluxes are not well-correlated.

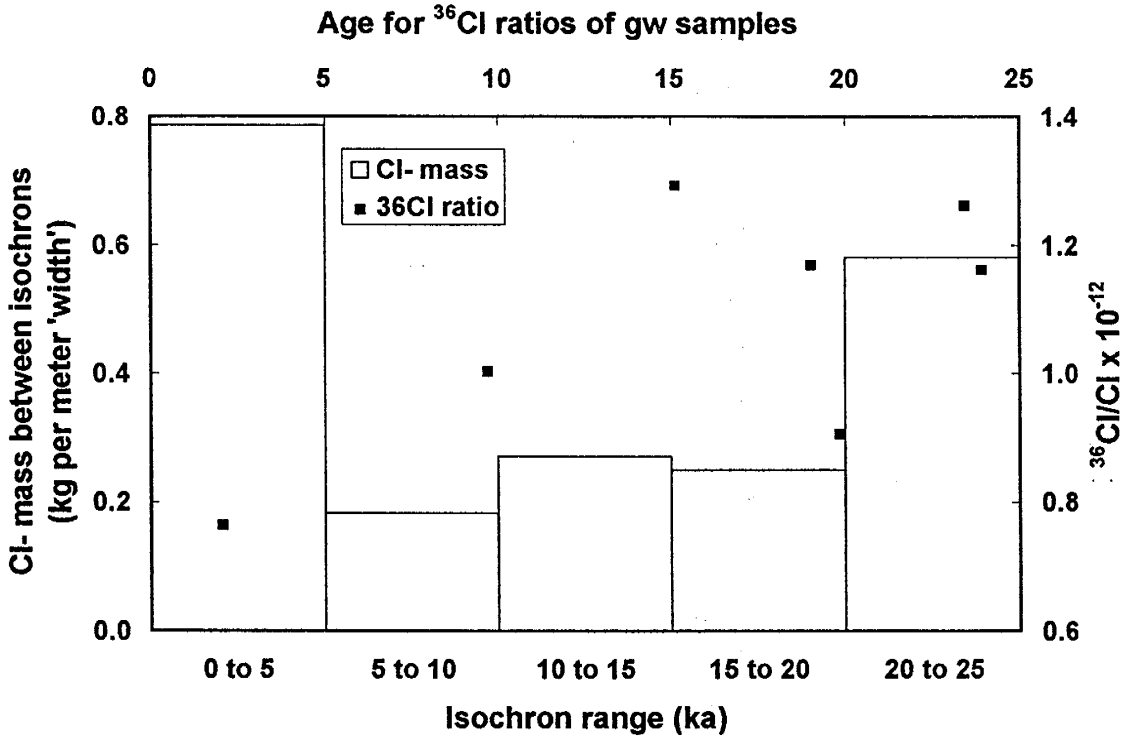

Figure 4-13. Mass of chloride deposited per meter width along an arbitrary flowline (open bars) and $^{36}Cl/Cl$ ratios of selected samples in the Ojo Alamo and Nacimiento versus age.

Summary and Conclusions

Radiocarbon ages, $^{36}Cl/Cl$ ratios and Cl/Br ratios were determined for 23 samples from the San Juan Basin in northern New Mexico. Based on Cl/Br ratios, many of these samples appeared to have been affected by in-situ geochemical changes that would significantly alter the measured $^{36}Cl/Cl$ ratio. For those samples within a narrow range of Cl/Br ratios close to that of modern precipitation in New Mexico, the temporal variation of $^{36}Cl/Cl$ ratios appears to follow the production signal calculated from paleointensity data. Radiocarbon chronology of the aquifer allows some comparison of $^{36}Cl/Cl$ ratios with Cl fluxes within

the aquifer, though such analysis relies heavily on estimates of aquifer thickness and Cl concentration distributions as well as the radiocarbon dating. Based on available information concerning those parameters in the San Juan Basin, $^{36}Cl/Cl$ ratios and Cl fluxes do not appear to be well correlated. This further supports the contention that variations in $^{36}Cl/Cl$ within the aquifer reflect changes in the atmospheric ^{36}Cl production rate, rather than variations in the flux of stable chloride to the region.

Carrizo Aquifer

Geography and Hydrogeology

The Carrizo aquifer is located in the gulf coastal plain of Texas in Atascosa and McMullen counties (approximate location 98°30'W 29°00'N) . The geologic unit is the Carrizo sandstone which is a confined, massive, medium grained sandstone aquifer of Eocene age. Stute *et al.* [1992] describe the unit as follows.

> *The sandstone outcrops out across the northwestern corner of Atascosa County at an elevation of about 200 m above sea level and dips towards the coast in a southeastern direction with a more or less constant slope of about 20 m per 1000 m. Rainfall recharges the aquifer in the outcrop and groundwater is following the structural/depositional dip until it discharges through confining beds into overlying aquifers [Hamlin, 1988]. A systematic hydrochemical evolution occurs along the flow path: the concentrations of total dissolved solids gradually increase, and waters rich in calcium, sodium, bicarbonate, and chloride change to waters rich in sodium-bicarbonate [Hamlin, 1988]. In deeper parts of the aquifer, some groundwater leaks upward into overlying layers. Just south of the border between Atascosa and McMullen counties (after a flow distance of about 75 km), cross-formational leakage along major faults causes mixing with groundwater of deeper origin.*

The Carrizo aquifer hydrogeology, hydrochemistry, and isotope hydrology have been well studied and previous ^{14}C research provides a timescale for the $^{36}Cl/Cl$ ratio measurements of this study. "In one of the classic studies on groundwater dating (Pearson, 1967), a systematic increase of the ^{14}C age with distance was found. [Stute *et al.*, 1993]." While well water samples often provide samples of dubious quality for ^{14}C dating due to contamination with water from other aquifers, Stute *et al.* [1993] indicate that such mixing between the Carrizo aquifer and other aquifers induced by leaky wells is limited and easily recognized through analysis of the geochemical data. Additional support for the general validity of the established ^{14}C ages has been provided by groundwater flow modeling. Brinkman [1981]

developed a numerical model of the aquifer and found that ages derived from that model were consistent with ^{14}C ages within about 20%.

Measurements of $^{36}Cl/Cl$ ratios in groundwater samples have also been made by previous investigators. Six ^{36}Cl measurements were performed in the early 80's [Bentley, 1986]. A slight increase of ^{36}Cl concentrations with age was observed and this was attributed to ion filtration. These $^{36}Cl/Cl$ ratio measurements and additional measurements made for the present study are discussed below in the context of evaluating the Carrizo aquifer as an archive of secular variations in the production rate of ^{36}Cl.

Sample collection and measurements

Samples measured for this study were obtained in October, 1990 by Martin Stute at L-DEO. Groundwater samples from the Carrizo aquifer were collected for measurements of hydrochemistry, noble gases, tritium, ^{14}C, Cl- and ^{36}Cl. Sample collection and results of these measurements are described in Stute *et al.* [1992]. Groundwater samples for $^{36}Cl/Cl$ ratio determination were collected from wells Tx-4, Tx-21, Tx-25, Tx-28 and Tx-33. Cl- concentrations in these samples were measured at L-DEO with a silver electrode automatic titrator. Samples for ^{36}Cl determination were collected in 500 ml glass bottles and shipped to NMIMT where they were processed to produce a relatively pure AgCl sample for AMS analysis. $^{36}Cl/Cl$ ratio determinations were performed with the tandem accelerator mass spectrometer at Purdue University according to techniques developed by Elmore and others [1979].

Sample processing at NMIMT

Groundwater samples were first acidified with nitric acid and $AgNO_3$ was then added to precipitate AgCl. The precipitate was then purified by repeatedly dissolving the samples in NH_4OH and reprecipitating AgCl by addition of nitric acid. $Ba(NO_3)_2$ was added during one or more of the dissolution steps to remove sulfate. Satisfactory purification was based on visual insptction and the final precipitate was rinsed several times in distilled deionized water before preparing for shipment. Cl- concentrations in these samples and sample volumes made addition of carrier chloride unnecessary and laboratory reported $^{36}Cl/Cl$

ratios thus directly reflect those of the actual groundwater samples. Details of the processing method are included as Appendix C.

Results and Discussion

Chronology

Groundwater sample ages were estimated as described in Stute *et al.* [1993]:

> *The linear relationship between ^{14}C ages [13] (Pearson and White, 1967) and distance from the recharge area along flowlines was used to convert distances into ages [15] (Stute et al., 1992). Ages in excess of 30 ka based on this linear extrapolation are less well constrained since the ^{14}C content is below the detection limit. The timescale used in this study is characterized by (systematic) errors in the range of a few thousand years.*

^{36}Cl variations

Results of the $^{36}Cl/Cl$ ratio determinations with corresponding ^{14}C ages and Cl-concentrations determined by Stute *et al.* [1993] are shown in †: Ages estimated by Martin Stute from interpolation between limited ^{14C} data.

Table 4-4. Because of the proximity of the aquifer to the coast, there is a definite dependence of stable Cl- flux on climate, in particular on sea level elevation changes and corresponding changes in distance from the aquifer to the coast. During the Pleistocene, sea level was approximately 120m lower than at present, due to the large amount of sea water trapped in glacial ice. Due to the bathymetry of the Gulf of Mexico, this translates to an approximately 125 km change in the distance from the aquifer to the coastline [Stute *et al.*, 1993]. Stute *et al.* used the modern spatial distribution of Cl flux ratios from NADP data to then convert the changing distance to the coast into an estimated present and paleo-chloride flux to the recharge area(Table 4-4).

Sample ID	Cl- conc. (meq/L)	Estimated age † (ka)	Decay-corrected $^{36}Cl/Cl$ ratio (x 10^{-15})	Cl- deposition rate ($mmol/m^2/yr$)	$^{36}Cl/Cl$ ratio normalized to Cl- flux
AL6851803	3.64	0	90	14.1	90
AL6859504	1.47	1.836	32	14.1	32
AL7805104	0.92	9.468	64	10.9	49
Tx 21	0.83	11.127	104	10.9	81
AL7812201	1.14	14.018	80	10.9	62
Tx 28	0.59	16.625	91	10.9	70
Tx 4	0.50	20.275	91	10.9	70
Tx 33	1.71	25.869	63	10.9	49
Tx-25	2.21	27.670	61	10.9	47
SU7836201	2.06	33.785	59	10.9	46
SU7851201	6.58	-	18	-	14

†: Ages estimated by Martin Stute from interpolation between limited ^{14}C data.

Table 4-4. Chloride and ^{36}Cl data for the Carrizo aquifer.

This flux of stable chloride to the aquifer recharge zone can be accounted for in estimating the initial $^{36}Cl/Cl$ ratio of the recharge by normalizing $^{36}Cl/Cl$ ratios to the present rate of chloride deposition. The ratios shown in the last column of Table 4-4 are so adjusted and these ratios are plotted in Figure 4-14. The VDM-based production signal in Figure 4-14 is arbitrarily normalized to a ratio of 30×10^{-15}. This is the ratio estimated for the recharge area of the Carrizo aquifer from the distribution predicted by Bentley *et al.* [1986]. Variations in the rate of chloride deposition could also be estimated using contoured ^{14}C ages, aquifer thicknesses and chloride concentration data, as was done for the San Juan basin. This would provide a better means of filtering out the stable chloride variation signal.

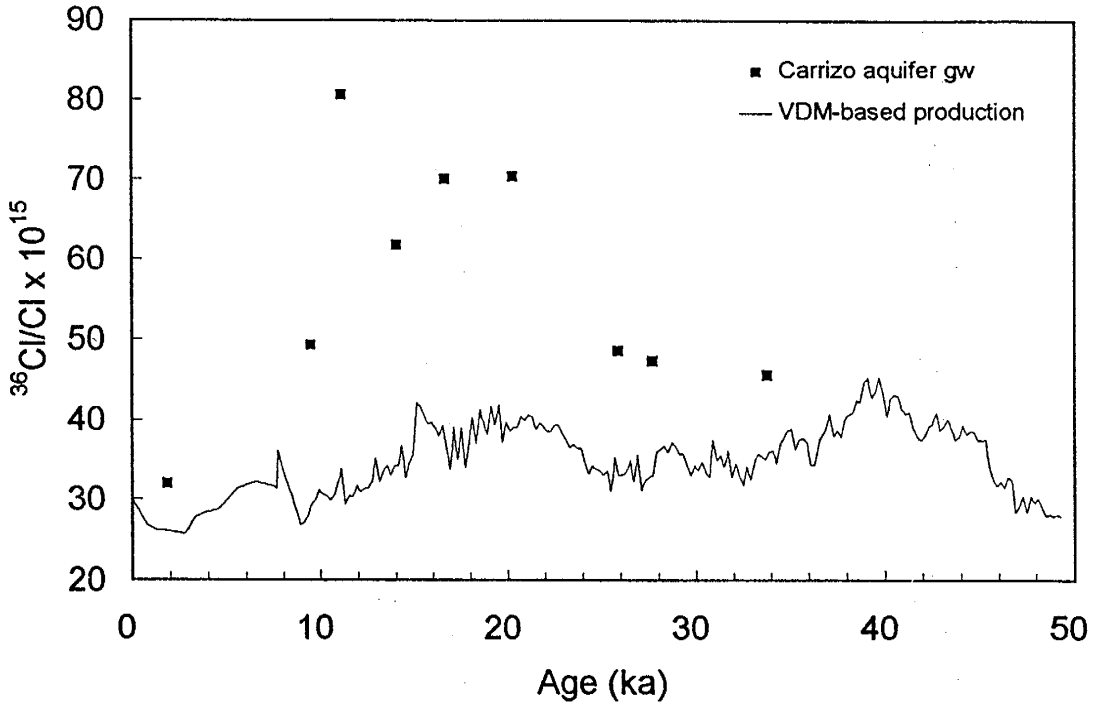

Figure 4-14. $^{36}Cl/Cl$ ratios of groundwater samples from the Carrizo aquifer, Texas, plotted against age determined by interpolation of existing ^{14}C data. The VDM-based production record is arbitrarily normalized to a ratio of 30 x 10^{-15}.

The resultant pattern of ^{36}Cl variation has a range of approximately a factor of two, much greater than the range anticipated from the VDM-based production signal. Disregarding the large difference in magnitudes, there is some similarity in the patterns of variation. Both signals show a broad peak centered at ~20 ka, with a steep increase in ratios from ~25 ka to 20 ka and a gradual decrease in ratios from ~16 ka to the present. Given uncertainty in the estimated change in Cl flux at the Pleistocene - Holocene transition, it is quite possible that the magnitude of the variation across that boundary is inaccurate. Errors in that estimate, however, would not affect $^{36}Cl/Cl$ ratios prior to the Holocene, where large variations are also observed.

Section Summary

Under the right conditions, groundwater samples provide a means of assessing long-term variations in the flux of conservative solutes such as chloride. ^{36}Cl concentrations in groundwater samples along a flowpath may thus provide a record of the secular variation of production of ^{36}Cl. In this study we examined $^{36}Cl/Cl$ ratios of groundwater samples from the San Juan Basin in northern New Mexico and from the Carrizo Aquifer in the gulf

coastal plain of Texas. The pattern of $^{36}Cl/Cl$ variation in these two systems is quite different. Discounting samples that appear to have been affected by in-situ sources of chloride, the San Juan data provide evidence that long-term variations in the atmospheric ^{14}C activity are directly related to variations in the strength of the earth's magnetic field. While the wide variations in Cl/Br ratios throughout the aquifers diminishes confidence in this interpretation, the basis for eliminating some samples from further analysis is arguably sound. On the other hand, the magnitude of variation in $^{36}Cl/Cl$ ratios in the Carrizo samples is much greater than that of the VDM-based production signal. That record suggests that ratios were at least twice as high as modern ratios between ~16 and 22 ka, but that ratios prior to 22 ka were only about 50% higher than modern. Because of the proximity of that aquifer to the Gulf Coast, chloride flux there changed dramatically at the end of the Pleistocene. Given the uncertainty in the magnitude of that change, it seems likely that variations in the flux of stable chloride to the recharge area have not been adequately filtered in the ^{36}Cl variation record. The Carrizo aquifer is not an ideal location to assess variations in ^{36}Cl flux and it may be prudent to place less confidence these data in our attempt to reconstruct the secular variation of cosmogenic nuclide production. Differences and similarities between these and other archives of cosmogenic nuclides are discussed in Section Five.

Section Five

Synthesis of Interpretation of ^{36}Cl Archives

> *Hume (Of Miracles, 1748) advanced the following principle which, echoing Okham, has been called Hume's Razor: "No testimony is sufficient to establish a miracle unless that testimony be of such a kind that its falsehood would be more miraculous than the fact which it endeavours to establish."*
>
> *- William Grey, Philosophy and the Paranormal. Part 2: Skepticism, Miracles, and Knowledge. Skeptical Inquirer 1994.*

In previous sections, I have summarized previous research regarding secular variation of cosmogenic nuclide production and extended study of that phenomenon with results of investigations of three archives of ^{36}Cl - fossil packrat middens, soil moisture and groundwater. From Section One, we may conclude that secular variations in atmospheric ^{14}C activity (as well as other cosmogenic nuclides) are not well understood, though it is widely accepted that the primary mechanism for such variation is modulation by a varying geomagnetic field. Archives of ^{14}C indicate that the atmospheric activity of ^{14}C was approximately 30% higher prior to ~15 ka but this difference has been variously attributed to oceanic venting [Edwards et al., 1993], geomagnetic control [Mazaud et al., 1991] or some combination of these factors. Polar archives of cosmogenic ^{10}Be and ^{36}Cl appear to record production rate variations due to solar modulation but are likely incapable of recording geomagnetically controlled variations because production at the poles is virtually independent of geomagnetic field strength effects. The dramatic decrease in ^{36}Cl and ^{10}Be concentrations that is seen in many polar ice cores during the transition from Pleistocene to Holocene is generally attributed to an increase in precipitation rates, rather than to production rate variations. The polar ^{10}Be archives do record two anomalous concentration peaks at ~35 and 60 ka B.P. These appear to reflect actual cosmogenic nuclide production rate increases and should be evident in other terrestrial archives of cosmogenic nuclides. The only study of low-latitude ^{10}Be variations that has been conducted indicates that cosmogenic nuclide production rates were approximately 20% higher during the last glacial maximum [Lao et al., 1992].

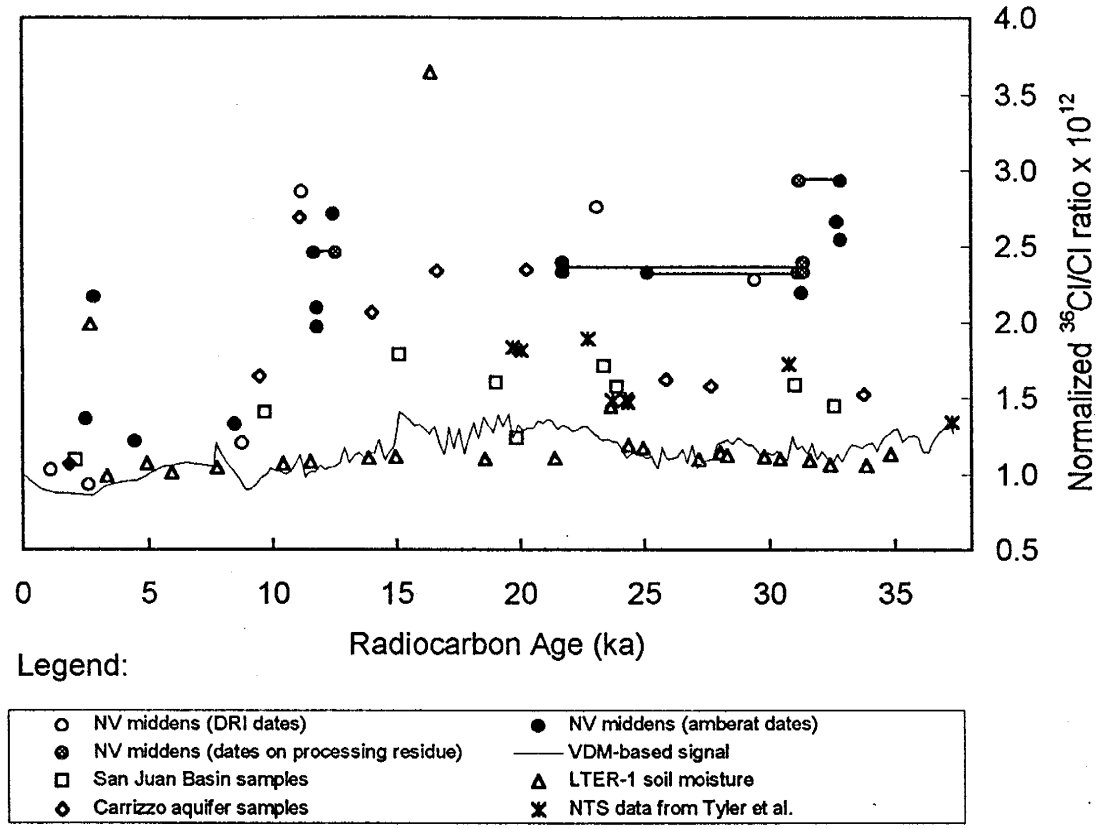

Figure 5-1. Composite plot of $^{36}Cl/Cl$ ratios measured for this study, each normalized to the respective estimated modern pre-bomb ratio. Corrections for decay are not included.

Results of the present study of several terrestrial archives that record $^{36}Cl/Cl$ variations over the last several thousand years are shown together in Figure 5-1, with each data set normalized to the estimated modern, pre-bomb $^{36}Cl/Cl$ ratio. Based on these data, I present the following conclusions.

Inferences about past cosmogenic nuclide production rates based solely on the packrat midden ^{36}Cl data reported in this study would be speculative at best. The number of data points currently available does not provide the necessary resolution and we currently have no means of determining whether variations in atmospheric distribution of ^{36}Cl or stable chloride flux may have affected $^{36}Cl/Cl$ ratios in the middens. In addition, the data from the California samples do not correspond well with the data from the Nevada middens and the New Mexico samples span a range of ages too short to evaluate long-term (10 ka+) $^{36}Cl/Cl$ variations. Variations in the $^{36}Cl/Cl$ ratio of chloride in the middens may well have

been caused by variations in the flux of stable chloride. The trend in the ratios of samples from Nevada is consistent with the hypothesis that an increase in the flux of continental dust occurred in the region at the termination of the Pleistocene.

While it seems likely that the flux of stable chloride and other aerosols would have increased as conditions became dryer at the close of the Pleistocene, there is no evidence to demonstrate that such a change actually occurred in the vicinity of the Mother Midden. Indeed, it may be argued that local sources of chloride-bearing arid dust are quite distant as well as upwind from the Mother Midden, so that $^{36}Cl/Cl$ ratios of infiltration at that location would be unaffected by their introduction. If we assume that stable chloride flux near the middens has been relatively constant then the $^{36}Cl/Cl$ variations may be attributed to ^{36}Cl production rate variations in the atmosphere. The fact that the pattern of variation does not match that based on the paleomagnetic data could be due to several factors.

Interpretation of the $^{36}Cl/Cl$ variations in the LTER-1 profile is hampered by the large chloride concentration fluctuations that occur over small depth intervals. While there are some similarities in the observed trend to that of the VDM-based production record, the correlation is too weak to suggest any clear conclusions regarding the cause of ^{36}Cl variations in the soil samples. Like the midden data, the record in the soil lacks a means of estimating ^{36}Cl flux variations independent of stable chloride flux variations. In spite of these objections, it should be noted that the overall trend in the $^{36}Cl/Cl$ ratios in the LTER-1 samples is not inconsistent with the midden record and other long-term indicators of cosmogenic nuclide production rate variations. Ratios in vadose zone samples from the Nevada Test Site [Tyler et al., submitted to IAEA] show an increasing trend from ~ 100 ka to 20 ka. While these data do not match the VDM-based signal well, the overall magnitude of variation is similar and the increasing trend in samples older than ~ 20 ka is actually similar to the trend in ratios seen in groundwater samples.

Chlorine-36/Cl ratio variations in groundwater samples have the advantage of allowing an independent means of estimating stable chloride and ^{36}Cl fluxes because the groundwater can be radiocarbon dated and fluxes inferred from concentrations and volumes of water

between isochrons. Our data from the San Juan Basin is well-correlated with the VDM-based production record where Cl/Br ratios are within a narrow range of the modern ratio in precipitation. This is the strongest evidence found in this study to confirm a magnetic field strength control of cosmogenic nuclide production. As noted above, ratios in vadose zone samples from the Nevada Test Site agree relatively well with the San Juan data for the period between ~35 ka and 20 ka. While the magnitude of variation observed in the Carrizo aquifer is much larger, $^{36}Cl/Cl$ ratios there may have been strongly affected by changes in stable chloride flux at the end of the Pleistocene, as distance from the aquifer to the coast was reduced. While such changes should not have affected the equally large variations seen before ~15 ka, it is apparent that $^{36}Cl/Cl$ ratios in the Carrizo aquifer are highly sensitive to climate variations because of its proximity to the coast.

The magnitude of $^{36}Cl/Cl$ variations in the Carrizo aquifer is quite similar to that seen in the packrat middens from Nevada. The major difference between these records is in the period between ~35 ka and 12 ka, where the middens suggest that ratios remained relatively high and the Carrizo data suggest that ratios increased from near-modern ratios to a broad peak centered at ~20 ka. It is possible that the variations observed in these records reflect $^{36}Cl/Cl$ variations throughout the southwest more accurately than does the record preserved in the San Juan aquifer, and that the magnitude of variation was considerably greater than is indicated by calculations based on available paleointensity records.

Considered together, the $^{36}Cl/Cl$ ratios recorded in the Nevada packrat middens and groundwater from the San Juan basin and Carrizo aquifer strongly suggest that $^{36}Cl/Cl$ ratios of infiltration in the southwest were at least 50% higher prior to about 12 ka, and perhaps as much as 100% higher. Although trends in $^{36}Cl/Cl$ ratios of deep soil moisture from boreholes in the Sevilleta are quite different from the midden and groundwater records, those profiles also support the premise that ratios were significantly higher in the past. These archives are all quite remote from one another, supporting the hypothesis that the source of the change is not simply introduction or increase of locally derived chloride-bearing arid dust. While the magnitude of the shift seen in the Mother Midden and Carrizo $^{36}Cl/Cl$ ratios is significantly greater than that indicated by the paleomagnetic data of Tric et

al. [1992], results of other investigators also suggest that production rates prior to ~12 ka may have been higher than is indicated that signal. Prior to ~15 ka, the Bard et al. [1990] data show a significant discrepancy between paleo-^{14}C-activities calculated from geomagnetic variations and paleo-activities measured in ancient corals. Discrepancies between the paleointensity-based production signal and archives of cosmogenic nuclides may be due to inaccuracies in the paleomagnetic measurements, variations in atmospheric circulation and distribution of cosmogenic nuclides, inaccurate calculations of the response of production to variations in the modulating factors or other unknown factors. Other archives of cosmogenic nuclides also show variations not seen in the paleointensity signal. ^{10}Be peaks in polar ice cores at ~35 ka and 60 ka can not be explained by geomagnetic variations and some of the discrepancies observed in some of the data collected for this study may be related to those unexplained variations.

The large ^{36}Cl/Cl variations observed in the midden samples and the groundwater samples from the Carrizo aquifer may well have been caused by changes in stable chloride flux. While this would not further our understanding of secular variation of the production of cosmogenic nuclides, the signal could still prove a valuable soil moisture and groundwater tracer. If ^{36}Cl/Cl ratios of infiltration changed due to a changing stable chloride flux, it is likely that the effect was associated with the climate change at the end of the Pleistocene. The mechanism for such a variation could be related to atmospheric circulation patterns or to dramatically increased production and distribution of arid dust in the southwest. In any case, the effect is apparently widespread across, at least, the southwest and these data will undoubtedly prove valuable in further attempts to use ^{36}Cl/Cl ratios as a tracer in the subsurface.

Suggestions for Further Research

A large increase in continental aerosol redistribution at the end of the Pleistocene should be evident in Cl concentrations in soil moisture and groundwater. Evidence of such a pronounced change might therefore be detected through examination of variations in constituents that are much less difficult to measure than ^{36}Cl.

Further efforts to attempt to define global variations in ^{36}Cl production variations might best be concentrated on further analysis of groundwater samples. There has been extensive study of long-term flow paths in the Great Artesian Basin, Australia with many radiocarbon and some ^{36}Cl measurements. This seems to be a promising place to continue research in to the record preserved in groundwater archives. If other groundwater records bear the same signature as the San Juan data, it would virtually confirm that ^{14}C activity variations in the atmosphere are due, at least in part, to magnetic field strength changes. This could lead to a greater understanding of other processes affecting ^{14}C activities as these other sources of variation could be deconvolved from the record of variation with the known VDM record.

Twomey [1977] notes that there has been little effort made to evaluate long-term trends in precipitation chemistry. Similarly, there appears to be little data regarding long-term chemical variations of natural recharge. Analysis of these variations can provide information about the sources of solutes in recharge as well as past rates of recharge (as demonstrated in the Carrizo study of and Stute *et al.* [1992]). Several researchers have used ratios of various ionic constituents to infer the origin of solutes in precipitation [Gambel, 1962; Junge and Werby, 1958]. This analysis could be extended to soil and groundwater samples using conservative ionic solutes such as Cl and Br.

There is relatively little data available regarding the actual spatial distribution of $^{36}Cl/Cl$ ratios in modern precipitation. While the distribution pattern described by Bentley *et al.* [1986] often provides a reasonable estimate of the modern pre-bomb ratio, recent research [S. Davis, pers. comm, Dec. 1995] indicates that the published $^{36}Cl/Cl$ distribution for the U.S is not very accurate. A better understanding of the atmospheric processes affecting $^{36}Cl/Cl$ ratios in precipitation and fallout would be very useful in interpretation of $^{36}Cl/Cl$ ratios and ratio variations in soil and groundwater.

Large concentration fluctuations over small changes in depth were observed in Cl, ^{36}Cl, and, in some cases, stable isotopes at the LTER site in the Sevilleta National Wildlife Refuge. Similarly "spiky" profiles have been observed in shallow vadose zone profiles in other areas of the arid southwest. These profiles are difficult to explain assuming standard advective

dispersive transport of conservative solutes. The soil moisture content data does not suggest the soils are dry enough to present an effective barrier to liquid transport. Given their apparently common occurrence in arid zone soil profiles, it would be worthwhile to pursue a better understanding of the phenomenon.

A common problem in interpretation of variations in environmental tracers is a lack of a local reference record of variation for environmental tracers. It seems likely that spatial variations in temporal variation patterns of solute deposition may persist even over long periods of time. This complicates interpretation of tracer data when one generally has available only a presumed global record of deposition variations. This is particularly problematic in profiles believed to represent tens of thousands of years of accumulation. In younger profiles however, it may be possible to compare variations within a soil profile to chemical and climatic variations inferred from dendrochronological records. Vroblesky and Yanosky [1990] demonstrated that chloride concentration variations in tulip tree rings appeared to record the arrival of a chloride front migrating from an upgradient landfill. Stable isotope variations are also recorded in tree rings [Feng and Epstein, 1994]. Analysis of soil moisture chemical and isotopic variations in an area where a reliable tree record of the same variations would provide an invaluable tool in interpretation of the factors affecting transport in the vadose zone.

References

Andrews, J.N., Florkowski, T., Lehmann, B.E., and Loosli, H.H. (1991). Underground production of radionuclides in the Milk River aquifer, Alberta, Canada, *Applied Geochemistry*, **6**: 425-434.

Bard, E., and Broecker, W.S. (1992). *The Last Deglaciation : Absolute and Radiocarbon Chronologies*, Springer-Verlag, Berlin; New York,

Bard, E., Hamelin, B., Fairbanks, R.G., and Zindler, A. (1990). Calibration of the 14C timescale over the past 30,000 years using mass spectrometric U-Th ages from Barbados corals, *Nature*, **345**: 405-410.

Beer, J., Baumgartner, St., Dittrich-Hannen, B., Hauenstein, J., Kubik, P., Lukasczyk, Ch., Mende, W., Stellmacher, R., and Suter, M. (1994). Solar variablity traced by cosmogenic isotopes, in *The Sun as a Variable Star: Solar and Stellar Irradiance Variations*, ed. J.M. Pap, C. Frohlich, H.S. Hudson and S.K. Solanki, Cambridge University Press, pp. 291-300.

Beer, J., Bonani, G., Hofmann, H.J., Suter, M., Synal, A., and Wolfli, W. (1987). 10Be measurements on polar ice comparison of Arctic and Antarctic records, *Nuclear Instruments and Methods in Physics Research*, **B29**: 203-206.

Beer, J., Joos, F., Lakasczyk, Ch., Mende, W., Rodriguez, J., Siegenthaler, U., and Stellmacher, R. (1994). 10Be as an indicator of solar variability and climate, in *The Solar Engine and its Influence on Terrestrial Atmosphere and Climate, NATO ASI Series*, ed. E. Nesme-Ribes, pp. 221-233.

Beer, J., Siegenthaler, U., Bonani, G., Finkel, R.C., Oeschger, H., Suter, M., and Wolfli, W. (1988). Information on past solar activity and geomagnetism from 10Be in the Camp Century ice core, *Nature*, **331**: 675-679.

Benson, L. (1993). Factors affecting 14C ages of lacustrine carbonates: Timing and duration of the last highstand lake in the Lahontan Basin, *Quaternary Research*, **39**: 163-174.

Benson, L., Currey, D., Lao, Y., and Hostetler, S. (1992). Lake-size variations in the Lahontan and Bonneville basins between 13,000 and 9000 14C yr B.P., *Palaeogeography, Palaeoclimatology, Palaeoecology*, **95**: 19-32.

Bentley, H.W., Phillips, F.M., and Davis, S.N. (1986). Chlorine-36 in the terrestrial environment, in *Handbook of Environmental Isotope Geochemistry*, ed. P. Fritz and J.C. Fontes, pp. 422-475.

Bentley, H.W., Phillips, F.M., Davis, S.N., Habernehl, M.A., Airey, P.L., Calf, G.C., Elmore, D., Gove, H.E., and Torgersen, T. (1986). Chlorine 36 dating of very old groundwater, 1, The Great Artesian Basin, Australia, *Water Resources Research*, **22**: 1991-2001.

Betancourt, J.L., and Van Devender, T.R. (1990). *Packrat Middens, The Last 40,000 Years of Biotic Change*, University of Arizona Press, Tucson,

Blinov, A. (1988). The dependence of cosmogenic isotope production rate on solar activity and geomagnetic field variations, in *Secular Solar and Geomagnetic Variations in the Last 10,000 Years*, ed. F.R. Stephenson and A.W. Wolfendale, Kluwer, Dordrecht, pp. 329-340.

Brinkman, J.E. (1981). Water age dating of the Carrizo Sand, *Thesis* ,University of Arizona, Tucson.

Chadwick, O.A., and Davis, J.O. (1990). Soil-forming intervals caused by eolian sediment pulses in the Lahontan basin, northwestern Nevada, *Geology*, **18**: 243-246.

Craig, H., and Gordon, L.I. (1965). Deuterium and oxygen-18 variations in the ocean and the marine atmosphere, in *Stable Isotopes in Oceanographic Studies and Paleotemperatures*, pp. 9-130.

Damon, P.E., Cheng, S., and Linick, T.W. (1989). Fine and hyperfine structure in the spectrum of secular variations of atmospheric 14C, *Radiocarbon*, **31**: 704-718.

Damon, P.E., Lerman, J.C., and Long, A. (1978). Temporal fluctuations of atmospheric 14C: causal factors and implications, *Ann. Rev. Earth Planet. Sci.*, 457-494.

Davis, O.K. (1992). A solar pacemaker for rapid climate change, *American Quaternary Association 12th Biennial Mtg. Program and Abstracts* ,University of California ,Davis.

Dowgiallo, J., Nowicki, Z., Beer, J., Bonani, G., Suter, M., Synal, H.A., and Wo:lfli, W. (1990). 36Cl in ground water of the Mazowsze Basin (Poland), *Journal of Hydrology*, **118**: 373-385.

Edwards, R.L., Beck, J.W., Burr, G.S., Donahue, D.J., Chappell, J.M.A., Bloom, A.L., Druffel, E.R. M., and Taylor, F.W. (1993). A large drop in atmospheric 14C/12C and reduced melting in the Younger Dryas, documented with 230Th ages of corals, *Science*, **260**: 962-968.

Elmore, D., Conard, N.J., Kubik, P.W., Gove, H.E., Wahlen, M., Beer, J., and Suter, M. (1987). 36Cl and 10Be profiles in Greenland ice: dating and production rate variations, *Nuclear Instruments and Methods in Physics Research*, **B29**: 207-210.

Elmore, D. , Fulton, B.R., Clover, M.R., Marsden, J.R., Gove, H.E., Naylor, H., Purser, K.H., Kilius, L.R., Beukens, R.P., and Litherland, A.E. (1979). Analysis of 36Cl in

environmental water samples using an electrostatic accelerator, *Nature*, **227**: 22-25.

Elsasser, W.E., Ney, E.P., and Winckler, J.R. (1956). Cosmic ray intensity and geomagnetism, *Nature*, **178**: 1226-1227.

Emerson, D.O., and Howard, W.E. (1978). Mineralogy of woodrat, neotoma cinerea, urine deposits from northeastern California, *Journal of Mammology*, **59**: 424-425.

Eriksson, E. (1960). The yearly circulation of chloride and sulfur in nature: meteorological, geochemical and pedological implication, Part II, *Tellus*, **12**: 63-109.

Eriksson, E. (1959). The yearly circulation of chloride and sulfur in nature: meteorological, geochemical and pedological implication, Part I, *Tellus*, **11**: 375-403.

Fabryka-Martin, J., Davis, S.N., and Elmore, D. (1987). Applications of 129I and 36Cl in hydrology, *Nuclear Instruments and Methods in Physics Research*, **B29**: .

Fabryka-Martin, J.T., Wightman, S.J., Robinson, B.A., and Vestal, E.W. (in press). Infiltration processes at Yucca Mountain inferred from chloride and chlorine-36 distributions, *Report LA-12970-MS* ,LANL.

Feng, X., and Epstein, S. (1994). Climatic implications of an 8000-year hydrogen isotope time series from Bristlecone Pine trees, *Science*, **265**: 1079-1081.

Feth, J.H. (1981). Chloride in natural continental water - a review, *Geological Survey Water-Supply Paper 2176* ,U.S. Gov't Printing Office.

Gambel, A.W., Jr. (1962). Indirect evidence of the importance of water-soluble continentally derived aerosols, *Tellus*, **14**: 91-95.

Hem, J.D. (1985). Study and interpretation of the chemical characteristics of natural water, *U.S.G.S. Survey Water Supply Paper 2254, 3rd edition.*

Hem, J.D. (1967). Composition of saline residues on leaves and stems of saltcedar (Tamarix pentandra pallas), *U.S.G.S. professional paper 491-C.*

Hendrickx, J. M. H., Hollanders, P., and Wierenga, P. J. Groundwater recharge through a bare sand soil in the chihuahan desert, *preprint.*

Hill, R.W. (1976). *Comparative Physiology of Animals - An Environmental Approach*, Harper & Row, New York, pp. 656 p..

Hoering, T.C., and Parker, P.L. (1961). The geochemistry of the stable isotopes of chlorine, *Geochimica et Cosmochimica Acta*, **23**: 186-199.

Junge, C.E. (1963). *Air Chemistry and Radioactivity*, Academic Press, New York.

Junge, C.E., and Werby, R.T. (1958). The concentration of chloride, sodium, potassium, calcium, and sulfate in rain water over the United States, *Journal of Meteorology*, **15**: 417-425.

Kaufmann, R., Long, A., Bentley, H., and Davis, S. (1984). Natural chlorine isotope variations, *Nature*, **309**: 338-340.

Knowlton Jr., R. G., Phillips, F. M., and Campbell, A. R. (1989). A stable-isotope investigation of water vapor during groundwater recharge in New Mexico, *Technical Completion Report No. 237*.

Kocharov, G.E. (1992). Radiocarbon and astrophysical-geophysical phenomena, in *Radiocarbon After Four Decades, An Interdisciplinary Perspective*, ed. R.E. Taylor, A. Long, and R.S. Kra, Springer-Verlag, New York, pp. 93-116.

Lal, D. (1992). Expected secular variations in the global terrestrial production rate of radiocarbon, in *The Last Deglaciation: Absolute and Radiocarbon Chronologies, NATO ASI Series*, ed. E. Bard and W.S. Broecker, Springer - Verlag, Berlin, pp. 113-126.

Lal, D. (1988). In situ-produced cosmogenic isotopes in terrestrial rocks, *Annual Review of Earth and Planetary Science Letters*, **16**: .

Lal, D. (1988). Theoretically expected variations in the terrestrial cosmic-ray production rates of isotopes, *Proc. 45th Conf. Solar - Terrestrial Relationships and the Earth Environment in the Last Millenia* ,Soc. Italiana di Fisica ,Bologna.

Lal, D. (1987). 10Be in polar ice: Data reflect changes in cosmic ray flux or polar meteorology, *Geophysical Research Letters*, **14**: 785-788.

Lal, D. (1985). Carbon cycle variations during the past 50,000 years: atmospheric 14C/12C ratio as an isotopic indicator, in *The Carbon Cycle and Atmospheric CO2: Natural Variations Archean to Present*, ed. E.T. Sundquist and W.S. Broeker, American Geophys. Union, Washington, D.C.,

Lao, Y., Anderson, R.F., Broeker, W.S., Trumbore, S.E., Hofmann, H.J., and Wolfli, W. (1992). Increased production of cosmogenic 10Be during the last glacial maximum, *Nature*, **357**: 576-578.

Legrand, M.R., Lorius, C., Barkov, N.I., and Petrov, V.N. (1988). Vostok (Antarctica) ice core: atmospheric chemistry changes over the last climatic cycle (160,000 years), *Atmospheric Environment*, **22**: 317-331.

Lorius, C., Jouzel, J., Ritz, C., Merlivat, L., Barkov, N.I., Korotkevich, Y.S., and Kotlyakov,

V.M. (1985). A 150,000 year climatic record from Antarctic ice, *Nature*, **316**: 591-596.

Mankinen, E.A., and Champion, D.E. (1993). Latest Pleistocene and Holocene geomagnetic paleointensity on Hawaii, *Science*, **262**: 412-416.

Mathias, A. D., Hassan, H. M., Ju, Y. -Q., Watson, J. E., and Warrick, A. W. (1986). Evapotranspiration estimates derived from subsoil salinity data, *Journal of Hydrology*, **85**: 209-223.

Mattick, J.L., Duval, T.A., and Phillips, F.M. (1987). Quantification of groundwater recharge rates in New Mexico using bomb-36Cl, bomb-3H and chloride as soil-water tracers, *WRRI Report No. 220*,NM WRRI.

Mayewski, P.A., Meeker, L.D., Whitlow, S., Twickler, M.S., Morrison, M.C., Alley, R.B., Bloomfield, P., and Taylor, K. (1993). The Atmosphere During the Younger Dryas., *Science*, **261**: 195-197.

Mazaud, A., Laj, C., Bard, E., Arnold, M., and Tric, E. (1992). A geomagnetic calibration of the radiocarbon time-scale, in *The Last Deglaciation: Absolute and Radiocarbon Chronologies, NATO ASI Series*, ed. E. Bard and W.S. Broecker, Springer - Verlag, Berlin, pp. 163-169.

Mazaud, A., Laj, C., Bard, E., and Tric, E. (1991). Geomagnetic field control of 14C production over the last 80 KY: Implications for the radiocarbon time scale, *Geophysical Research Letters*, **18**: 1885-1888.

McElhinny, M.W., and Senanayake, W.E. (1982). Variations in the Geomagnetic Dipole 1: the past 50,000 years, *Journal of Geomagnetism and Geoelectricity*, **344**: 39-51.

Meynadier, L., Valet, J.-P., Weeks, R., Shackleton, N.J., and Hagee, V.L. (1992). Relative geomagnetic intensity of the field during the last 140 ka, *Earth and Planetary Science Letters*, **114**: 39-57.

Mifflin, M.D., and Wheat, M.M. (1979). Pluvial lakes and estimated pluvial climates of Nevada, *Bulletin 94*,Nevada Bureau of Mines and Geology ,Reno.

Newell, R.E. (1971). The global circulation of atmospheric pollutants, *Scientific American*, **224**: 32-42.

Oeschger, H., and Beer, J. (1990). The past 5000 years history of solar modulation of cosmic radiation from 10Be and 14C studies, *Phil. Trans. R. Soc. Lond.*, **330**: 471-480.

Papke, K.G. (1976). Evaporites and brines in Nevada playas, *Bulletin 87*,Nevada Bureau of Mines and Geology ,Reno.

Paterne, M., Guichard, F., Labeyrie, J., Gillot, P.Y., and Duplessy, J.C. (1986). Tyrrhenian Sea tephrochronology of the oxygen isotope record for the past 60,000 years, *Marine Geology*, **72**: 259-285.

Paterne, M., Guichard, F., and Labeyrie, J.L. (1988). Explosive activity of the south Italian volcanoes during the past 80,000 years as determined by marine tephrochronology, *Journal of Volcanology and Geothermal Research*, **34**: 153-172.

Phillips, F.M. (1994). Environmental tracers for water movement in desert soils of the American southwest. *Soil Science Society of America Journal*, **58**: 15-24.

Phillips, F.M., Bentley, H.W., Davis, S.N., Elmore, D., and Swanick, G.B. (1986). Chlorine 36 dating of very old groundwater 2. Milk River Aquifer, Alberta, Canada, *Water Resources Research*, **22**: 2003-2016.

Phillips, F.M., Mattick, J.L., Duval, T.A., Elmore, D., and Kubik, P.W. (1988). Chlorine 36 and tritium from nuclear weapons fallout as tracers for long-term liquid and vapor movement in desert soils, *Water Resources Research*, **24**: 1877-1891.

Phillips, F.M., Peeters, L.A., Tansey, M.K., and Davis, S.N. (1986). Paleoclimatic inferences from an isotopic investigation of groundwater in the central San Juan Basin, New Mexico, *Quaternary Research*, **26**: 179-193.

Phillips, F.M., Tansey, M.K., Peeters, L.A., Cheng, S., and Long, A. (1989). An isotopic investigation of groundwater in the central San Juan Basin, New Mexico: Carbon 14 dating as a basis for numerical flow modeling, *Water Resources Research*, **25**: 2259-2273.

Raisbeck, G.M., Yiou, F., Bourles, D., and Kent, D.V. (1990). Evidence for an increase in cosmogenic 10Be during a geomagnetic reversal, *Nature*, **315**: 315-317.

Raisbeck, G.M., Yiou, F., Bourles, D., Lorius, C., Jouzel, J.J, and Barkov, N.I. (1987). Evidence for two intervals of enhanced 10Be deposition in Antarctic ice during the last glacial period, *Nature*, **326**: 273-277.

Raisbeck, G.M., Yiou, F., Fruneau, M., Loiseaux, J.M., Lieuvin, M., Ravel, J.C., and Lorius, C. (1981). Cosmogenic 10Be concentrations in Antarctic ice during the past 30,000 years, *Nature*, **292**: 825-826.

Raisbeck, G.M., Yiou, F., Jouzel, J., and Petit, J.R. (1990). 10Be and del2H in polar ice cores as a probe of the solar variability's influence on climate, *Pil. Trans. R. Soc. Land*, **330**: 463-470.

Schmidt-Neilsen, K. (1964). *Desert Animals, Physiological Problems of Heat and Water*, Oxford University Press, London,

Sequeira, R. (1993). On the large-scale impact of arid dust on precipitation chemistry of the continental northern hemisphere, *Atmospheric Environment*, **27A**: .

Sonett, C.P., Morfill, G.E., and Jokipii, J.R. (1987). Interstellar shock waves and 10Be from ice cores, *Nature*, **330**: 458-460.

Stephens, D.B, and Knowlton Jr., R. (1986). Soil-water movement and recharge through sand at a semi-arid site in New Mexico, *Water Resources Research*, **22**: 881-889.

Sternberg, R.S. (1992). Radiocarbon fluctuations and the geomagnetic field, in *Radiocarbon After Four Decades, An Interdisciplinary Perspective*, ed. R.E. Taylor, A. Long, and R.S. Kra, Springer-Verlag, New York, pp. 93-116.

Stuiver, M., and Braziunas, T.F. (1991). Climatic, solar, oceanic, and geomagnetic influences on late-glacial and Holocene atmospheric 14C/12C change, *Quaternary Research*, **35**: 1-24.

Stuiver, M., and Quay, P.D. (1980). Changes in atmospheric carbon-14 attributed to a variable sun, *Science*, **207**: 11-19.

Stute, M., Clark, J.F., and Bonani, G. (1995). A 30,000 yr continental paleotemperature record derived from noble gases dissolved in groundwater from the San Juan Basin, New Mexico, *Quaternary Research*, **43**: 209-220.

Stute, M., Schlosser, P., Clark, J.F., and Broecker, W.S. (1992). Paleotemperatures in the southwestern United States derived from noble gas temperatures, *Science*, **256**: 1000-1003.

Suess, H.E. (1986). Secular variations of cosmogenic 14C on earth: their discovery and interpretation, *Radiocarbon*, **28**: 259-265.

Tansey, M.K. (1984). An integrated isotopic/physical approach to a numerical model of groundwater flow in the San Juan Basin, *Master's Thesis* ,NMIMT ,Socorro, NM.

Tauxe, L. (1993). Sedimentary records of relative paleointensity of the geomagnetic field: theory and practice, *Reviews of Geophysics*, **31**: 319-354.

Tauxe, L., and Valet, J.-P. (1989). Relative paleointensity of the earth's magnetic field from marine sedimentary records: a global perspective, *Phys. Earth Planet. Inter.*, **56**: 59-68.

Thompson, R.S., Benson, L., and Hattori, E.M. (1986). A revised chronology for the last Pleistocene lake cycle in the central Lahontan basin, *Quaternary Research*, **25**: 1-9.

Thouveny, N., Creer, K.M., and Williamson, D. (1993). Geomagnetic moment variations in the last 70,000 years, impact on production of cosmogenic isotopes, *Global and Planetary Change*, **7**: 157-172.

Torgersen, T, Habermehl, M.A., and Phillips, F.M. (1992). Chlorine 36 dating of very old groundwater 3: further studies in the Great Artesian Basin, *Water Resources Research*, **27**: 3201.

Tric, E., Valet, J.-P., Tucholka, P., Paterne, M., LaBeyrie, L., Guichard, F., Tauxe, L., and Fontugne, M. (1992). Paleointensity of the geomagnetic field during the last 80,000 years, *Journal of Geophysical Research*, **97**: 9337-9351.

Tucholka, P., Fontugne, M., Guichard, F., and Paterne, M. (1987). The Blake magnetic polarity episode in cores from the Mediterranean Sea, *Earth and Planetary Science Letters*, **86**: 320-326.

Turekian, K., Nozaki, Y., and Benninger, L.K. (1977). Geochemistry of atmospheric radon and radon products, *Annual Review of Earth and Planetary Science*, **5**: 227-255.

Turin, H.J. (1995). Geochemistry of cave pool water in Lechuguilla Cave, NM, *GSA Abstracts.*

Tweit, S.J. (1992). *The Great Southwest Nature Fact Book*, Alaska Northwest Books, Seattle, pp. 223.

Twomey, S. (1977). *Atmospheric Aerosols*, Elsevier Scientific, New York, pp. 290-293.

Tyler, S.W., Chapman, J.B., Conrad, S.H., and Hammermeister, D. (1994). Paleoclimatic response of a deep vadose zone in southern Nevada, U.S.A. as inferred from soil water tracers, *Proceedings of the First International Symposium on Application of Tracers in Arid Zone Hydrology* ,IAEA ,Vienna, Austria.

Tyler, S.W., Chapman, J.B., Conrad, S.H., Hammermeister, D.P., Blout, D., Miller, J., and Ginanni, J.M. (~1995). Soil water flux on the Nevada Test Site: spatial and temporal variations over the last 120,000 years, *submitted to IAEA.*

Valet, J.-P., and Meynadier, L. (1993). Geomagnetic field intensity and reversals during the past four million years, *Nature*, **366**: 234-238.

Vroblesky, D.A., and Yanosky, T.M. (1990). Use of tree-ring chemistry to document historical ground-water contamination events. *Groundwater*, **28**: 677-684.

Wilson, J.L., and Gelhar, L.W. (1974). Dispersive mixing in a partially saturated porous medium, *Technical Report No. 191* ,Dept. of Civil Eng., M.I.T..

Yiou, F., Raisbeck, G.M., Bourles, D., Lorius, C., and Barkov, N.I. (1985). 10Be in ice at Vostok, Antarctica during the last climatic cycle, *Nature*, **316**: 616-617.

Yurtsever, Y. (1975). Worldwide survey of stable isotopes in precipitation, *Rep. Sect.*

Isotope Hydrol. ,IAEA.

Appendix A

Chloride Extraction Method for Processing Rat-Urine Samples for ^{36}Cl Ratio Determination

These notes are intended to provide a guideline for processing packrat midden samples for ^{36}Cl ratio measurement. As such, the notes describe the method in considerable detail but omit most of the details concerning proper cleaning of the associated glassware and plasticware. Proper cleaning before and during the process, to avoid contamination with any sources of chloride other than the midden itself, is essential but may vary depending on the equipment and cleaning compounds available in the laboratory, It should be noted that the processing described here is intended only to yield a sample of purity suitable for AMS measurement. If other information from the midden is required, such as concentrations of various inorganic ions including chloride, other methods may be required. In general the method requires few careful measurements of mass or volumes involved; the most critical part of the process is to scrupulously avoid introducing other sources of chloride during processing.

1) Break up a portion of the sample and select a subsample that consists of as pure amberat as possible. The samples are typically very well-indurated and can often be broken only with a rock hammer or another such instrument. If the sample is of suitable size, a hacksaw may provide a better means of selecting a subsample. If the sample is large, it is recommended that efforts be taken to select a precise subsample; this helps to limit complications due to possible spatial variations within the midden.

2) Set aside sufficient sample for radiocarbon dating as well as the following procedure. (Actual samples for ^{14}C dating are best selected using a microscope to pick out pieces of relatively pure amberat). These samples should be a split of the same portion to ensure that the ^{14}C data and ^{36}Cl data are obtained from the same material.

3) Use previous data regarding chloride concentrations in solid amberat, and efficiency of extraction procedure, to estimate mass of amberat required to obtain approximately 40 mg of chloride (this should be approximately 10 grams of midden material).

4) Dissolve sufficient solid amberat in 18-megaohm deionized water to obtain ~40 ml of solution (a volume chosen to optimize ease of filtration). Shake for several hours before further processing to ensure that all of the amberat is dissolved.

5) Filter sample using clean Millipore filter setup, 0.45-micron filter(s), and labeled filtration flasks. Save undissolved solids from the filtration in a separate container for possible supplemental radiocarbon dating. If sufficient filtration flasks are available, it may be expedient to rinse once and save the labeled filtration flasks for further processing of the same samples. Note that if Cl- concentration measurements are to made on the

samples, one must take care to limit the amount of water introduced during the filtering process.

6) Measure chloride concentrations of the samples if desired. Note that samples must be diluted by a factor of approximately 10 prior to measurement with the ion specific electrode. Use a minimum of three fresh standards in a range of approximately 50 to 500 ppm Cl- and a blank. Refer to ion-specific electrode measurement procedures for further details.

7) Transfer the samples to 250-ml centrifuge containers (if sufficient Cl- is available, save some of the sample in a separate beaker as a precaution against processing errors). Using data obtained in step 5, dilute the samples to approximately 100 mg/l with 18 megaohm deionized water. The dilution is not critical and it may be most effective to simply dilute the solution by adding only enough ultrapure water to fill the centrifuge container. Add approximately 5 ml concentrated HNO3 to the samples and check for precipitate. If a precipitate develops, separate and discard it by either (1) filtration or (2) centrifuging the samples, pouring off the supernatant to clean containers (or the saved filtration flasks), and removing the precipitate via a vigorous ultra-pure rinse.

8) Add 0.1 Molar $AgNO_3$ solution in approximately the following proportion: 1.5 moles Ag : 1 mole Cl in sample (The amount of $AgNO_3$ added is again not critical and is chosen to ensure that sufficient Ag is available to combine with the Cl in the sample yet avoiding the always unwise excess. It is also possible to simply add $AgNO_3$ until precipitate no longer forms upon the addition). Place samples in a warm area or warm them in a water bath at 60 - 90 degrees C for 2 to 3 hours to allow AgCl to precipitate and settle. Pour off supernatant, retaining the solid AgCl.

9) Transfer remaining precipitate and solution and centrifuge for ten minutes to concentrate AgCl. Carefully remove solution, pour off supernatant, and again keep the precipitate (solid AgCl).

10) Rinse the AgCl in ultra-pure water and transfer to 50-ml glass or teflon centrifuge tube. Let AgCl sit in the tube of DI water for 1 hour or more at room temperature, then centrifuge and decant off DI water, retaining solid AgCl.

11) Dissolve the solid AgCl in concentrated NH_4OH.

12) Add HNO_3 to precipitate AgCl. (The amount of HNO_3 required is slightly greater than the amount required to neutralize the solution).

13) Centrifuge and decant, retaining solid AgCl.

14) Dissolve the AgCl in ~3 ml of NH_4OH and add ~1.5 ml of $Ba(NO_3)_2$ to precipitate $BaSO_4$. Let the solution stand for at least 8 hours (but preferably longer).

15) Centrifuge the tube, then carefully remove and retain the AgCl solution using a clean glass pipette. Place it in another glass centrifuge tube and label it twice.

16) Repeat steps 11 through 13 three times to remove as many contaminants as possible.

17) Note: Each repetition of this procedure should cause the color of the AgCl precipitate to become increasingly lighter, grading to a slightly lavender color as AgCl purity increases.

18) Again add sufficient HNO_3 to precipitate AgCl and let stand for approximately 2 hours. Decant off the acidic solution and rinse the AgCl 3 times in DI water. Make sure the pH of the final rinse is about 7.

The remaining processing details describe one method of drying the samples for packing in one type of AMS holder. The AMS laboratory should be contacted as to the appropriate method of packing the samples before proceeding with these steps. In some cases the laboratory may accept wet samples and packing may include only labeling of appropriately clean containers..

1) Transfer the AgCl onto a clean watch glass. Remove excess water using a small glass pipette. Cover the glass with aluminum foil leaving several holes near the edges to allow water vapor to escape. Place two labels on the foil.

2) Place the sample in the oven for 24 hours. Set the temperature to approximately 60° (this is about 4.0 on the oven in the isotope lab at NMIMT).

3) Remove the samples from the oven and pack in holders. If samples are not packed immediately, cover the samples with parafilm to prevent contamination.

4) When packing samples, record the number written on the metal holder itself and make sure that that number matches the number printed on the plastic cover of the holder. Holders should be packed completely full; if insufficient sample is available, the sample may be mixed with AgBr to ensure that the holder is completely filled.

NOTES:

(1) "Centrifuge" implies 10 minutes or more at 25,000 rpm.

Appendix B

Sample ID	Ca (mg/kg)	Mg (mg/kg)	K (mg/kg)	Na (mg/kg)	Cl (mg/kg)	Br (mg/kg)	N as urea (mg/kg)
LSM091282LP1(1)	6279	4273	32528	12630	18905	ND	1221
PH140889 PEW2(1,5)	7675	3251	58891	4775	5776	ND	< 300
PH150990 PEW1(1,4)b	14738	1857	14429	1601	< 6200	ND	< 300
PH150990 PEW1(6,6)	29773	3377	6360	1901	< 6200	ND	< 300
PH180589 PEW3(2,1)	12776	3053	18945	4803	5997	ND	482

Results of analyses of 5 midden samples for urea-nitrogen and several cations and anions. Concentrations are mg solute per kilogram midden material. ND indicates non-detection of that species. Analyses performed by the Reference Laboratory, Albuquerque, NM.

Appendix C

Chloride Extraction Method for Processing Soil and Groundwater Samples for ^{36}Cl Ratio Determination

These notes are intended to provide a guideline for processing soil and groundwater samples for ^{36}Cl ratio measurement. As such, the notes describe the method in considerable detail but omit most of the details concerning proper cleaning of the associated glassware and plasticware. Proper cleaning before and during the process, to avoid contamination with any sources of chloride other than the sample itself, is essential but may vary depending on the equipment and cleaning compounds available in the laboratory, It should be noted that the processing described here is intended only to yield a sample of purity suitable for AMS measurement. If other information from the samples is required, such as concentrations of various inorganic ions including chloride, additional steps may be required. In general this process requires few careful measurements of mass or volume; the most critical part of the process is to scrupulously avoid introducing other sources of chloride during processing.

1. Weigh out sufficient sample mass to provide the amount of Cl necessary for the analysis. This depends largely on the chloride concentration of the material. If concentrations are less than 5 ppm and only small samples are available chloride yield may be very low. In such cases, it may be necessary to add single-isotope chloride as a carrier/tracer.
2. Add the sample to a clean container. If concentrations are high enough, it is advisable to place the samples in containers that will fit into some type of agitator.
3. Add an equal mass of ultra-pure water to the sample containers and allow to leach for at least 24 hours.
4. Turn off the agitating device and place the samples upright to allow mineral matter to settle.
5. Centrifuge the samples if possible. Pour off the solution into a clean container and filter through with 0.45 μm filter(s) to remove any remaining mineral material. If mineral material does not settle easily or is difficult to filter, the pH of the solution can be lowered just prior to centrifugation or settling to encourage aggregation.
6. Remove an aliquot of the filtered solution for Cl analysis and/or other analyses.
7. If solution concentrations are high enough, AgCl may now be precipitated by addition of $AgNO_3$ and pH adjustment. Again, it is advisable to perform these steps in containers which may be readily centrifuged. If concentrations are too dilute, silver chloride may not precipitate in aggregate particles large enough to settle easily. In this case, a sub-process such as described below may be required.

a) Adjust pH to neutral or slightly basic and place on hot plate in a vented hood to evaporate water and concentrate Cl. Temperature should be set so that samples are steaming but not boiling. Samples should be periodically monitored during this process so that solution does not become too concentrated. Do not allow all of the water to evaporate.

8. Adjust pH to ~2 by addition of pure concentrated HNO_3.

9. Add sufficient $AgNO_3$ to precipitate slightly more AgCl than should be possible based on the estimated mass of Cl in solution. Place samples in a warm area or warm them in a water bath at 60 - 90 degrees C for 2 to 3 hours to allow AgCl to precipitate and settle.

10. If possible, centrifuge samples so that precipitate forms a cohesive mass in the bottom of the container.

11. Pour off solution, rinse by addition and agitation in ultra-pure water and repeat step 10.

12. Pour off solution; dissolve AgCl precipitate in NH_4OH and transfer to 50-ml glass centrifuge tube.

13. Continue processing starting with step 12 of the method for extracting Cl from packrat middens (Appendix A).

Appendix D

Tabulated Data for LTER-1 and LTER-2

Sample	Sample average depth (m)	Soil Type	** Best est. of interval bottom (m)	** Interval age (ka)	** Total age (ka)	** Sample age (ka)	Dry Sample Mass (g)	Mass H2O (g)	Volumetric water content	** Cumulative Chloride (g/m^2)	** Cumulative water (m^3/m^2)	ISE mg Cl- per Kg soil	* ISE mg Cl- per m^2	$\delta^{18}O$ 1	$\delta^{18}O$ 2	$\delta^{18}O$ 3	Lab 36Cl Ratio /10^15 Cl	+ / -	Decay-Corrected 36Cl Ratio /10^15 Cl	** Soln. Cl Conc. (mg/liter)
LTER1-01	0.05	sand	0.05	0.061	0.061	0.061	202.53	3.94	0.033	4.5	0.002	53.73	4,540				-	-	-	2762
LTER1-02	0.15	sand	0.15	0.176	0.237	0.237	137.58	4.04	0.050	17.7	0.007	78.11	13,201				-	-	-	2660
LTER1-03	0.30	sand	0.45	0.218	0.454	0.345	223.25	10.62	0.080	34.1	0.031	32.20	8,163				-	-	-	677
LTER1-04	0.53	sand	0.70	0.143	0.597	0.500	127.79	7.63	0.101	44.8	0.056	25.30	9,834	-4.75			-	-	-	424
LTER1-05	0.80	sand	1.00	0.280	0.877	0.690	95.35	5.51	0.098	65.7	0.085	41.40	18,891	-3.5			-	-	-	716
LTER1-06	1.00	sand	1.25	0.128	1.005	0.877	116.26	6.61	0.096	75.4	0.109	22.80	7,706	-4.96			-	-	-	401
LTER1-07	1.43	sand	1.50	0.290	1.295	1.214	138.91	6.72	0.082	97.1	0.130	51.49	37,418	-4.15			-	-	-	1064
LTER1-08	1.68	sand	1.80	0.154	1.449	1.387	123.52	5.82	0.080	108.7	0.154	22.77	9,620	-4.47			-	-	-	483
LTER1-09	2.25	sand	2.40	1.620	3.069	2.664	110.03	5.69	0.087	230.1	0.206	119.79	115,394	-4.34			1389	20	1,398	2316
LTER1-10	2.93	sand	3.28	0.395	3.463	3.306	122.51	6.87	0.095	259.7	0.289	19.90	22,869	-4.87			690	16	695	355
LTER1-11	3.63	sand	3.75	1.967	5.430	4.928	100.97	5.00	0.084	407.2	0.329	185.70	219,683	-4.88			749	24	758	3750
LTER1-12	3.86	sand	4.10	1.546	6.976	5.916	122.80	5.79	0.080	523.2	0.357	196.03	76,197	-4.97			708	31	718	4158
LTER1-13	4.30	sand	4.68	2.239	9.215	7.748	106.04	5.14	0.082	691.1	0.404	171.33	127,401	-5.56			730	20	744	3535
LTER1-14	4.84	clay	4.93	1.893	11.108	10.427	110.01	16.05	0.160	833.1	0.444	517.00	306,679	-7.42	-7.43		747	16	765	3544
LTER1-15	5.02	sand	5.25	1.426	12.534	11.509	62.83	13.06	0.351	940.1	0.557	197.75	60,156	-7.73			756	11	777	951
LTER1-16	5.55	sand	5.70	2.005	14.539	13.871	116.01	7.79	0.113	1090.4	0.608	197.75	177,125	-7.1			772	11	797	2945
LTER1-17	5.83	sand	6.15	1.389	15.928	14.941	110.59	5.77	0.088	1194.6	0.647	137.00	64,828	-5.8			779	11	806	2626
LTER1-18	6.30	sand	6.30	0.463	16.391	16.391	101.50	22.15	0.369	1229.4	0.703	137.00	108,819	-7.81			**2552**	37	2,650	628
LTER1-19	6.60	clay	6.80	3.625	20.017	18.567	104.13	19.68	0.208	1501.2	0.807	495.00	163,127	-7.44			770	12	803	2619
LTER1-20	6.97	clay	7.20	3.205	23.221	21.379	117.89	17.84	0.166	1741.6	0.873	547.00	222,325				774	11	813	3615
LTER1-21	7.71	sand	8.08	0.752	23.973	23.657	124.53	2.68	0.036	1798.0	0.905	37.93	47,435	-4.9			1008	17	1,064	1762
LTER1-22	8.45	sand	8.80	0.756	24.729	24.362	126.30	4.21	0.056	1854.7	0.946	46.58	58,253	-6.83	-7.98		834	13	882	1397
LTER1-23	9.13	sand	9.51	0.474	25.203	24.949	113.89	5.30	0.079	1890.2	1.001	29.63	34,051	-7.63			821	12	869	637
LTER1-24	9.76	sand	10.11	0.455	25.658	25.393	131.34	3.43	0.044	1924.4	1.028	33.66	35,838	-6.9			-	-	-	1289
LTER1-25	10.45	sand	10.55	1.952	27.611	27.167	95.59	17.16	0.303	2070.8	1.161	196.92	229,628	-7.39			769	31	818	1097
LTER1-26A	10.65	clay	10.65	0.410	28.020	28.020	-	-	0.220	2101.5	1.183	279.63	61,435				798	16	851	1398
LTER1-26B	10.75	clay	10.90	0.707	28.727	28.303	79.64	18.02	0.249	2154.5	1.245	193.00	21,201	-8			786	12	839	853
LTER1-27	11.14	sand	11.23	1.438	30.164	29.772	114.14	10.03	0.149	2262.3	1.295	193.33	127,424	-6.57	-6.01		781	11	836	2200
LTER1-28	11.32	sand	11.59	1.040	31.205	30.425	124.42	11.18	0.152	2340.4	1.349	128.26	39,017	-7.23	-7.56	-7.2	769	16	825	1427
LTER1-29	11.91	clay	12.05	0.583	31.788	31.610	97.63	19.32	0.217	2384.1	1.449	86.53	56,081	-7.61	-7.84		762	23	819	437
LTER1-30	12.20	clay	12.40	1.513	33.301	32.436	108.97	25.76	0.260	2497.6	1.540	295.15	94,024	-8.08	-8.01	-8.08	743	11	801	1249
LTER1-31	12.59	clay	12.70	0.894	34.195	33.867	105.33	22.84	0.238	2564.6	1.612	203.43	87,152	-7.68	-7.69		739	18	799	938
LTER1-32	12.87	sand	13.01	1.144	35.339	34.822	107.76	14.01	0.220	2650.4	1.680	163.76	77,491	-7.79	-7.79		791	25	857	1260

** represents revised calcs based on new estimates of interval top and bottom

1.5 =bulk density of mix
1.7 =bulk density of sand
1.1 =bulk density of clay

Sample No.	soil type	bulk density	Depth (m)	d18O	Sample age	Volumetric water content	mg Cl/Kg soil	Cum. chloride (g/kg)	Cum. chloride (g/m^2)	Cum. water content (m^3/m^2)	Cl- conc. (mg/L)
LTER2-1	mix	1.5	0.05	5.09	0.14	0.051	162	162	108	0.003	4737
LTER2-2	mix	1.5	0.20	2.81	0.48	0.063	130	292	195	0.012	3115
LTER2-3	mix	1.5	0.38	-0.28	0.53	0.058	15	307	205	0.022	391
LTER2-4	mix	1.5	0.55	-2.52	0.60	0.053	26	333	222	0.031	734
LTER2-5	mix	1.5	0.80	-4.23	3.99	0.160	782	1115	743	0.071	7354
LTER2-6	mix	1.5	1.54	-5.57	7.56	0.177	278	1393	929	0.202	2357
LTER2-7	mix	1.5	1.80	-5.59	8.90	0.248	322	1715	1143	0.267	1948
LTER2-8	mix	1.5	2.23	-6.20	11.56	0.213	357	2072	1381	0.358	2514
LTER2-9	mix	1.5	2.48	-5.28	12.60	0.170	240	2312	1541	0.401	2114
LTER2-10	clay	1.1	2.92	-5.42	14.38	0.068	190	2502	1714	0.431	3069
LTER2-11	clay	1.1	3.16	-4.99	14.93	0.119	133	2635	1835	0.459	1231
LTER2-12	mix	1.5	3.63	-4.33	15.59	0.068	81	2716	1889	0.491	1782
LTER2-13	mix	1.5	3.95	-3.74	16.05	0.058	83	2799	1944	0.510	2158
LTER2-14	mix	1.5	4.35	-4.90	16.81	0.046	109	2908	2017	0.528	3539
LTER2-15	mix	1.5	5.01		17.47	0.021	58	2966	2056	0.542	4143
LTER2-16	mix	1.5	5.23		18.09	0.088	163	3129	2164	0.561	2785
LTER2-17	clay	1.1	5.73				176	3305	2324	0.561	
LTER2-18	clay	1.1	5.98	-5.60	20.31	0.114	161	3466	2471	0.590	1556
LTER2-19	clay	1.1	6.41	-5.00	21.45	0.094	152	3618	2609	0.630	1783
LTER2-20	clay	1.1	6.63		22.10	0.111	171	3789	2764	0.655	1696
LTER2-21	mix	1.5	7.79		24.63	0.035	126	3915	2848	0.695	5415
LTER2-22	mix	1.5	7.97	-3.66	24.86	0.022	73	3988	2897	0.699	4932
LTER2-23	mix	1.5	9.19	-4.60	27.82	0.075	140	4128	2990	0.790	2815